Inaugural dissertation

for

obtaining the doctoral degree

of the

Combined Faculty of Mathematics, Engineering and Natural Sciences

of the

Ruprecht - Karls - University

Heidelberg

Presented by

M.Sc. Andrea Zanotti

born in San Giovanni in Persiceto (BO), Italy

Oral examination: 13.06.2023

Characterisation of
the human signal peptidase complex
as a quality control enzyme
for membrane proteins

Referees: Prof. Dr. Matthias P. Mayer

Prof. Dr. Marius K. Lemberg

Summary

During membrane protein biogenesis, cells need to detect and degrade faulty proteins. Despite a key role in cellular homeostasis and human diseases, little is known about the underlying mechanisms. In recent years, few endoplasmic reticulum (ER)-resident proteases have been linked to quality control by cleaving their clients and thereby facilitating membrane extraction and degradation via the ER-associated degradation (ERAD) pathway. The major ER-resident protease in mammalian cells is the signal peptidase complex (SPC), a tetra subunit complex discovered in the 1970s to be responsible for the removal of signal sequences from ER-targeted and secretory proteins. Until now, this was thought to be the only function of the SPC besides a few studies reporting a role in the maturation of viral polyproteins.

In this work, I show that the SPC also acts as a membrane protein quality control factor. First, through proteome-wide computational analyses, I identified approximately 1500 membrane proteins containing SPC cryptic cleavage sites after N-terminal and internal type-II oriented transmembrane domains (TMDs). I then validated SPC cleavage for several candidate substrates (Cx32, Cx26, Cx30.3, PMP22, iRhom2 and Hrd1) and revealed that SPC cleavage relies on the accessory subunit SPCS1 as recognition factor to discern between signal sequences and TMDs. Moreover, I show that the SPC cleaves membrane proteins when they fail to fold properly or assemble correctly into their native complexes, thus exposing cryptic cleavage sites. I also show that this SPC cleavage mechanism cooperates with the ERAD pathway to help maintain a functional membrane proteome and confers a fitness advantage to cells exposed to ER stress. Finally, I report first data on the possible role of the SPC in controlling protein abundance beyond its quality control function.

Overall, this thesis characterises a novel function of the SPC, expanding its substrate spectrum, extending the knowledge on the essential cellular functions performed by this protease and laying the foundations for future work at the organismal level in quality control-related diseases and beyond.

Zusammenfassung

Während der Biogenese von Membranproteinen müssen Zellen fehlerhafte Proteine erkennen und abbauen. Trotz einer Schlüsselrolle bei der zellulären Homöostase und menschlichen Krankheiten ist sehr wenig über die zugrundeliegenden Mechanismen bekannt. In den letzten Jahren wurden nur wenige im Endoplasmatischen Retikulum (ER) ansässige Proteasen mit der Qualitätskontrolle in Verbindung gebracht, indem sie durch Proteolyse ihrer Klienten deren Membranextraktion im ER-assoziierten Abbauweg (ERAD) erleichtern. Die wichtigste ER-lokalisierte Protease in Säugerzellen ist der Signalpeptidase-Komplex (SPC), ein in den 1970er Jahren entdeckter Komplex aus vier Untereinheiten, der für die Entfernung von ER-Signalsequenzen verantwortlich ist. Seitdem wurde angenommen, dass abgesehen von vereinzelten Studien über eine Rolle bei der Reifung viraler Polyproteinen, dies die einzige Funktion von SPC ist.

In dieser Arbeit zeige ich nun, dass die SPC auch als Qualitätskontrollfaktor für Membranproteine fungiert. Durch Proteom-weite bioinformatische Analyse identifizierte ich ungefähr 1500 Membranproteine, die kryptische SPC-Spaltstellen nach N-terminalen sowie internen Typ-II-orientierten Transmembrandomänen (TMDs) enthalten. Anschließend validierte ich die SPC-Spaltung für mehrere Kandidatensubstrate (Cx32, Cx26, Cx30.3, PMP22, iRhom2 und Hrd1) und zeigte, dass die SPC-vermittelte Spaltung auf der akzessorischen Untereinheit SPCS1 als Erkennungsfaktor beruht, um zwischen Signalsequenzen und TMDs zu unterscheiden. Darüber hinaus zeige ich, dass die SPC Membranproteine spaltet, wenn sie sich nicht richtig falten oder sich nicht korrekt zu ihren nativen Komplexen zusammensetzen, wodurch kryptische Spaltstellen freigelegt werden. Ich zeige auch, dass dieser SPC-Spaltungsmechanismus mit dem ERAD-Weg kooperiert, um die Aufrechterhaltung eines funktionellen Membranproteoms zu unterstützen und Zellen, die ER-Stress ausgesetzt sind, einen Fitnessvorteil zu verleihen. Abschließend berichte ich erste Daten über eine mögliche Rolle der SPC bei der Kontrolle der Proteinhäufigkeit über die Qualitätskontrollfunktion hinaus. Alles in allem charakterisiert diese Arbeit eine neue SPC-Funktion, die ihr Substratspektrum vergrößert, wodurch das Wissen über die wesentlichen zellulären Funktionen dieser Protease

erweitert und die Grundlagen für zukünftige Arbeiten auf der Ebene des Organismus bei Krankheiten im Zusammenhang mit der Qualitätskontrolle und darüber hinaus gelegt werden.

Table of Contents

Contributions

This project was performed in a close collaboration with the group of Prof. Dr. Matthias Feige (Technische Universität München, TUM, Munich).

The vast majority of the results presented in this thesis were recently published in *Science* (Zanotti et al. 2022)[1], with the exception of Fig. 1D, 2A, 3, 9C, 12B-C and 13.

Prof. Dr. Marius Lemberg and Prof. Dr. Matthias Feige helped with and supervised the conceptualisation of this work.

Computational analyses in Fig.1, 4 and 5 are based on my own analyses that were extended in collaboration with Dr. Gurdeep Singh (Russell Group, BioQuant, Heidelberg).

SPCS1 mutant constructs used in Fig. 7 were designed by me and generated by Marina Tauber.

I performed the Cycloheximide chase analyses in Fig.11B, which were subsequently replicated by Dr. Dönem Avci.

I conceived the qRT-PCR analysis in Fig. 12A, which was carried out by Dr. Dönem Avci.

I conceived the interactome analysis in Fig.13B, which was carried out by Dr. Dönem Avci and Marina Tauber.

I designed and performed all the other experiments reported in this thesis.

List of abbreviations

ATP	Adenosine triphosphate
CHOP	C/EBP homologous protein
CHX	Cycloheximide
CPA	Cyclopiazonic acid
Cx	Connexin
DMSO	Dimethylsulfoxide
DTT	Dithiothreitol
EMC	ER membrane protein complex
ER	Endoplasmic reticulum
ERAD	ER-associated degradation
GTP	Guanosine triphosphate
HEK	Human embryonic kidney
IRE1	Inositol-requiring enzyme 1
KO	Knockout
PAGE	Polyacrylamide gel electrophoresis
PERK	double-stranded RNA-activated protein kinase (PKR)-like ER kinase
RQC	Ribosome-associated quality control
SPC	Signal peptidase complex
SPP	Signal peptide peptidase
SRP	Signal recognition particle
TA	Tail-anchored
TMD	Transmembrane domain
UPR	Unfolded protein response
UPS	Ubiquitin-proteasome system
XBP1	X-box binding protein 1

List of Figures

List of Tables

1. Introduction

1.1 Membrane protein biogenesis

An essential characteristic of all organismal life is the presence of lipid membranes that are key to maintaining separation between the intracellular and extracellular environment as well as segregating the content of the different intracellular compartments. Embedded into these, otherwise impermeable, lipid membranes are integral membrane proteins, which are fundamental for the transport of molecules (e.g. ions and nutrients), metabolites and signals from the extracellular environment into the cells and across the different intracellular compartments. In all analysed species, membrane proteins constitute about 25-30% of the whole proteome[2,3] and perform fundamental functions as metabolic enzymes and mediators of cell-to-cell interaction and adhesion[4]. Membrane protein biogenesis is, therefore, a fundamental process which is evolutionarily conserved and required to be tightly regulated (see section 1.2 for more details).

In prokaryotic organisms, characterised by the absence of intracellular membrane-bound organelles, membrane proteins are inserted directly in the plasma membrane, where they exert their functions[5]. In eukaryotic organisms, characterised by the presence of several distinct intracellular membrane-bound organelles (e.g. mitochondria, chloroplasts, lysosomes and peroxisomes), the majority of membrane proteins are inserted into the endoplasmic reticulum (ER) membrane before undergoing maturation processes (e.g. glycosylation, folding and assembly into protein complexes) and possibly trafficking to their final destination in the cell[6,7]. The portion of the protein that spans the membrane is predominantly composed of α-helical structures, transmembrane domains (TMDs), mainly containing hydrophobic amino acid residues[8]. In human cells, ~5000 membrane proteins contain ~20000 TMDs displaying a wide variety of sequences, biophysical properties, localisation and membrane orientations (topology). Approximately half of these are single pass proteins, possessing one single TMD inserted in the membrane in different orientations: type I if the C-terminus faces the cytosol, type II if it faces the ER lumen or tail-anchored (TA) if the TMD is at the very C-terminus of the protein with a type II orientation. The other half are multipass membrane proteins containing

multiple TMDs. This high diversity implies that the machinery involved in membrane protein biogenesis is highly versatile and consists of different pathways selective for the different types of substrates[9]. Overall, the process of membrane protein biogenesis can be subdivided in four crucial steps: targeting, insertion, folding and assembly.

1.1.1 Membrane protein targeting

As a general rule, membrane protein targeting to the ER is driven by the presence of hydrophobic domains located at the N-terminus and it happens co-translationally[10] when the protein is still being synthesised by the ribosomes. This hydrophobic sequence can either be a cleavable targeting sequence, called signal sequence[11–13] (see section 1.3 for more details), which is removed immediately after translocation into the ER membrane, or the first proper TMD of the protein, called signal anchor, which is part of the mature inserted protein. However, for TA proteins, the targeting signal is located at the very C-terminus and the targeting process happens post-translocationally[14], when the synthesis by the ribosomes is complete. On average, the hydrophobic core of signal sequences is ten amino acids long compared to the 20 amino acids of TMDs and is highly variable in sequence and hydrophobicity. Together with the targeting signal's different location, this consequently highlights the necessity of different pathways or targeting mechanisms to accommodate the different substrates.

1.1.1.1 Co-translational targeting

The essential factor for co-translational targeting of membrane proteins is the signal recognition particle (SRP)[15,16], a highly conserved ribonucleoprotein complex[17]. In mammalian cells, it is constituted by a 7SL RNA in complex with six protein subunits SRP9, SRP14, SRP19, SRP54, SRP68 and SRP72. SRP recognises the hydrophobic targeting sequences as soon as they arise from the ribosome exit tunnel[18,19] and hands them over to the SRP receptor at the ER membrane. The recycling of SRP after binding and targeting to the receptor is driven by a GTP hydrolysis cycle performed by the SRP subunit SRP54 and the α-subunit of the SRP receptor[20]. SRP54 also contains a hydrophobic substrates-binding groove which is usually autoinhibited by an amphipathic helix found at the C-terminus of SRP54 itself[19]. This helix is then displaced in the presence of signal peptides or TMDs and is used to hold the substrates in place. This

autoinhibitory mechanism is likely the reason for reduced off-target binding and high specificity towards signal peptides and TMDs. Ensuring reduced promiscuity towards non-substrates, the nascent polypeptide-associated complex (NAC), a cytoplasmic protein that binds to the exit tunnel of nearly all ribosomes, also plays a role. The biological relevance of NAC in target specificity is highlighted by SRP binding to ribosome translating protein lacking a signal sequence or TMD and by extensive mistargeting in the absence of NAC[21,22]. In summary, membrane proteins containing N-terminal signal peptides or signal anchors are targeted co-translationally to the ER membrane through a process including recognition of the targeting sequence by SRP, with the help of NAC, and subsequent docking of the translating ribosome to the ER membrane via the action of the SRP receptor.

1.1.1.2 Post-translational targeting

Post-translational targeting is predominantly used for TA proteins and it involves an entirely different set of factors and a different pathway, called GET pathway[23]. Since the TMD (targeting sequence) is found at the C-terminus and therefore arises from the ribosome exit tunnel late in the translation process, a pre-targeting complex formed by GET4, GET5, the chaperone SGTA and the control factor BAG6 engages with the nascent chain before handing over to the actual targeting factor, the homodimeric GET3 (TRC40 in mammals) chaperone[24,25]. TRC40 binds the C-terminal TMD of TA proteins[26–28] and delivers it to the ER membrane via the interaction with the receptor and translocase GET1-GET2[29]. In contrast with the SRP pathway, the recycling of the GET pathway components is driven by an ATP hydrolysis cycle performed by GET3 and GET1-GET2[30].

1.1.2 Membrane protein insertion

The next step in membrane protein biogenesis following targeting to the ER membrane is membrane insertion of the hydrophobic TMD(s). Per se, inserting hydrophobic helixes into the hydrophobic membrane bilayer is an energetically favoured reaction. However, a few challenges render this a complex process: unwanted interactions between TMDs before targeting (e.g. aggregation), translocation of hydrophilic TMDs flanking regions (e.g. loops) and insertion of the TMDs in the correct orientation. On the one hand, unwanted interactions before

targeting are controlled by targeting factors and chaperones (see section 1.1.1). On the other hand, loop translocation and correct orientation of TMDs are achieved with the help of components of the insertion machineries.

TA proteins can be inserted through two distinct mechanisms, based on the hydrophobicity of the TMD. TA proteins containing high hydrophobicity TMDs are inserted via the GET1-GET2 heterodimer[31,32]. GET1 belongs to the Oxa1 family of protein insertases[33] and present a cytosolic-facing hydrophilic vestibule required for insertion of the engaged TMD into the membrane[34]. Conversely, TA proteins containing medium to low hydrophobicity TMDs are inserted via the ER membrane protein complex (EMC)[35]. The EMC is constituted by ten subunits. One of those, EMC3, belongs to the Oxa1 family of protein insertases[33] and exploits the hydrophilic vestibule for membrane insertion of TMDs, in the same manner as GET1.

For all the other membrane proteins, the insertion route involves the Sec61 complex, also called translocon, an evolutionarily conserved protein-conducting channel constituted by three subunits: the large subunit Sec61α, which forms the aqueous channel through the ER membrane and possesses a lateral gate opening in the plane of the membrane, and two small peripheral subunits Sec61β and Sec61γ[36–38]. When inactive, the lateral gate is closed and the channel is plugged by a short helix. When signal peptides or signal anchors bind to the translocon, the lateral gate opens and dislocates the plug, consequently opening the channel[39]. Specifically, signal peptides bind with the N-terminus towards the cytosol so that translation elongation results in the C-terminal portion to be pushed through the channel in an orientation allowing cleavage of the signal sequence by the signal peptidase complex[40] (SPC; see section 1.3). Consequently, the TMD following the signal sequence possesses a type I orientation and is inserted in the membrane through the open lateral gate.

Membrane proteins without a signal sequence use the first TMD (signal anchor) as targeting signal (see section 1.1.1) and face the challenge of two possible orientations during the insertion process. Type II-oriented signal anchors follow the same route as signal peptides through the Sec61 later gate[41]. It has been recently reported that, instead, type I-oriented signal anchors are inserted by the EMC[42]. The EMC samples signal anchors after the release from the SRP and before the engagement with the traslocon, inserting type I- and skipping type II-oriented signal anchors, which are then inserted by the Sec61 translocon[43].

The Sec61 translocon associates with various proteins and complexes, including the SPC for signal sequence removal, the oligosaccharyltransferase (OST) complex for nascent chain N-glycosylation[44], the Sec62-Sec63 complex to support posttranslational translocation[45], the translocon associated (TRAP) complex[46] and the translocating chain-associated membrane protein (TRAM)[47], whose function is still poorly characterised.

Recently, a specialized translocon has been reported for insertion of multipass membrane proteins[48,49]. It is characterised by the association of three different complexes to the Sec61 translocon during synthesis of multipass membrane proteins: (i) the GET- and EMC-like (GEL) complex, constituted by TMCO1, belonging to the Oxa1 family of protein insertases[33], and C20orf24, (ii) the protein associated with translocon (PAT) complex, constituted by Asterix and CCDC47, and (iii) the back of Sec61 (BOS) complex, constituted by Nicalin, TMEM147 and NOMO. These complexes form a membrane-exposed lipid-filled cavity behind the Sec61 translocon, at the opposite site of the later gate, where TMDs can be inserted sequentially in a controlled environment. In this multipass translocon, newly synthesised proteins can be inserted through the later gate of Sec61 or via TMCO1 (as seen for GET1 and EMC3). It appears that the route used depends on the length of the loops: TMDs followed by long loops are inserted through the later gate of Sec61, while TMDs followed by short loops through TMCO1[49].

All in all, the translocon is a dynamic complex whose assembly is driven by the wide variety of clients to provide optimal conditions for membrane insertion.

1.1.3 Membrane protein folding and assembly

Following insertion into the membrane, multipass membrane proteins need to correctly fold their TMD bundles. TMD bundles are stabilised by hydrophobic interactions but also by interactions between hydrophilic amino acids from adjacent TMDs, especially in channel-forming proteins.

In comparison to the well-studied folding mechanisms for soluble proteins[50,51], folding mechanisms for membrane proteins are still poorly characterised. As described above, TMDs of multipass membrane proteins are inserted sequentially via the multipass translocon (see section 1.1.2). It has been recently described that the lipid-filled cavity formed by the complexes

of this specialised translocon provided a protected environment to allow proper folding[52]. In particular, the Asterix subunit of the PAT complex interacts with newly synthesised TMDs through exposed hydrophilic amino acids to help preventing degradation via quality control mechanisms (see section 1.2) until the next interacting TMD is synthesised and inserted. Moreover, the EMC and Calnexin has also been reported to act as chaperones to facilitate folding of membrane proteins[53–55].

The last step in membrane protein biogenesis is assembly into protein complexes. The easiest model would be that subunits freely diffuse in the membrane until they encounter the partners to form protein complexes. However, in a crowded cellular environment, as for isolated TMDs, also membrane proteins isolated from their complex partners are prone to aggregation and subjected to degradation via quality control mechanisms[56] (see section 1.2), rendering this mechanism not really efficient. Therefore, there might exist assembly factors that helps shield the subunits until interaction with the partner subunits is achieved. Such factors are still ill-defined. For soluble protein complexes, eukaryotic cells use mechanisms of co-co assembly[57], where two nascent chains of complex subunits are assembled together during translation, and co-post assembly[58], where one nascent chain of a subunit is assembled with an already translated subunit, to overcome aggregation and degradation issues of orphan subunit in a crowded environment. It would be interesting to understand if such mechanisms exist also for membrane protein complexes.

1.2 Protein homeostasis

Due to the essential cellular functions performed by membrane proteins, their complex biogenesis (see section 1.1) requires tight regulation of every step to prevent failures. Membrane proteins are intrinsically susceptible to misfolding[59]. Folding is an error prone process. Consequently, approximately 15% of newly synthesised proteins need to be degraded by the ubiquitin-proteasome system (UPS)[60]. When cells fail to clear misfolded proteins, the accumulation of such faulty proteins is linked to several diseases, such as diabetes, cancer and neurodegenerative disorders[59,61]. Therefore, cells have in place several quality control mechanisms for every step of the biogenesis pathway which are essential to maintain protein homeostasis[60].

The first layer of quality control occurs at the ribosome if translation is stalled. Ribosome-associated quality control (RQC) is used to clear partially translated proteins via ubiquitin-mediated proteasomal degradation, recycling of ribosomes and degradation of mRNAs and it can occur at the cytosol and at the ER membrane[62–64]. The second layer concerns the targeting step. Cytosolic factor, such as BAG6, interacts with E3 ubiquitin ligases to degrade membrane proteins that are mislocalised to the cytosol[65,66].

1.2.1 Quality control at the ER

Besides being mislocalised to the cytosol, proteins directed to the ER can be mistargeted to other organelles (e.g. mitochondria). In this case, an AAA-ATPase (Msp1/ATAD1) is used to extract the mislocalised protein[67,68]. An analogous factor (P5A-ATPase) is found in the ER membrane to drive extraction of mitochondrial protein that are mistargeted to the ER[69]. The last step of quality control occurs when proteins are inserted into the ER. Proteins in the ER are modified by removal of signal peptides by the SPC, addition of oligosaccharides by the OST complex and disulphide bonds formation to reach their mature form and proper conformation. Quality control at this level is achieved by a network of several factors[50,70,71]: soluble chaperones of the Hsp70 and Hsp90 families (e.g. BiP and GRP94[72]), co-chaperones (e.g. ERdj3), carbohydrate-binding chaperones (e.g. Calnexin and Calreticulin[73]), folding catalysts (e.g. protein disulphide isomerases (PDIs)) and membrane chaperones (e.g. Calnexin[55], EMC[53,54] and PAT complex[52]). In case of failure or saturation of the quality control mechanisms, faulty proteins accumulate in the ER lumen and membrane. The ER-associated degradation (ERAD) pathway is responsible for clearance of erroneous proteins from the ER environment[74]. However, excessive accumulation of damaged proteins can trigger the unfolded protein response (UPR) as a mechanism to cope with ER stress conditions and restore homeostasis[75,76].

1.2.2 The UPR

The UPR is a signalling transduction pathway and is activated in response to stress conditions in the ER. These can derive from imbalances in protein folding capacity or even from imbalance in ER membrane lipid composition[77,78]. In general, UPR activation leads to ER expansion,

upregulation of quality control and folding factors, upregulation of lipid synthesis enzymes and reduction of protein flux into the ER[75]. In metazoan, there are three distinct branches of the UPR that acts in parallel[75,79].

The first branch is mediated by the inositol-requiring enzyme 1 (IRE1) and it is the most conserved and studied branch[80]. When inactive, IRE1 is bound to BiP and monomeric[81]. Upon ER stress and accumulation of misfolded proteins, BiP detaches from IRE1 to engage with misfolded proteins. Furthermore, misfolded proteins also bind directly to IRE1[82]. Both events lead to oligomerisation of IRE1 which self-phosphorylates and mediates alternative splicing of X-box binding protein 1 (XBP1) mRNA, producing XBP1(s), an UPR-specific transcription factor[83,84]. This transcription factor then upregulates the transcription of chaperones, lipid synthesis enzymes and ERAD components[85].

The second branch is mediated by the transmembrane transcription factor ATF6, which it is transported to the Golgi upon accumulation of misfolded proteins in the ER. In the Golgi, site-1 and site-2 proteases (S1P and S2P) remove the membrane anchor, thereby allowing the cytosolic domain to enter the nucleus and to upregulate transcription of folding factors, such as BiP, GRP94 and PDIs[86,87].

The third branch is mediated by the double-stranded RNA-activated protein kinase (PKR)-like ER kinase (PERK), a transmembrane kinase which oligomerises upon ER stress and self-phosphorylates and phosphorylates the translation initiation factor eIF2α, thereby inhibiting translation and reducing ER protein load[81,88,89]. eIF2α phosphorylation also leads to upregulation of the transcription factor ATF4, which in turn upregulates expression of transcription factor C/EBP homologous protein (CHOP) and growth arrest and DNA damage-inducible 34 (GADD34)[90]. These two factors control PERK signalling in a feed-back loop and leads to apoptosis and cell death if ER stress is not resolved.

1.2.3 The ERAD pathway

ERAD is a process that consists of several parallel branches employed by the ER to degrade misfolded protein or to control their abundance[74,91,92]. Based on the location of the folding problem, ERAD is divided in ERAD-L if it is in the ER lumen, ERAD-M if it is in the ER membrane and ERAD-C if it is in the cytosol. In general, ERAD functions through membrane-bound E3

ubiquitin ligases forming complexes with cofactors to facilitate substrates recognition, ubiquitination and retrotranslocation[93]. Since the UPS is located in the cytosol, substrate needs to be translocated out of the ER to be ubiquitinated and subsequently degraded. The driving force for retrotranslocation is provided by the AAA+ ATPase p97/VCP[94].

The molecular details and specificity of the E3 ubiquitin ligases are well understood in yeast, where the Hrd1 complex is handling ERAD-L and ERAD-M substrates, while the Doa10 complex is mainly handling ERAD-C substrates[92]. Moreover, yeast also uses the Asi complex in the inner nuclear membrane to degrade mislocalised membrane proteins and orphan complex subunits[95,96]. In mammalian cells, the network of ERAD factors is more complex and employs several different E3 ubiquitin ligases to promote adaptation to different conditions and accommodate a wide variety of substrates[93]. Some E3 ubiquitin ligases have specialised functions, such as RNF26, in complex with TMEM33-43, ENDOD1 and TMED1, in regulation of immune signalling[97] or RNF185, in complex with TMUB1/2 and Membralin, in degradation of a specific subset of integral membrane proteins[98]. Other E3 ubiquitin ligases have a more general function, such as Hrd1 and gp78[74,92], or are still poorly characterised. In yeast, Hrd1 assembles with the derlin Dfm1 to degrade ERAD-M substrates and with Hrd3, Usa1, Yos9 and the derlin Der1 to degrade ERAD-L substrates[99]. In mammalian cells, the Hrd1 complex is constituted by (i) Herp and FAM8A1, which drives complex assembly and oligomerisation[100,101], (ii) SEL1L, OS9 and XTP3B, which mediate substrates recognition[102], (iii) Ube2j1 and Ube2g2, which are E2 ubiquitin-conjugating enzymes required for substrates ubiquitination and (iv) Derlin1/2/3.

Proteins of the derlin family are central components of the ERAD pathway due to their interaction with E3 ubiquitin ligases and their function has been linked to the retrotranslocation process[103,104]. For example, yeast Dfm1 is reported to be the central component of the retrotranslocation machinery for ERAD-M substrates[105]. Additionally, yeast Der1 in complex with Hrd1 and Hrd3 and mammalian Derlin1 in a tetrameric state have been reported to form protein conducting channels for retrotranslocation of ERAD-L substrates[106,107]. However, also Hrd1 alone has been reported to form a retrotranslocation channel[108,109]. These studies have extended the view on retrotranslocation by also showing that local membrane thinning by ERAD factors contributes to efficient membrane protein extraction[106,110]. This highlights that extraction of membrane proteins poses a challenge due to their stable integration into the lipid bilayer[111].

One way to reduce the energy barrier and thereby facilitating membrane extraction would be proteolysis of the membrane domain. Indeed, the intramembrane protease signal peptide peptidase (SPP), initially identified to cleave signal peptides after their removal by the SPC[112], and the rhomboid protease RHBDL4 have been described to function in specific ERAD branches[113–118]. Finding other ER-resident proteases involved in the ERAD pathway would provide further understanding on the molecular mechanisms of the ERAD machinery.

1.3 Signal sequences and signal peptidases

As described above (see section 1.1), proteins are often targeted to the ER via N-terminal signal sequences recognized by the SRP pathway. Signal sequences are then removed immediately after import completion by the action of enzymes named Signal Peptidases (SPases). The targeting process via signal sequences is conserved from bacteria to humans[119]. Signal sequences do not share sequence homology but possess three conserved domains[11,120]: (i) a positively charged, unstructured, domain at the N-terminus, called n-region, which regulates membrane topology by driving nascent chain orientation in the Sec61 translocon[121] (ii) a strictly hydrophobic α-helical domain, generally shorter than TMDs, called h-region, and (iii) an extended non-helical β-structure polar region at the C-terminus, typically around 4-7 amino acids, containing the cleavage site and the two crucial positions relative to the scissile peptide bond (-1 and -3) occupied by small neutral amino acids. SPases are membrane-embedded enzymes and belong to the family of serine proteases. As signal sequences, SPase's function is also evolutionarily conserved[119].

1.3.1 Prokaryotic signal peptidases

Different types of SPases, based on the substrates specificity, are found in prokaryotic cells: (i) type I SPases cleave N-terminal signal sequences from outer membrane and periplasmic proteins in gram-negative and proteins exported outside the cells in gram-positive bacteria[122], (ii) type II SPases cleave lipoproteins precursors [123] and (iii) type IV SPases cleave prepilins and prepilin-like proteins[124]. Type I SPases are the most studied and the first type I SPase was purified from *Escherichia coli* [125]. Type I SPases contain two N-terminal TMDs that anchor the

enzyme to the membrane and a C-terminal periplasmic domain. This domain contains the substrates binding region with the catalytic site, formed by a serine-lysine catalytic dyad, and a hydrophobic region, which drives interaction with the membrane and most likely permits the catalytic activity of the enzyme at the membrane surface[119,126]. Type I SPases are rather unusual serine proteases because they are not inhibited by standard serine protease inhibitors but by β-lactams and lipopeptides[127]. In line with their essential function, type I SPases have been reported to be required for cell viability[119]. Therefore, type I SPases are investigated as antibacterial targets[127].

1.3.2 The eukaryotic signal peptidase

In eukaryotic cells, the SPase localised to the ER and cleaves off signal sequences form ER targeted and secretory proteins[128]. Unlike the prokaryotic monomeric SPases, the eukaryotic counterpart is a multi-subunit complex generally formed by five membrane proteins, as identified from the first purified signal peptidase complex (SPC) from dog pancreas microsomes[129].

In mammalian cells, the different subunits are named SPC12, SPC18, SPC21, SPC22/23 and SPC25 based on their apparent molecular weight and encoded by the SPCS1, SEC11A, SEC11C, SPCS3 and SPCS2 genes, respectively. SPCS1 and SPCS2 possess two TMDs, N- and C- terminal domains protruding in the cytosol and a really short loop in the lumen[130]. SEC11A, SEC11C and SPCS3 possess one TMD with a type II orientation and big luminal domains. Of note, yeast SPC contains only four subunits: Sec11, SPC1, SPC2 and SPC3[131]. SEC11A and SEC11C are the catalytic subunits and harbour the catalytic site constituted by the catalytic triad serine-histidine-aspartate, in contrast to the catalytic dyad of bacterial type I SPases. However, also the eukaryotic SPC is not inhibited by the common serine proteases. They are highly homologous between each other and share high homology with yeast Sec11[119]. Sec11, as type I SPases, is essential for cell viability[132]. SPCS1, SPCS2 and SPCS3 are accessory subunits that do not possess catalytic activity and whose functions are only partially characterised. SPCS3 is glycosylated and the yeast homologue is essential for the SPC activity and cell growth[133,134], most likely because it helps maintaining the structure of the catalytic domain. SPCS2 and SPCS1 yeast homologues are not essential for activity of the complex and

for cell viability[135,136]. Nevertheless, SPCS2 is reported to interact with the Sec61 translocon, both in yeast and mammals[137,138]. SPCS1 is the least characterised subunit. It is reported to be essential for embryonic development in *Drosophila*[139], even though the mechanism is still uncharacterised, and to restrain SPC activity based on the length of the n-region and {Bibliography}hydrophobicity of the h-region of signal sequences in yeast[140].

1.3.3 The human signal peptidase complex

In dog, rat, mouse and human the SPC presents the two catalytic subunits SEC11A and SEC11C[119]. The fact that all the other eukaryotic species possess only one catalytic subunit raises intriguing questions on the necessity of having the SEC11 gene duplicated, the functions of the two catalytic subunits and if they both coexist in the same complex.

Last year, the cryo-electron microscopy (cryo-EM) structure of the human SPC was published[40]. This is the first structure of any SPC ever reported and provides important insights into the subunits arrangement. First, SEC11A and SEC11C are not in the same complex but form two paralogous complexes, each including the three accessory subunits SPCS1, SPCS2 and SPCS3. The subunits form a "window frame"-like structure, causing membrane thinning in the complex's core. This is suggested to function as "molecular ruler" to specifically accommodate signal sequences and not TMDs, which possess a longer hydrophobic sequence that do not match the length of the thinned lipid bilayer, providing another determinant for SPC specificity toward signal sequences. Second, SEC11A and SPCS3 forms the catalytic core and SPCS1 and SPCS2 were not recovered in stoichiometric amount with SEC11A and SPCS3. This highlights once more the relevance of addressing the functions of SPCS1 and SPCS2.

Recent studies reported that the human SPC can be hijacked by some viruses (e.g. flaviviruses such as West Nile, dengue, Zika, and Japanese encephalitis viruses, Pestiviruses, Influenza C virus and Hepatitis C virus) to promote cleavage and maturation of their polyproteins[141–145], which differs structurally from signal sequences. In this process, an essential role is played by the SPCS1 subunit[141,143]. Moreover, by screening for compound to block flavivirus replication, the first SPC inhibitor was identified, a natural product of fungal origin called cavinafungin[146].

These recent discoveries might suggest that SPC function is not limited to signal sequences removal and that accessory subunits might be required for unknown functions in substrates recognition.

1.4 Aim of the thesis

In the 1970s, Blobel and colleagues formulated the signal hypothesis, one of the pillars of molecular and cell biology, where they postulated that proteins contain signals in their amino acid sequences to target them to membranes. Later in the 1970s and in the 1980s, these signal sequences were identified to be at the N-terminus of ER-targeted and secretory proteins and to be cleaved off immediately after translocation. In 1986, the ER-resident protease for this cleavage was identified: a five subunits complex called the signal peptidase complex (SPC). Since then, the SPC has been relegated to this only function. Recently, however, a few studies reported SPC cleavage of a few substrates, especially viral polyproteins, not possessing signal sequences. The aim of this thesis is, therefore, to identify new SPC substrates besides signal sequences and to characterise possible new functions of this essential protease.

2. Results

2.1 Identification and validation of noncanonical substrates

Since its discovery in the 1970s, the SPC has been known to solely have the function of cleaving off signal sequences from ER targeted and secretory proteins; however, recent studies suggested this might not be the only function of this complex. With the aim of possibly expanding the substrates spectrum of this enzyme, I performed a computational analysis of the whole human proteome by using the existing software SignalP[147], in collaboration with Dr. Gurdeep Singh (Russell Lab, BioQuant, Heidelberg). SignalP is a neural network-based method that predicts the presence of N-terminal signal sequences and SPC cleavage sites, based on the properties of protein sequences. It gives three different scores as output (Fig. 1A): the s-score displays the probability of each amino acid in the sequence to be part of a signal sequence, the c-score displays the probability of each amino acid to be the first one at the N-terminus in the mature protein following the cleavage by the SPC and, the y-score which is a combination of the previous two scores and displays the predicted cleavage site. Moreover, SignalP consists of (i) a network trained to distinguish if a hydrophobic stretch is part of a signal sequence or if it is a proper TMD (SignalP_TM), and (ii) of an additional network which is not trained to do so (SignalP_noTM) and, therefore, recognizes also TMDs as signal sequences. In order to identify putative SPC cleavage sites not linked to the presence of a signal sequence, I ran the whole proteome in both SignalP networks and compared the y-scores obtained. By plotting both outputs against each other and by setting thresholds for cleavage prediction (see Methods section 4.2.4 for details), I obtained a scatterplot divided in quadrants (Fig. 1B) with: (i) the upper-right quadrant containing proteins predicted to be cleaved in both networks and already annotated as carrying a signal sequence, (ii) the bottom-left quadrant containing proteins not predicted to be cleaved in any of the two networks and (iii) the bottom-right quadrant containing the proteins of interest of this study, which are predicted to be cleaved in the SignalP_noTM network but not in the SignalP_TM one. The latter proteins contain predicted SPC cleavage sites without actually carrying a signal sequence. I will refer to such sites as cryptic cleavage sites. By filtering for membrane proteins located along the secretory pathway with a type II-oriented N-terminal TMD, this approach identified 262 proteins containing a cryptic

cleavage site following the first N-terminal TMD. These proteins were further ranked based on mutations linked to human diseases reported in three different databases: Uniprot[148], ClinVar[149] and COSMIC[150] (Fig. 1C).
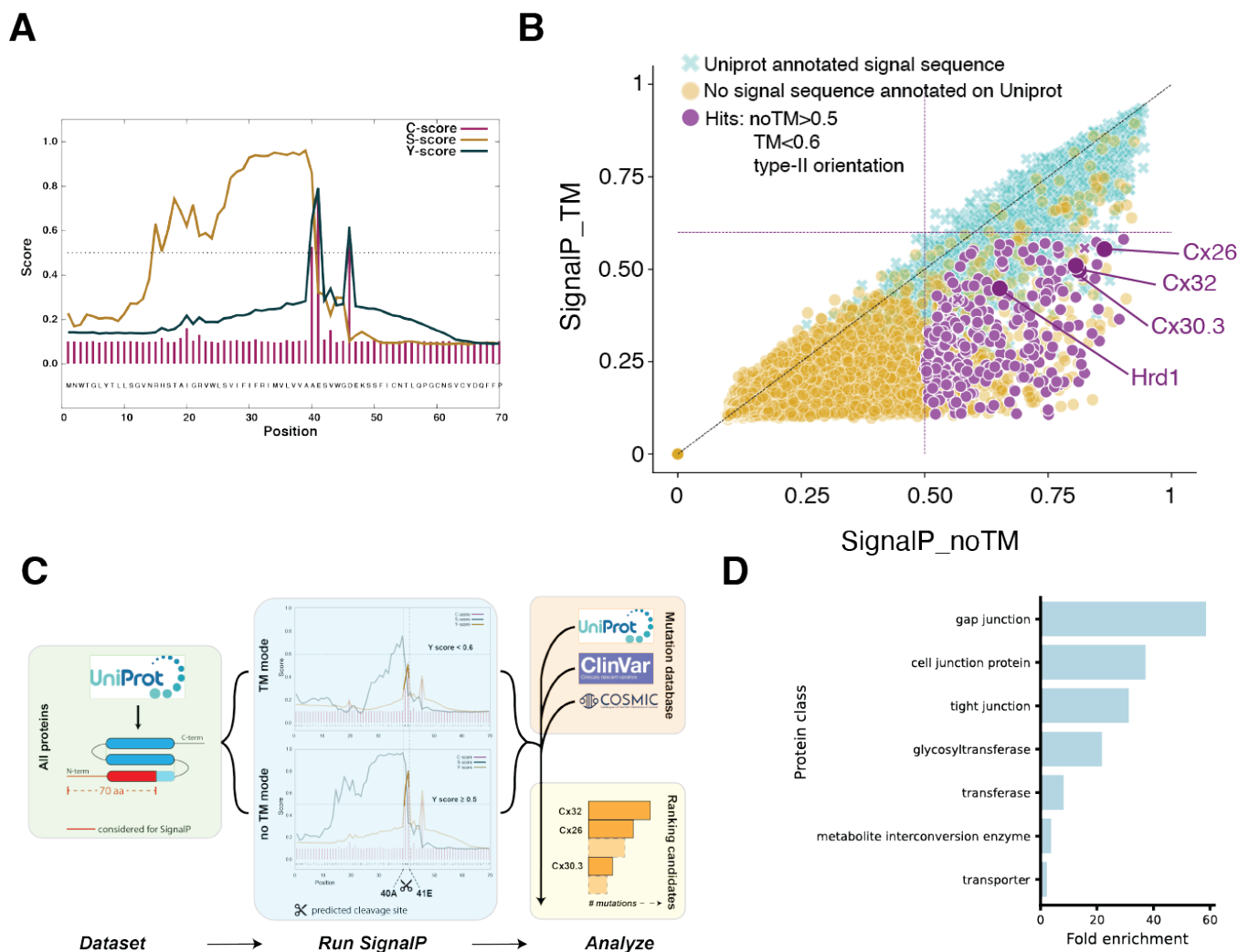
Figure 1. Computational approach to identify noncanonical SPC substrates. A. Example of graphical output of SignalP4.1 (noTM network) showing the 3 different scores for Cx32. **B.** Analysis of cryptic SPC cleavage sites in the human proteome. Scatter plot of Y scores (combined cleavage site scores) obtained by SignalP4.1 analysis of the first 70 amino acids of all human proteins, exploiting the two different neural networks available (noTM and TM, see methods for details). Cyan crosses represent proteins with an annotated signal peptide according to UniProt. Yellow circles represent proteins with no annotated signal peptide. Light purple circles represent hits that pass the applied filtering steps and are thus candidates for cryptic SPC cleavage sites. Dark purple circles represent hits further analysed in this study. Dotted purple lines correspond to the thresholds. **C.** Schematic of the workflow for the computational analysis. **D.** Fold enrichment analysis of protein classes in the list of protein containing N-terminal putative SPC cryptic cleavage sites, performed by using Gene Ontology Resource[151–153].

In addition, I also performed an enrichment analysis of protein classes represented in the hit list (Fig. 1D). This analysis revealed that, among the proteins containing putative cryptic cleavage sites, there is a strong enrichment for proteins involved in cell-to-cell junctions and, in particular, of proteins belonging to the gap junction class. These proteins are represented by the Connexin (Cx) protein family. Connexins are tetra-spanning proteins which assemble into hexameric structures called connexons. These oligomers reach the plasma membrane where they dock onto other connexons from adjacent cells to form gap junctions allowing direct communication of two cells and direct transfer of small molecules and ions[154,155]. Proteins of the Connexin family were also on top of the hit list (Fig. 1C) due to the high abundance of naturally occurring mutations linked to human diseases [156]. Based on these observations and since previous studies already indicated aberrant signal peptidase-like processing[157–159], I decided to focus the validation of candidates on this protein family, using mainly Connexin32 (Cx32) as a candidate substrate. Of note, Cx32 has more than 200 naturally occurring mutations linked to neurodegenerative diseases and neuropathies, in particular to the X-linked dominant Charcot-Marie-Tooth disease[160–162]. The group of Prof. Dr. Matthias Feige (TUM, Munich) examined several naturally occurring variants introducing polar residues in the four different TMDs[1] and I predominantly focused on the cysteine201→arginine (C201R) variant[163]. When ectopically expressed in human embryonic kidney (HEK) 293T cells, a cell line which does not physiologically produce connexin proteins, all analysed Cx32 mutants interestingly gave rise to two distinct species on SDS-PAGE gels[1], in contrast to the wt Cx32 protein, which appeared as one single band (Fig. 2A). This pattern might be an indication of proteolytic processing, as predicted by the computational approach.

By introducing a FLAG-tag either at the C-terminus or at the N-terminus of the Cx32 variants and by mutating the cleavage site into inert amino acids (e.g. proline, alanine and leucine)[1], the group of Prof. Dr. Matthias Feige showed that the processing is indeed happening at the N-terminus and at the predicted cleavage site. Notably, they also observed the same double band pattern for Cx32 mutants in the Schwannoma cell line sNF96.2, which strongly resembles Schwann cells which endogenously express Cx32[1].

To unequivocally prove that the processing of Cx32 mutants is mediated by the SPC, I treated HEK293T cells expressing FLAG-tagged Cx32[C201R] with cavinafungin, a natural product recently identified to selectively inhibit the SPC by blocking the catalytic subunit SEC11 as

primary target[146]. Indeed, inhibiting SPC activity resulted in a complete loss of the Cx32 cleavage fragment (Fig. 2B), ultimately confirming that SPC can cleave transmembrane proteins which do not contain a signal sequence.
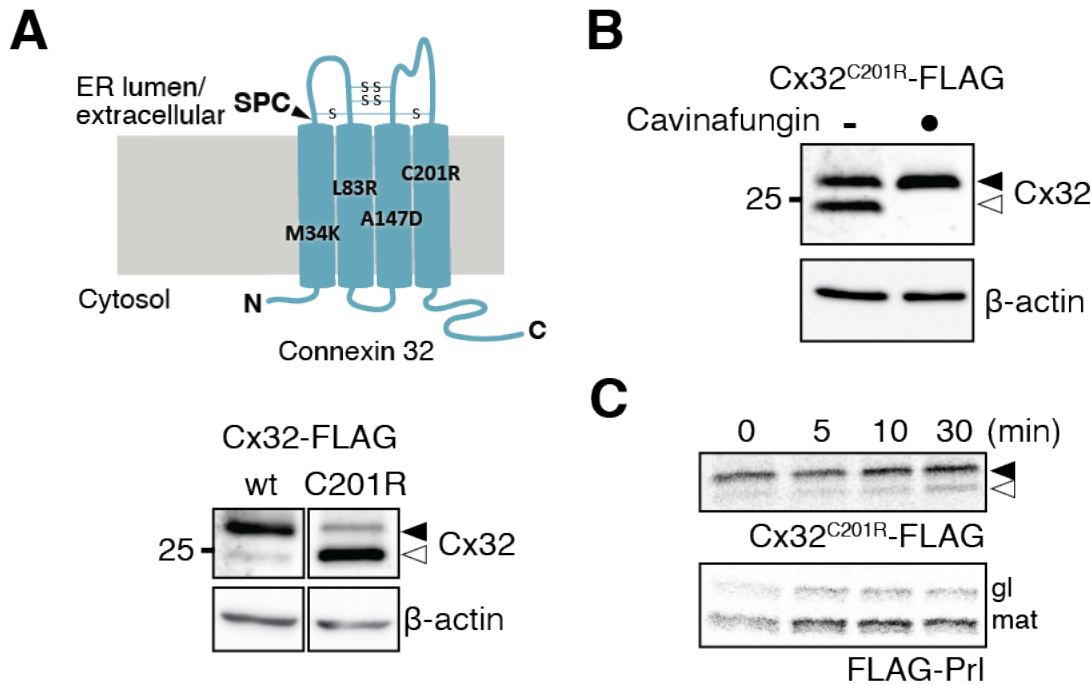
Figure 2. The SPC post-translocationally cleaves membrane proteins. A. Top, schematic of Cx32 highlighting mutations in the transmembrane domains and the predicted SPC cleavage site. Bottom, immunoblot analysis of FLAG-tagged Cx32 (wt and C201R) ectopically expressed in HEK293T. Full and empty arrowhead represents full-length and processed Cx32. Actin was used as loading control. **B.** Immunoblot analysis of FLAG-tagged Cx32[C201R] ectopically expressed in HEK293T treated with the SPC inhibitor cavinafungin (1 μM), where indicated. Full and empty arrowhead represents full-length and processed Cx32. Actin was used as loading control. **C.** Autoradiograph of immunoprecipitated FLAG-tagged Cx32[C201R] and the canonical SPC substrate prolactin (FLAG-Prl) labelled with ^{35}S-cys/met mix for 2 min and chase for the indicated times. Full and empty arrowhead represents full-length and processed Cx32. Glycosylated prolactin (gl) and mature prolactin (mat) are indicated.
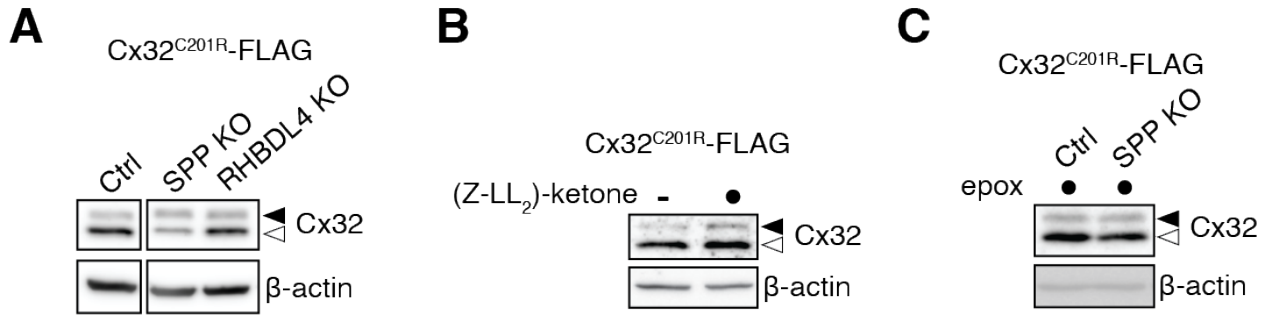
Figure 3. Other ER resident proteases do not affect Cx32 cleavage. A. Immunoblot analysis of FLAG-tagged Cx32^{C201R} ectopically expressed in HEK293T wt (Ctrl), SPP KO or RHBDL4 KO cells. Full and empty arrowhead represents full-length and processed Cx32. Actin was used as loading control. **B.** Immunoblot analysis of FLAG-tagged Cx32^{C201R} ectopically expressed in HEK293T treated with the SPP inhibitor (Z-LL$_2$)-ketone (50 μM), where indicated. Full and empty arrowhead represents full-length and processed Cx32. Actin was used as loading control. **C.** Immunoblot analysis of FLAG-tagged Cx32^{C201R} ectopically expressed in HEK293T wt (Ctrl) or SPP KO cells treated with the proteasome inhibitor epoxomicin (2 μM), where indicated. Full and empty arrowhead represents full-length and processed Cx32. Actin was used as loading control.

Canonically, the SPC cleaves off signal sequences from translated nascent chains during the translocation process[128]. In complete opposition to this, Cx32^{C201R} cleavage occurs at a later stage (Fig. 2C), when the translocation process is over and the protein is already inserted in the membrane. I could prove this by means of radioactive pulse-chase analysis, where Cx32^{C201R} processing initiates slowly, approximately 30 minutes after synthesis. This is in contrast to what I observed with Prolactin, a canonical SPC substrate containing a signal sequence, where the unprocessed form is not detected, even immediately after synthesis (Fig. 2C).

For completeness, I verified that the other two major ER-resident proteases, signal peptide peptidase (SPP)[112,164] and rhomboid protease RHBDL4[117,165,166], are not involved in this process. To this end, I ectopically expressed FLAG-tagged Cx32^{C201R} in HEK93T ctrl, SPP KO[167] and RHBDL4 KO[117] cells (Fig. 3A). The lack of RHBDL4 does not affect Cx32^{C201R} processing while, interestingly, the lack of SPP seems to partially prevent it (Fig. 3A). Treating cells with (Z-LL)$_2$-ketone, a known SPP inhibitor[112], has no impact on Cx32^{C201R} cleavage (Fig. 3B) and treating SPP KO cells with epoxomicin, to inhibit proteasomal degradation, completely

stabilises the cleavage fragment (Fig. 3C), suggesting that SPP catalytic activity is not required for this process. Nevertheless, it seems that the presence of SPP itself helps to stabilize the SPC-derived fragment. To clarify this aspect, further investigation would be required.

Having demonstrated that the SPC can also cleave after proper TMDs located at the N-terminus of a protein, I wondered if this could also happen after internal TMDs. With the help of Dr. Gurdeep Singh, I performed the same computational analysis described above, this time including peptides starting from each and every TMD of the whole membrane proteome (Fig. 4A). Remarkably, this approach identified approximately 1300 membrane proteins containing putative SPC cryptic cleavage sites after internal TMDs (Fig. 4B), with proteins predicted to have even more than one cleavage site. Among these, I verified SPC cleavage for the rhomboid pseudoprotease iRhom2, a protein with seven TMDs whose cleavage site is predicted after the first TMD at position 432 (Fig. 4C). iRhom2 is known to control trafficking and activation of the plasma membrane sheddase ADAM17 (A Disintegrin And Metalloprotease domain-containing protein 17)[168] – also called TACE (tumor necrosis factor-α converting enzyme) – together with FRMD8 (a FERM domain containing protein)[169]. Despite being a 97 kDa protein, ectopically expressed FLAG-tagged iRhom2 presents one additional band at 55 kDa, known from the literature to represent the N-terminal domain, including the first TMD[169]. However, until now, the origin of this fragment was unknown. Treating cells with the SPC inhibitor cavinafungin leads to a complete loss of the 55 kDa band (Fig. 4C), confirming the prediction of the computational analysis. Of note, in contrast to Cx32, iRhom2 is cleaved in the wt state, not carrying any mutation. In support of the SPC-derived cleavage, very recently, the group of Matthew Freeman (Sir William Dunn school of Pathology, Oxford) also identified the SPC as the responsible protease for the generation of the 55 kDa iRhom2 fragment[170].

Concomitantly, the group of Prof. Dr. Matthias Feige validated internal cleavage by the SPC in another candidate protein, PMP22 (peripheral myelin protein 22)[1]. PMP22, as Cx32, is also linked to the neuropathy Charcot-Marie-Tooth disease[171,172] and is cleaved when carrying a mutation in the second TMD[1]. They could show that PMP22 cleavage occurs after the third TMD, as predicted by the computational approach, and that the fragment is stabilized by inhibition of the proteasome and of the AAA-ATPase p97[1], suggesting a possible involvement of the ERAD pathway.
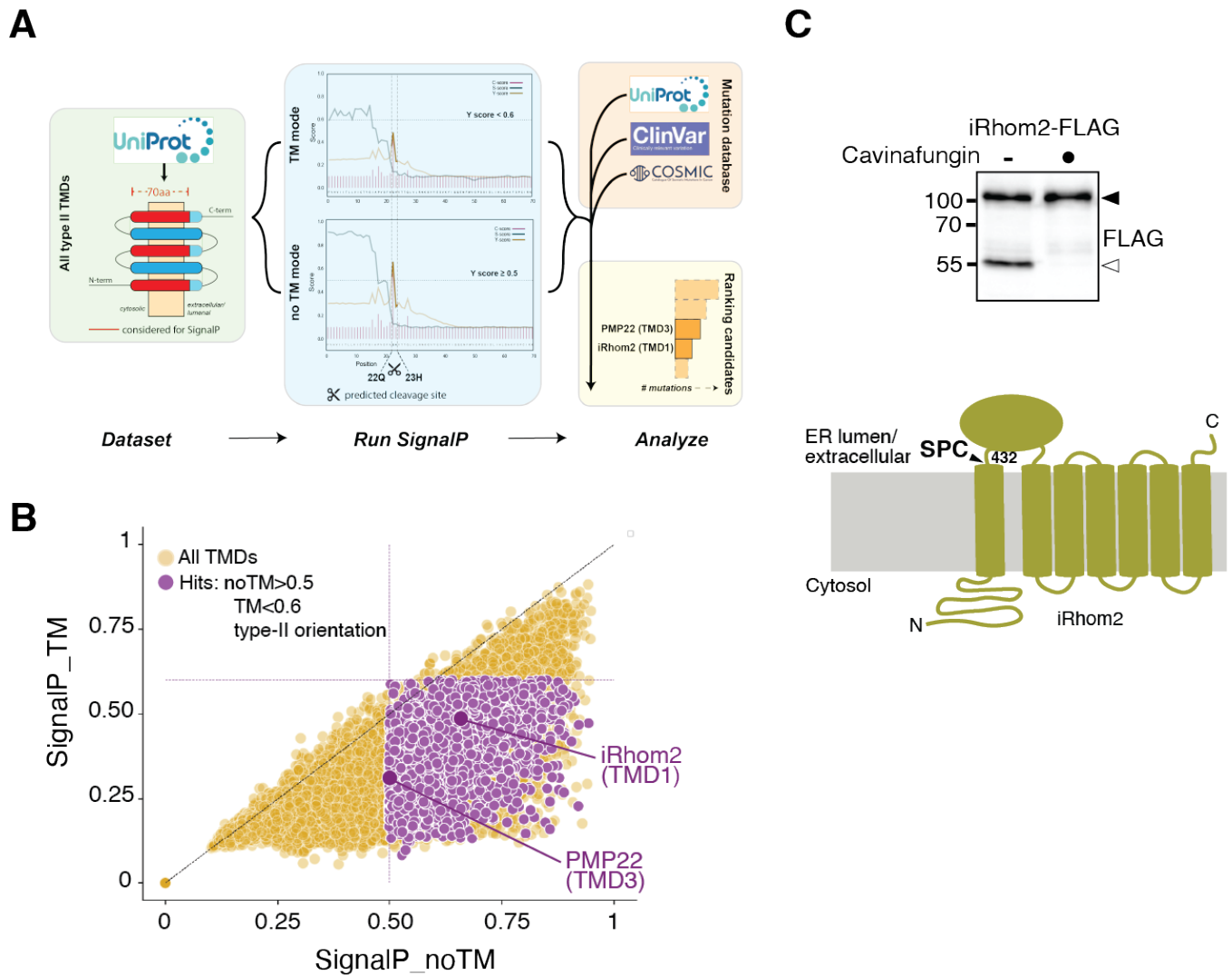
Figure 4. The SPC can cleave also after internal TMDs. A. Schematic of the workflow for the computational analysis. **B.** Analysis of cryptic SPC cleavage sites in the human membrane proteome. Scatter plot of Y scores (combined cleavage site scores) obtained by SignalP4.1 analysis of the first 70 amino acids of all human proteins, exploiting the two different neural networks available (noTM and TM, see methods for details). Yellow circles represent all TMDS. Light purple circles represent hits that pass the applied filtering steps and are thus candidates for cryptic SPC cleavage sites. Dark purple circles represent hits further analysed in this study. Dotted purple lines correspond to the thresholds. **C.** Top, immunoblot analysis of FLAG-tagged iRhom2 ectopically expressed in HEK293T treated with the SPC inhibitor cavinafungin (1 μM), where indicated. Full and empty arrowhead represents full-length and processed iRhom2. Bottom, schematic of iRhom2 highlighting the predicted SPC cleavage site.
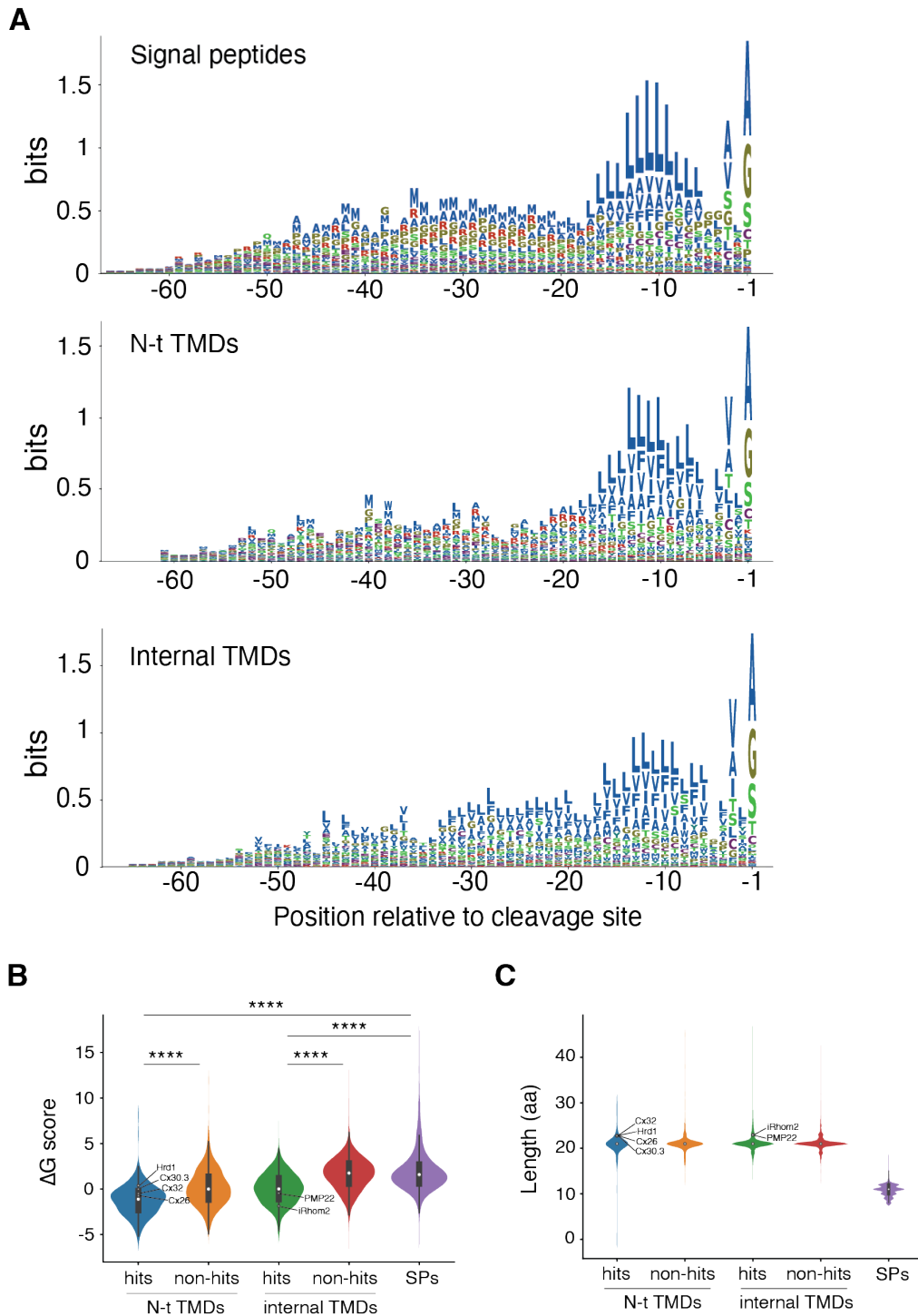
Figure 5. Noncanonical SPC substrates have different properties compared to canonical signal peptides.
A. Sequence analysis of canonical (signal peptides) and noncanonical (N-terminal TMD and internal TMD) SPC substrates using Logomaker[173]. **B.** Violin plot comparing the ΔG score for membrane insertion of canonical (signal peptides) and noncanonical (N-terminal TMD and internal TMD, hits and non-hits) SPC substrates, highlighting the hits validated in this study. **** P<0.0001; Wilcoxon Rank Sum Test. **C.** Violin plot comparing the length of the

hydrophobic core of canonical (signal peptides) and noncanonical (N-terminal TMD and internal TMD, hits and non-hits) SPC substrates, highlighting the hits validated in this study.

Furthermore, to rule out that this noncanonical cleavage is simply due to the fact that the cryptic cleavage sites follow TMDs which show more signal peptide-like features, I performed computational analyses comparing different physicochemical properties of signal peptides and TMDs of the newly identified noncanonical substrates, in collaboration with Dr. Gurdeep Singh (Fig. 5). Despite the similarity in the amino acids profiles in the sequence logo (Fig. 5A), TMDs of noncanonical substrates display significantly lower free energy (ΔG score) for membrane integration in comparison to signal peptides as well as to TMDs not containing a cryptic cleavage site (Fig. 5B). Moreover, classical signal peptides' h-regions are, on average, significantly shorter than TMDs of noncanonical substrates and TMDs of membrane proteins not containing a cryptic cleavage site (Fig. 5C). Together, these analyses confirm that the newly described noncanonical SPC cleavage does not occur after TMDs with signal peptide-like features but after proper TMDs.

All in all, so far, I have provided clear evidences that the SPC can unexpectedly cleave multipass membrane proteins at cryptic cleavage sites following proper TMDs, therefore, substantially expanding its substrate spectrum, which was previously restricted to signal peptides and viral polyproteins.

2.2 The accessory subunit SPCS1 is essential for noncanonical cleavage

The findings outlined above raise the question on how cleavage of multipass membrane proteins by the SPC is regulated, since TMDs have different physicochemical properties compared to signal peptides and do not fulfil the general requirements for SPC canonical cleavage[11,40,174]. As already described in the introduction, recent work by the group of Dr. Michael Diamond (Saint Louis, Missouri, USA) showed that the SPC is important for cleavage and maturation of flaviviral polyproteins, with a key role played by the accessory subunit SPCS1[141]. This suggests that the SPCS1 subunit may have a function in the processing of substrates not linked to signal peptides. Hence, I sought to understand if SPCS1 has a role in cleavage of multipass membrane proteins. By using HEK293T SPCS1 KO cells[141], I ectopically

expressed FLAG-tagged Cx32[C201R] in these cells and in wt HEK293T cells as control (Ctrl). Remarkably, the lack of SPCS1 leads to a significant reduction of Cx32 cleavage, which is almost completely re-established upon exogenous expression of SPCS1 (Fig. 6A). Notably, I could observe dependency on SPCS1 also for cleavage of other multipass membrane proteins containing cryptic cleavage sites, namely Cx26 and Cx30.3 (Fig. 6B), iRhom2 (Fig. 6C) and PMP22 (Fig. 6D). This supports the idea that SPCS1 plays a key role in SPC noncanonical cleavage. Another question is if also removing the other SPC subunits displays the same effect on Cx32 cleavage. The group of Prof. Dr. Matthias Feige analysed Cx32[C201R] cleavage in knockdown conditions for SPCS1, SPCS2, SPCS3 and SEC11A, reporting that knockdown of all subunits but SEC11A – the catalytic one – affects cleavage to different extents[1]. This indicates that there might be a more intricate interaction between the subunits, which cannot be simply explained by a general destabilization of the complex when one of the subunits is not present.

To further validate the role of SPCS1 and to better understand the kinetics of the process, I performed radioactive pulse-chase analyses in HEK293T wt (Ctrl) and SPCS1 KO cells. Indeed, in the absence of SPCS1, after a slight initial increment, Cx32 cleavage is substantially blocked (Fig. 6E). In contrast, the lack of SPCS1 does not affect processing of canonical signal peptides as shown for Calnexin, PDIA6, TCRα and ERdj3[1]. In addition, I could show that Prolactin secretion, which requires signal peptide removal, is increased by approximately 4-fold (Fig. 6F). These data strongly support the important and specific role of SPCS1 in cleavage of membrane proteins by the SPC and its dispensability for canonical signal peptide removal.

Next, I wanted to understand how the SPCS1 subunit acts in this process. SPCS1 is a fairly small protein (12 kDa) with two TMDs; it does not have a catalytic site or any amino acid exposed to the luminal side[40] where the catalytic site of the catalytic subunit SEC11A is located. Hence, SPCS1 is unlikely to directly influence the catalytic activity of the complex in any manner. I, therefore, hypothesized that SPCS1 might work as a recognition factor to recruit TMDs into the complex. A first hint towards the corroboration of this hypothesis came from co-immunoprecipitation analyses. By pulling down ectopically expressed FLAG-tagged iRhom2, I could co-precipitate SPCS1 (Fig. 7A). As control, SPCS1 did not co-precipitate with the iRhom2 binding partner TACE (Fig. 7A). This experiment clearly shows a physical interaction between SPCS1 and a noncanonical SPC substrate.
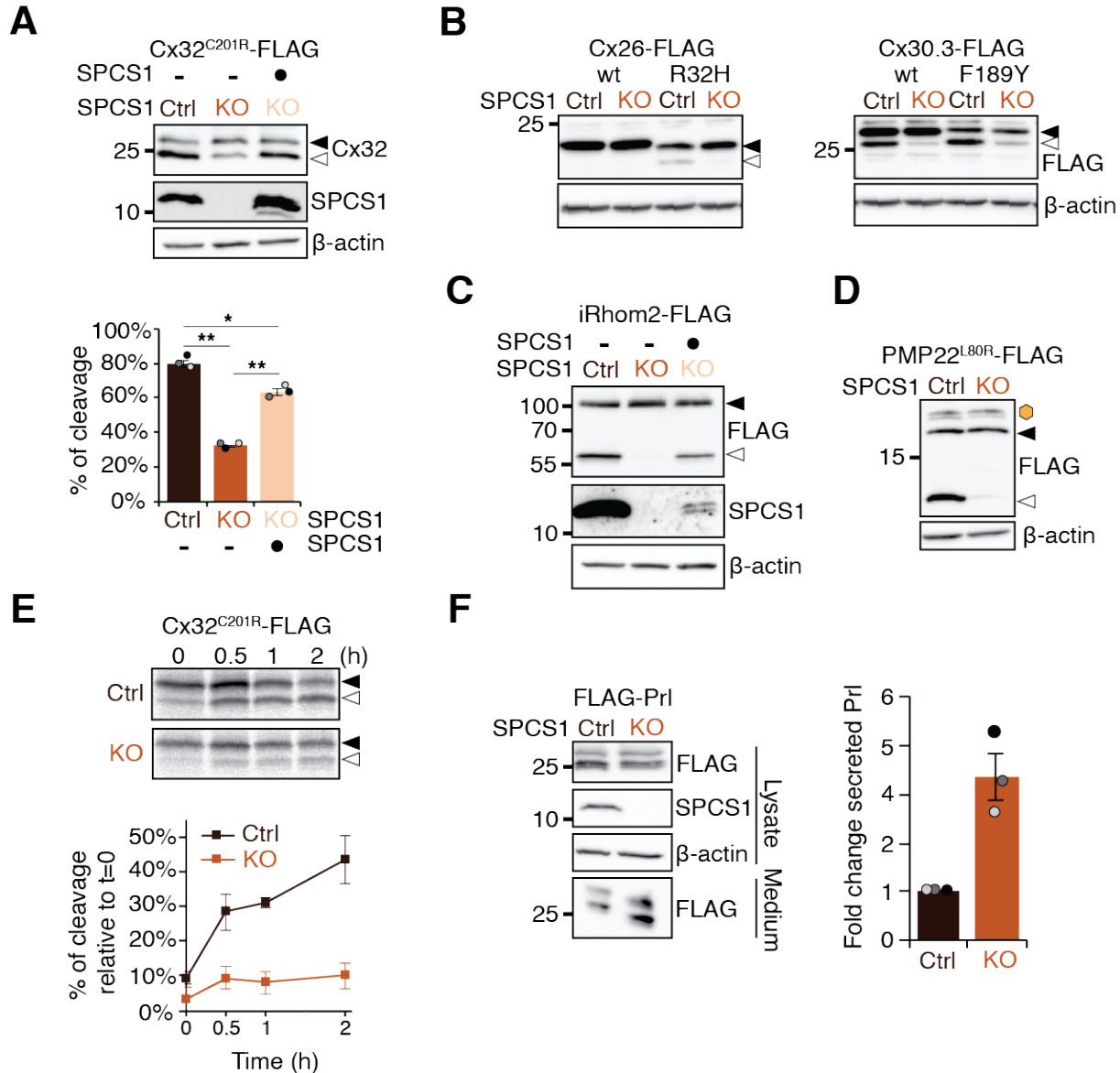
Figure 6. The accessory subunit SPCS1 is key for noncanonical cleavage but does not affect canonical signal peptide processing. A. Top**,** immunoblot analysis of FLAG-tagged Cx32[C201R] ectopically expressed in HEK293T wt (Ctrl), SPCS1 KO and SPCS1 KO cells with exogenous expression of SPCS1. Full and empty arrowhead represents full-length and processed Cx32. Actin was used as loading control. Bottom, quantification of percentage of Cx32[C201R] cleavage (n=3; mean± s.e.m.; * P<0.05; ** P<0.01; paired t test). **B.** Immunoblot analysis of FLAG-tagged Cx26 and Cx30.3 variants ectopically expressed in HEK293T wt (Ctrl) or SPCS1 KO cells. Full and empty arrowhead represents full-length and processed Cx26 or Cx30.3. Actin was used as loading control. **C.** Immunoblot analysis of FLAG-tagged iRhom2 ectopically expressed in HEK293T wt (Ctrl), SPCS1 KO cells or and SPCS1 KO cells with exogenous expression of SPCS1. Full and empty arrowhead represents full-length and processed iRhom2. Actin was used as loading control. **D.** Immunoblot analysis of FLAG-tagged PMP22[L80R] ectopically expressed in HEK293T wt (Ctrl) or SPCS1 KO cells. Full and empty arrowhead represents

full-length and processed PMP22. Orange hexagon represent glycosylated PMP22. Actin was used as loading control. **E.** Top, autoradiograph of immunoprecipitated FLAG-tagged Cx32^{C201R} labelled with ^{35}S-cys/met mix for 5 min and chased for the indicated times. Full and empty arrowhead represents full-length and processed Cx32. Bottom, quantification of percentage of Cx32^{C201R} cleavage relative to t=0 (n=3; mean± s.e.m.). **F.** Left, immunoblot analysis of FLAG-tagged Prolactin ectopically expressed in HEK293T wt (Ctrl) or SPCS1 KO cells. Extracellular medium was analysed to assess secretion. Actin was used as loading control. Right, Quantification of secreted Prolactin (n=3; mean± s.e.m.).

Next, I identified which SPCS1 residues are important for its function in the recognition of noncanonical SPC substrates. Notably, the amino acid sequence and structure of SPCS1 suggest that its interaction with membrane proteins can most likely only happen at the TMD regions. For this reason, I focused my attention on the SPCS1 TMD2 and took into consideration predominantly conserved bulky and hydrophobic amino acids protruding into the membrane bilayer (Fig. 7B), being good candidates for the interaction with hydrophobic TMDs. Consequently, I generated several different SPCS1 constructs harbouring the following mutations: W47A, M53A, F58A, L61-62A, P65G, W67A, Y70A, W67A-Y70A and R71-72A. The idea was to ectopically express these constructs together with FLAG-tagged iRhom2 in SPCS1 KO cells and assess their effect on iRhom2 processing. Strikingly, ectopic expression of the SPCS1$^{W67A-Y70A}$ mutant did not rescue iRhom2 cleavage, in contrast to wt SPCS1 (Fig. 7C-D). However, I had the concern that this effect might simply be due to the fact that the SPCS1$^{W67A-Y70A}$ mutant is not able to assemble in complex with the other SPC subunits. By co-expressing HA-tagged SEC11A and the different SPCS1 mutants and by pulling down on the HA tag, I could prove that SPCS1$^{W67A-Y70A}$, and all the other mutants, can co-precipitate with the catalytic subunit SEC11A (Fig. 7E), thereby confirming physical interaction and erasing the abovementioned concern. Of note, SPCS1$^{L61-62A}$ expression led to a slight but significant overrescue of iRhom2 cleavage compared to SPCS1^{wt} expression (Fig. 7C-D).

Together, these findings suggest that the SPCS1 subunit functions as a docking site for recognition of noncanonical SPC substrates, namely multipass membrane proteins containing cryptic SPC cleavage sites, and that the patch in the TMD2 formed by the residues L61, L62, W67 and Y70 is important for this function (Fig. 7F).

2.3 Membrane protein misfolding and failed complex assembly promote SPC-mediated cleavage

The data presented so far shows that the SPC can also cleave multiple membrane proteins at cryptic sites, with an essential role played by the accessory subunit SPCS1. Notably, this occurs not only following the first TMD, but also after downstream TMDs. Distinct clients and various mutations all giving rise to cleavage products suggest that a common denominator underlies this type of cleavage by the SPC.

All the mutations giving rise to SPC-mediated cleavage introduced charged residues in TMDs that are embedded in the hydrophobic environment of the lipid bilayer. Thus, I hypothesized that these mutations may cause folding problems to the proteins, leading to the exposure of otherwise buried, cryptic, cleavage sites which become subsequently susceptible to processing by the SPC. Hence, I started investigating if this new SPC function could be linked to quality control of membrane proteins.

Initial data supporting this hypothesis was produced by the group of Prof. Dr. Matthias Feige by means of microscopy and western blot analysis. All Cx32 mutants validated for SPC cleavage displayed ER localization and were unable to form gap junctions[1], suggesting that these mutants were retained in the ER due to their incorrect folding. To control that the SPC-mediated cleavage is not simply caused by prolonged exposure to the SPC in the ER after retention, Cx32[wt] was artificially retained in the ER by adding an ER-retention signal at the C-terminus. This Cx32 variant localized to the ER and did not show any processing[1], confirming that prolonged exposure to the SPC is not sufficient. Furthermore, if misfolding is the trigger for SPC-mediated cleavage and is, indeed, caused by the mutations, compensating those with a stabilizing, opposing, mutation should prevent Cx32 cleavage. Indeed, compensating the C201R mutation with F29D, V84E or R142D mutations, all forming salt bridges as computationally evaluated by molecular dynamics simulations, led to a reduction of Cx32 cleavage[1].

Of note, only those mutations disrupting structural features (e.g. introducing charges in the TMDs or disrupting cysteines involved in disulphide bridge formation), but those in the N- or C-terminal part of the protein or in the loops, induced SPC-mediated cleavage of Cx32[1].
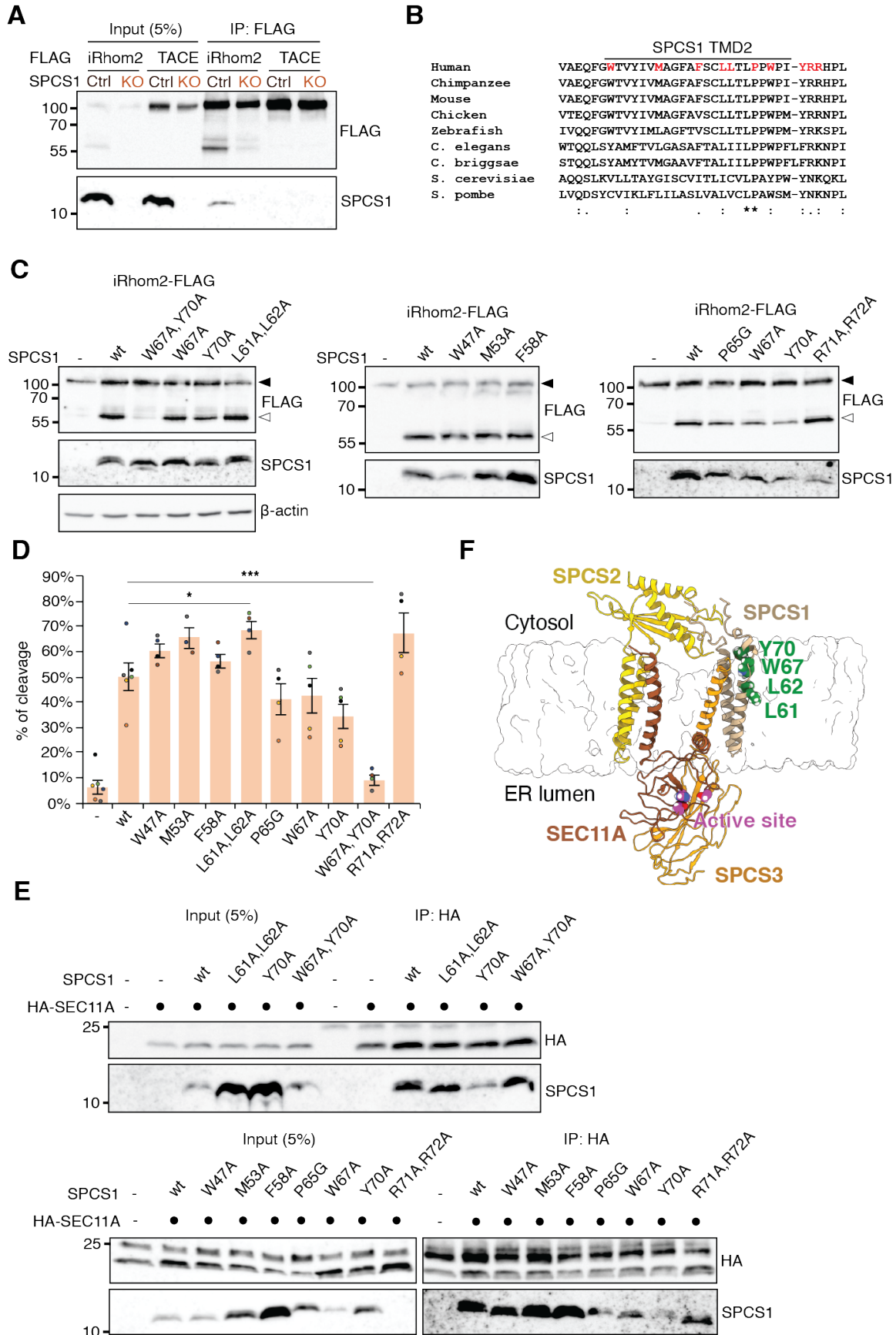
Figure 7. The SPCS1 subunit functions as a recruitment factor for noncanonical substrates. A. Co-immunoprecipitation analysis of ectopically expressed FLAG-tagged iRhom2 and TACE and endogenous SPCS1 in HEK293T wt (Ctrl) or SPCS1 KO cells. **B.** Multiple sequence alignment of TMD2 and flanking region of SPCS1 from the indicated species using Clustal Omega[175]. Residue analysed by mutagenesis are highlighted in red. **C.** Immunoblot analysis of different SPCS1 variants ectopically expressed in SPCS1 KO cells together with FLAG-tagged iRhom2. Full and empty arrowhead represents full-length and processed iRhom2. Actin was used as loading control. **D.** Quantification of percentage of iRhom2 cleavage (n=3-6, coloured dots represent different replicates; mean $\pm$ s.e.m.; * P<0.05; *** P<0.001; unpaired t test). **E.** Co-immunoprecipitation analysis of ectopically expressed HA-tagged SEC11A and different SPCS1 variants in SPCS1 KO cells. **F.** Model of the SPC highlighting SPCS1 residues affecting iRhom2 cleavage (green) and the active catalytic site (purple) on the SEC11A subunit. Adapted from Zanotti et al. 2022[1].

To conclusively corroborate the idea that misfolding is, indeed, the trigger for SPC-mediated cleavage, I induced acute misfolding by disrupting disulphide bonds in Cx32^{C201R} by means of the reducing agent DTT and analysed the kinetics of its SPC-mediated cleavage via radioactive pulse-chase analyses. When DTT was added during the pulse at time point 0 (t=0), Cx32^{C201R} cleavage was accelerated compared to the untreated condition (Fig.8A-B). Surprisingly, when DTT was instead added with a 30 minutes delay during the chase, Cx32^{C201R} cleavage was abruptly accelerated, even more than upon DTT addition at t=0 (Fig. 8A-B). This latter observation suggests that the SPC-mediated cleavage is more effective at later stages of biosynthesis when the translocation process is already completed (see Fig. 1), the newly synthesized protein has left the translocon environment and its folding factors have dissociated, rendering the misfolded protein with the exposed cleavage site accessible to the SPC (Fig. 8C). Of note, treating cells with the ER stressor Tunicamycin does not accelerate cleavage of Cx32^{C201R} [1], indicating that the effect observed upon DTT is due specifically to disruption of structural disulphide bridges and not to a general effect of ER stress induction. Together, the findings presented here support the idea that SPC cleavage plays a role in post-translocational quality control of membrane proteins.
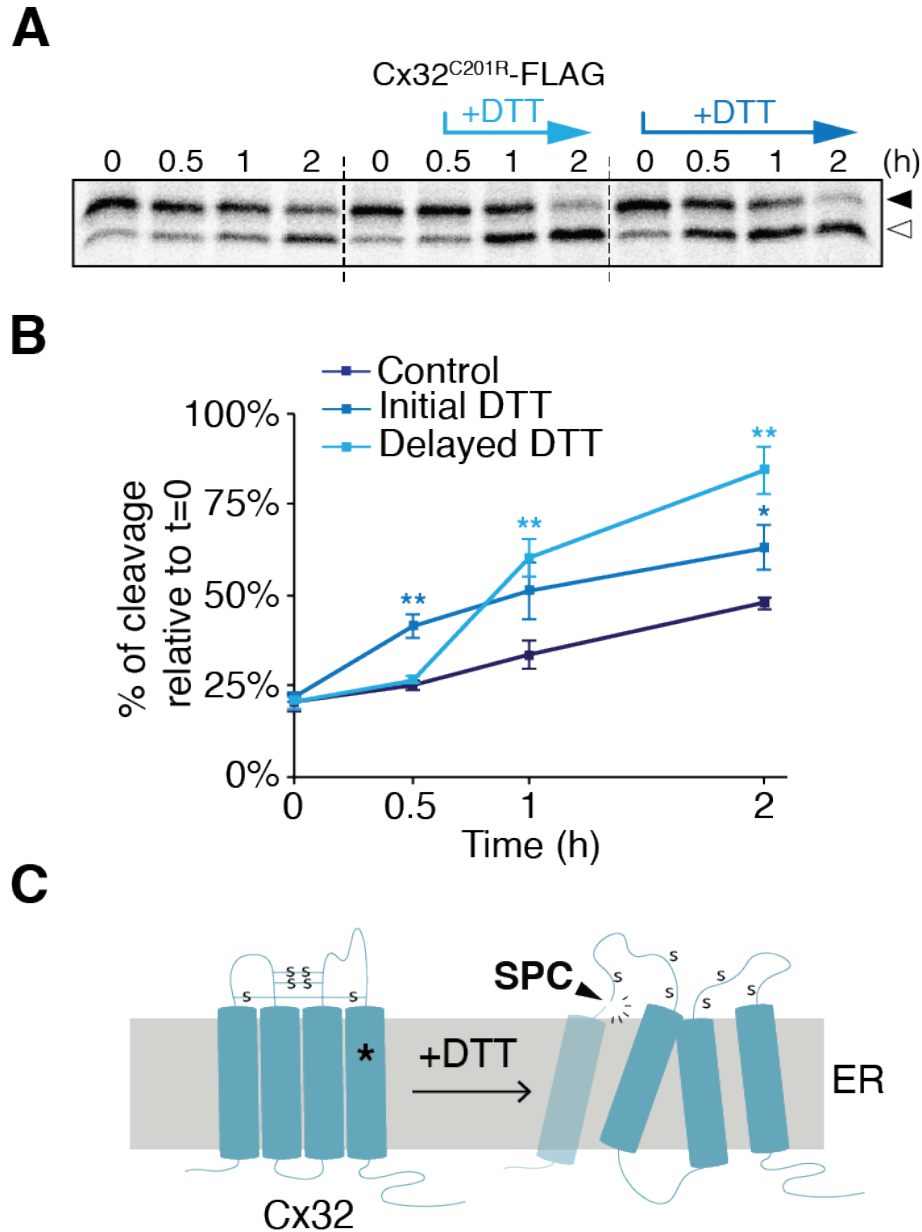
Figure 8. Misfolding promotes SPC-mediated cleavage. A. Autoradiograph of immunoprecipitated FLAG-tagged Cx32^{C201R} labelled with ^{35}S-cys/met mix for 5 min and chased for the indicated times. Full and empty arrowhead represents full-length and processed Cx32. DTT was added at the indicated time points (blue arrows). **B.** Quantification of percentage of Cx32^{C201R} cleavage relative to t=0 (n=3; mean± s.e.m.; * P<0.05; ** P<0.01; unpaired t test). **C.** Schematic representation of misdolding causing exposure of cryptic SPC cleavage sites and subsequent cleavage by the SPC.
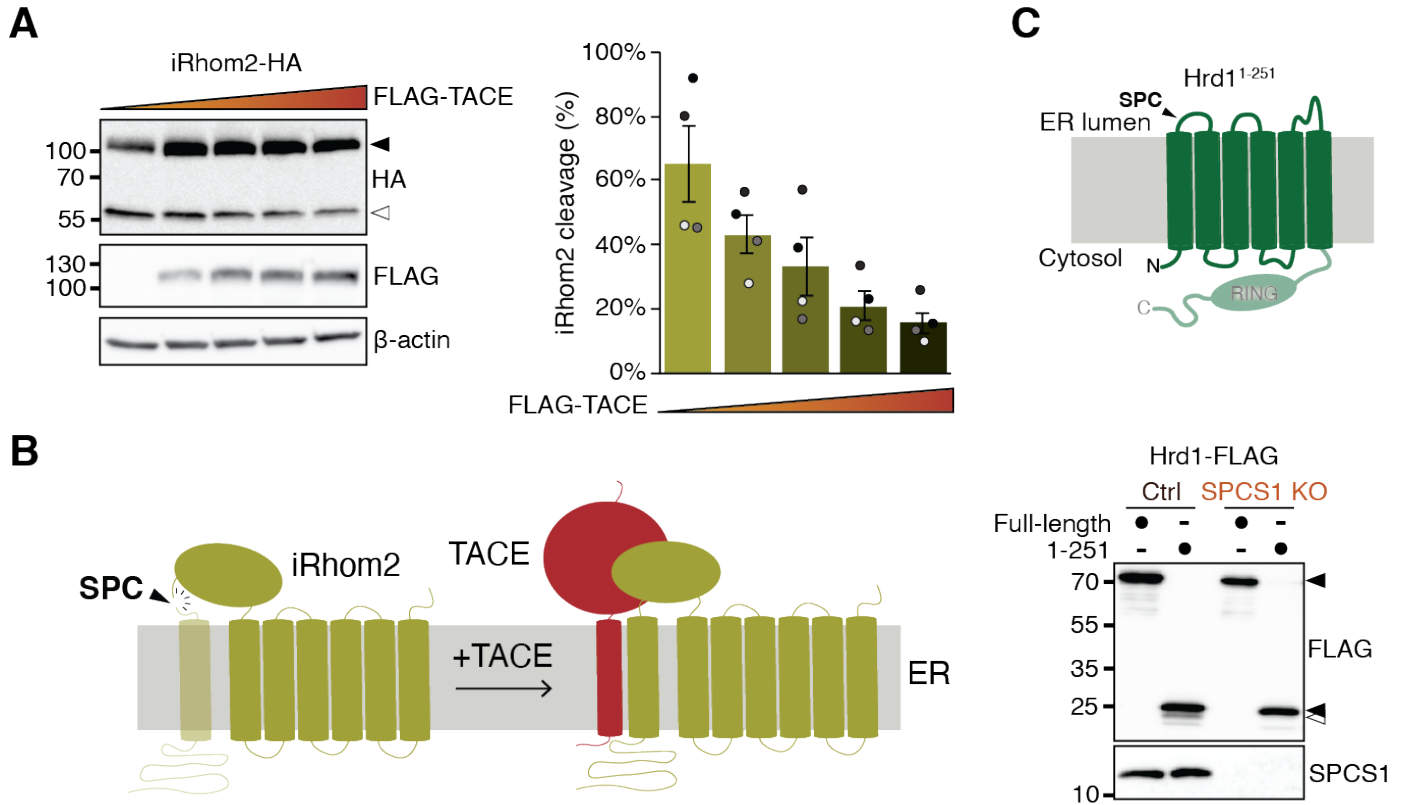
Figure 9. Failed complex assembly promotes SPC-mediated cleavage. A. Left, immunoblot analysis of HA-tagged iRhom2 expressed in HEK 293T cells together with increasing amount of its interaction partner FLAG-tagged TACE. Full and empty arrowhead represents full-length and processed iRhom2. Actin was used as loading control. Right, quantification of percentage of iRhom2 cleavage (n=4, grey scale dots represent different replicates; mean ± s.e.m.). **B.** Schematic representation of how complex formation may protect the SPC cleavage site. **C.** Top, schematic representation of Hrd1[1-251] mutant lacking the C-terminal cytosol portion contain the RING domain. Bottom, immunoblot analysis of two different FLAG-tagged Hrd1 constructs expressed in HEK 293T cells. Full and empty arrowhead represents full-length and processed Hrd1.

Importantly, misfolding can be the reason why Cx32 mutants are cleaved by the SPC, but it cannot explain why iRhom2 is cleaved in its wild-type form (see Fig. 4C and 6C). As already stated, iRhom2 is required to form a complex with its interaction partner TACE to allow its activation in the Golgi and its export towards the plasma membrane, where TACE exerts its several cellular functions, including roles in TNFα and EGFR signalling[176]. Therefore, I hypothesized that, as for proper protein folding, proper complex assembly may mask SPC cleavage sites as well. When protein complexes fail to assemble correctly, this may lead to subunits instability[56], subsequently exposing cryptic cleavage sites. Hence, I sought to assess

if this is the case for iRhom2. By ectopically expressing iRhom2 in HEK 293T cells together with increasing amount of TACE, cleavage of iRhom2 decreases proportionally with increasing amount of TACE (Fig. 9A). This indicates that the stoichiometric imbalance caused by ectopic expression of iRhom2, leading to SPC-mediated cleavage, can be compensated by the addition of its interaction partner TACE, preventing the access to iRhom2's cleavage site. To further support the hypothesis that also failed complex assembly induces SPC-mediated cleavage of membrane proteins, I analysed Hrd1, another protein which was predicted by the computational analysis to have an N-terminal cryptic cleavage site (see Fig.1B). Hrd1 is a six TMDs RING-domain ER resident E3 ubiquitin ligase[177], which assembles into different high molecular complexes with functions in the ERAD pathway[178,93,179,100]. Full-length Hrd1 ectopically expressed in HEK293T cells does not show any SPC-derived cleavage fragment (Fig. 9C). However, a hrd1 mutant lacking the C-terminal portion shows a cleavage fragment, which disappears in SPCS1 KO cells (Fig. 9C), suggesting SPC-mediated cleavage. This mutant was previously reported to be defective in assembly with core components of the Hrd1 complex[100], such as FAM8A1 and Herp. Thus, this observation, together with the data on iRhom2, confirm that also failure in protein complex assembly may lead to SPC-mediated cleavage.

Conclusively, the data presented in this section provides evidence that SPC cryptic cleavage sites can be exposed due to misfolding or absence of interaction partners, highlighting a role for this noncanonical SPC-mediated cleavage in quality control of membrane proteins.

2.4 The SPC quality control function cooperates with the ERAD pathway

In the previous sections, I outlined the identification of a noncanonical cleavage by the SPC linked to the quality control of membrane proteins. One fate that a protein can undergo when misfolded or when failing to form native complexes is clearance by degradation pathways[60], such as the ERAD pathway in the ER[91,180–182]. Since a few recent studies showed involvement of the ER resident proteases RHBDL4 and SPP in such pathway[116,115,114,166,117], I sought to investigate if this noncanonical function of the SPC synergizes with ERAD as well.
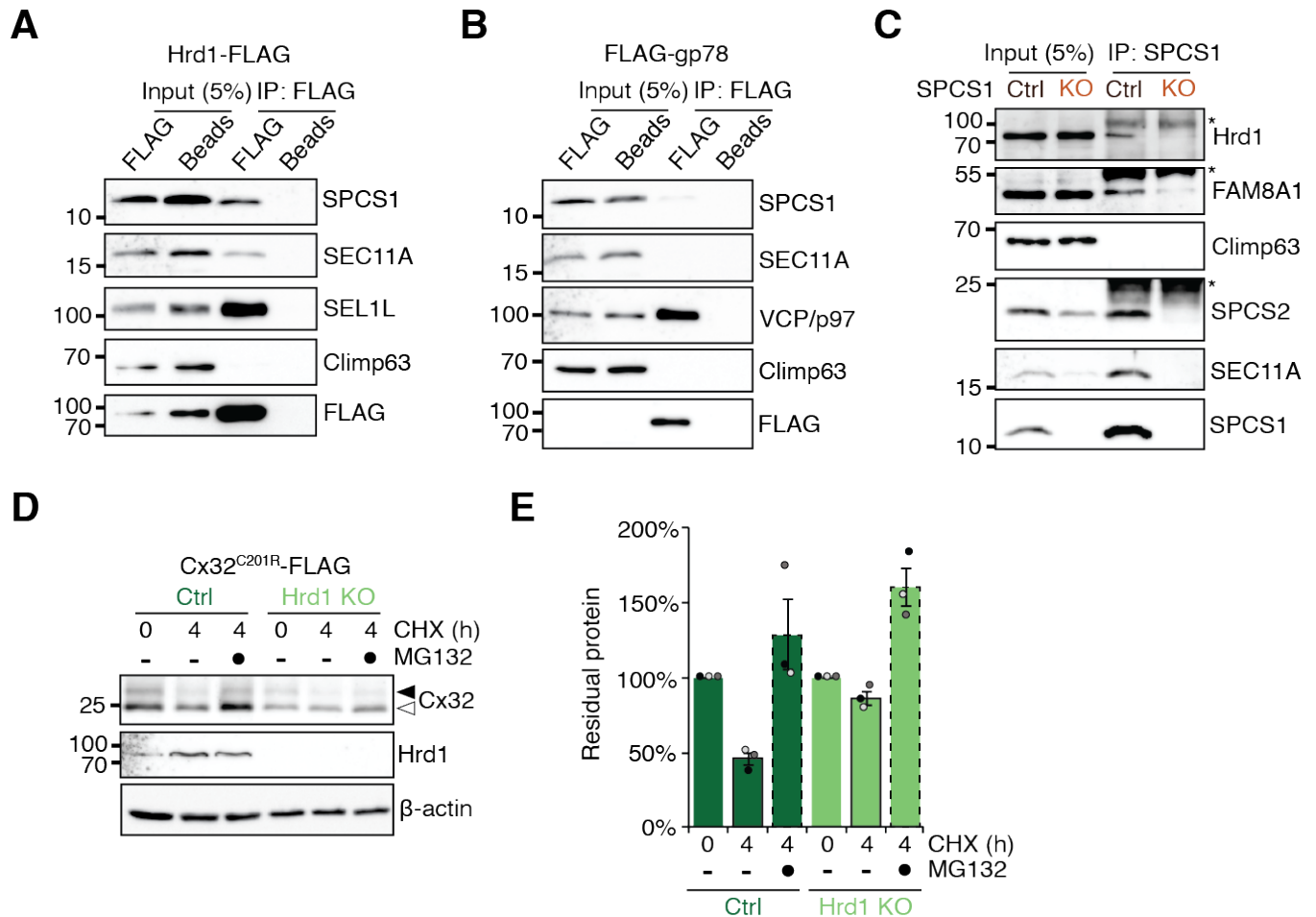
Figure 10. The SPC cooperates with Hrd1 to degrade membrane proteins. A. Co-immunoprecipitation analysis of ectopically expressed FLAG-tagged Hrd1 and endogenous SPC subunits (SPCS1 and SEC11A) in HEK293T wt. SEL1L and Climp63 were used as positive and negative control, respectively. **B.** Co-immunoprecipitation analysis of ectopically expressed FLAG-tagged gp78 and endogenous SPC subunits (SPCS1 and SEC11A) in HEK293T wt. VCP/p97 and Climp63 were used as positive and negative control, respectively. **C.** Co-immunoprecipitation analysis of the endogenous SPC subunit SPCS1 and endogenous components of the Hrd1 complex (Hrd1 and FAM8A1) in HEK293T wt. Other subunits of the SPC (SPCS2 and SEC11A) were used as positive controls and Climp63 as negative control. **D.** Immunoblot analysis of FLAG-tagged Cx32[C201R] ectopically expressed in HEK293T wt (Ctrl) or Hrd1 KO cells[117] treated with CHX and MG132 as indicated. Actin was used as loading control. **E.** Quantification of residual Cx32[C201R] relative to t=0 (n=3, grey scale dots represent different replicates; mean ± s.e.m.).

A Cx32^C201R-FLAG
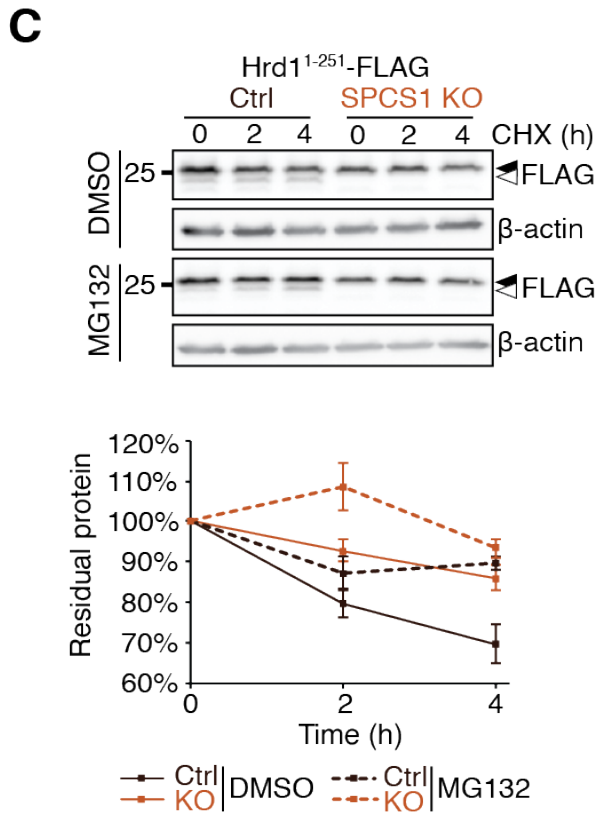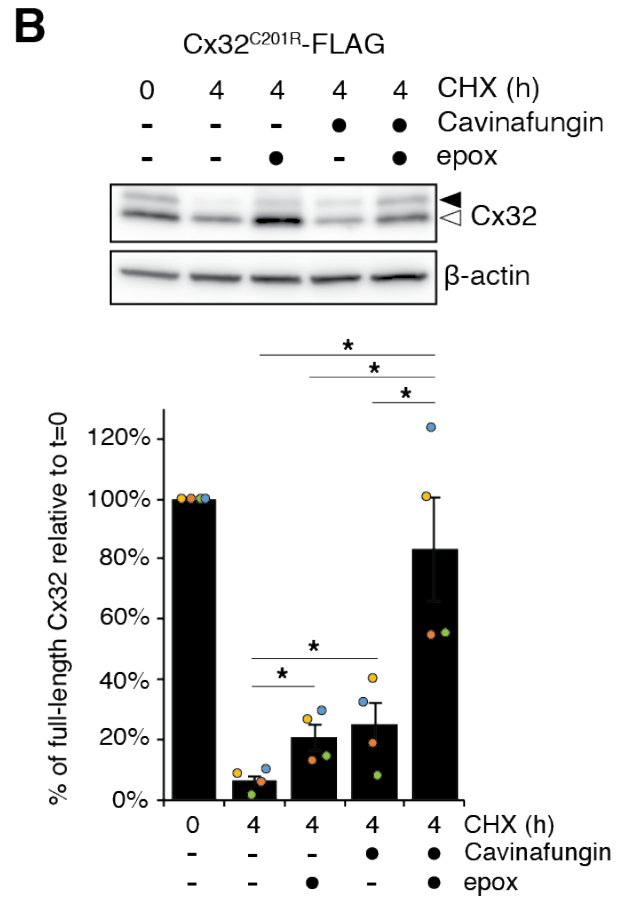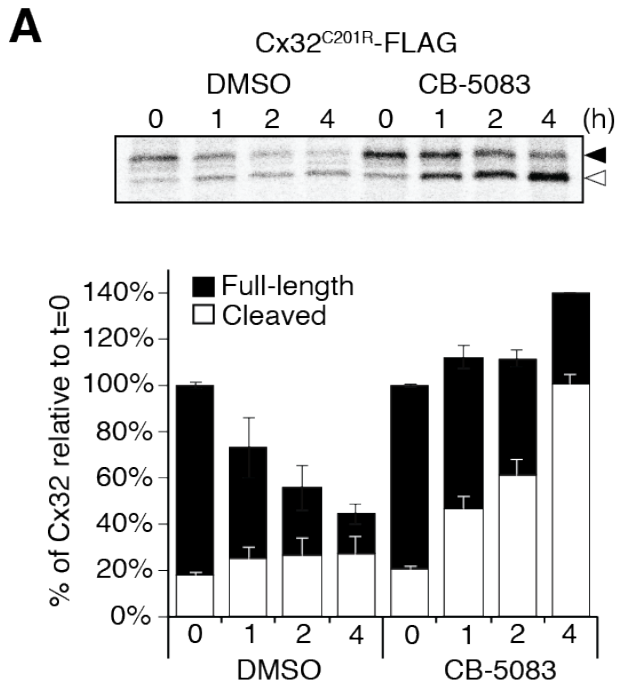
B Cx32^C201R-FLAG

C Hrd1^1-251-FLAG

Figure 11. The SPC cooperates with ERAD to cleave and degrade membrane proteins. A. Top, autoradiograph of immunoprecipitated FLAG-tagged Cx32^{C201R} labelled with ^{35}S-cys/met mix for 10 min and chased for the indicated times. The VCP/p97 inhibitor was used where indicated. Full and empty arrowhead represents full-length and processed Cx32. Bottom, quantification of Cx32^{C201R} species relative to t=0 (n=3; mean ± s.e.m.). **B.** Top, immunoblot analysis of FLAG-tagged Cx32^{C201R} ectopically expressed in HEK293T wt cells treated with CHX, epoxomicin and cavinafungin as indicated. Actin was used as loading control. Bottom, quantification of percentage of full-length Cx32^{C201R} relative to t=0 (n=4; coloured dots represents different replicates; mean ± s.e.m.; * P<0.05; paired t test). Top, immunoblot analysis of FLAG-tagged Hrd1$^{1-251}$ ectopically expressed in HEK293T wt (Ctrl) or SPCS1 KO cells treated with CHX and MG132 as indicated. Actin was used as loading control. Bottom, quantification of residual Hrd1$^{1-251}$ relative to t=0 (n=3; mean ± s.e.m.). **C.** Top, immunoblot analysis of FLAG-tagged Hrd1$^{1-251}$ ectopically expressed in HEK293T wt (Ctrl) or SPCS1 KO cells treated with CHX and MG132 as indicated. Actin was used as loading control. Bottom, quantification of residual Hrd1$^{1-251}$ relative to t=0 (n=3; mean ± s.e.m.).

Essential players in the ERAD pathway are E3 ubiquitin ligases[183,184]. A previous study analysing the interaction map of several E3 ligases reported a putative interaction of Hrd1 with components of the SPC[97]. In light of the work presented so far, this putative interaction may acquire physiological relevance. To validate this interaction, I initially ectopically expressed FLAG-tagged Hrd1 in HEK293T cells and performed co-immunoprecipitation analysis. Indeed, Hrd1 shows physical interaction with the SPC subunits SPCS1 and SEC11A (Fig. 10A). On the contrary, FLAG-tagged gp78, the other major ERAD-linked ER-resident E3 ubiquitin ligase, does not show significant interaction with the SPC subunits (Fig. 10B), suggesting that the interaction observed is specific to Hrd1 and not a general artefact of ectopic expression. To confirm this finding further, I executed co-immunoprecipitation analysis on endogenous SPC and Hrd1 complex components. By pulling down endogenous SPCS1, endogenous Hrd1 and another component of the complex (FAM8A1) co-precipitate (Fig. 10C), highlighting the interaction between the SPC and the Hrd1 complex. To start addressing the functional role of this interaction, I performed cycloheximide chase analysis of Cx32^{C201R} in Hrd1 KO cells[117]. Compared to wt cells, where the SPC-derived Cx32^{C201R} fragment is reduced by 50% in a 4-hour time frame, in Hrd1 KO cells the fragment is completely stable (Fig. 10D-E). This already hinted towards the fact that the SPC cooperates with the ERAD component Hrd1 to degrade misfolded membrane proteins. With the aim to further investigate the possible link between the

SPC and ERAD, I carried out radioactive pulse-chase analyses to address the kinetics of cleavage and degradation of Cx32^{C201R} upon inhibition of the ERAD pathways via prevention of membrane dislocation by chemical inhibition of the AAA-ATPase VCP/p97[185].

Over time, full-length Cx32^{C201R} should theoretically decrease possibly due to degradation and/or processing by the SPC, while SPC-derived Cx32^{C201R} fragment should increase due to processing of full-length Cx32^{C201R} and decrease at the same time due to degradation. In vehicle control (DMSO) treated cells, the SPC-derived Cx32^{C201R} fragment signal only slightly increases, while full-length Cx32^{C201R} signal, as well as the total protein signal, decreases overtime (Fig. 11A). In contrast, in cells treated with the VCP/p97 inhibitor (CB-5083), the total protein signal is completely stable and the full-length Cx32^{C201R} signal still decreases, while a clear accumulation of the SPC-derived Cx32^{C201R} fragment signal can be observed (Fig. 11A). The reason why Cx32^{C201R} fragment signal does not increase in DMSO samples compared to the treated ones has to be ascribed to degradation. Additionally, the fact that full-length Cx32^{C201R} signal still decreases in CB-5083 treated samples indicates that processing by the SPC is the major player for the observed decreased. This experiment suggests that processing by the SPC is a prerequisite for ERAD-mediated degradation of mutant membrane proteins.

To further validate this conclusion, I performed Cycloheximide chase analysis on Cx32^{C201R} upon blockage of SPC processing, by its inhibitor cavinfungin, and assessed the degradation of the full-length protein because the SPC-derived fragment already present at steady state is not affected by the cavinafungin treatment. After 4 hours, full-length Cx32^{C201R} is barely detected due to processing and degradation (Fig. 11B). Upon proteasome inhibition with epoxomicin, full-length Cx32^{C201R} is only partially stabilized (Fig. 11B), due to the SPC activity which is still cleaving it. Similarly, upon SPC inhibition with cavinafungin, full-length Cx32^{C201R} is, again, only partially stabilized (Fig. 11B), suggesting that there might be another pathway which plays a role in the degradation of Cx32^{C201R}. Indeed, upon treatment with both inhibitors together, full-length Cx32^{C201R} is fully stabilized (Fig. 11B), showing an additive effect indicating the involvement of another ERAD pathway, together with the SPC. Of note, Hrd1$^{1-251}$, another noncanonical SPC substrate (see Fig. 9C), shows SPCS1-dependent degradation (Fig. 11C), further highlighting the cooperation of the SPC quality control function and ERAD. Taken together, these results demonstrate that the newly uncovered quality control function of the

SPC indeed cooperates with ERAD to degrade faulty membrane proteins, rendering the SPC-mediated proteolysis an option to mark proteins for degradation via the ERAD pathway.
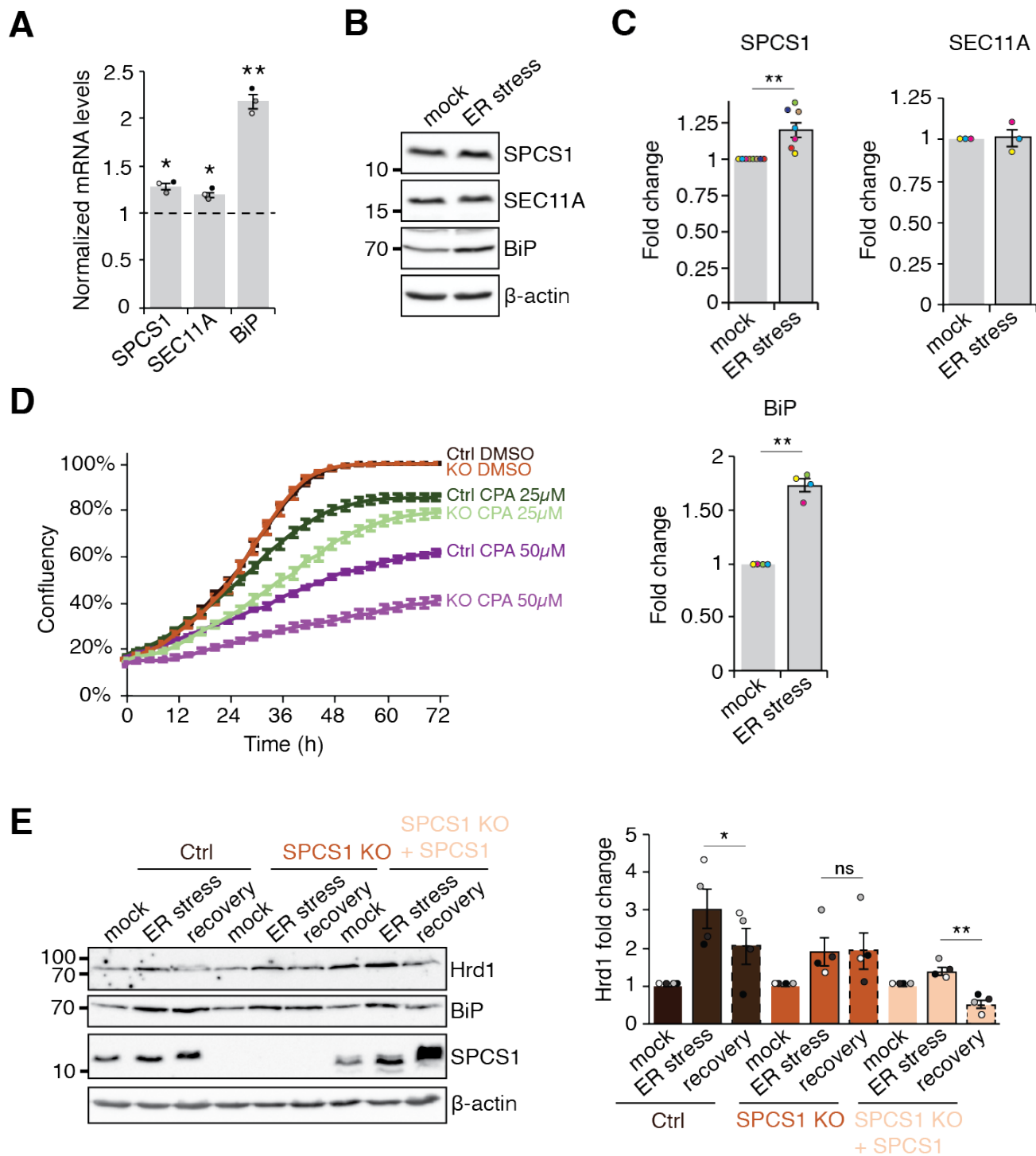
Figure 12. The SPC helps cells during ER stress and recovery. A. Quantification of the levels of the indicated mRNAs extracted from HEK293T cells upon ER stress induction with CPA. Levels were normalized to vehicle control samples and to actin mRNA (n=3; mean ± s.e.m.; * P<0.05; ** P<0.01; paired t test). **B.** Immunoblot analysis of endogenous SPC subunits (SPCS1 and SEC11A) in HEK293T wt upon ER stress induction by CPA. BiP was used as control for ER stress induction. Actin was used as loading control. **C.** Quantification of SPCS1 (n=8), SEC11A (n=3) and BiP (n=4) amount relative to mock. (mean ± s.e.m.; ** P<0.01; paired t test). **D.** Growth curves of HEK293T wt (Ctrl) and SPCS1 KO cells treated with vehicle control DMSO (n=9; mean ± s.e.m.) or two different CPA concentrations to induce ER stress (25 µM; mean ± s.e.m; n=9 or 50 µM; mean ± s.e.m; n=6). **E.** Left, immunoblot analysis of endogenous Hrd1 HEK293T wt (Ctrl), SPCS1 KO and SPCS1 KO cells with exogenous expression of SPCS1 before (mock) and after ER stress induction by CPA and after recovery post-ER stress upon wash-out of CPA. Bip was used as control for ER stress induction. Actin was used as loading control. Right, quantification of Hrd1 amount relative to mock (n=4; grey scale dots represent different replicates; mean ± s.e.m.; * P<0.05; ** P<0.01; paired t test).

2.5 SPC-mediated ERAD is beneficial for coping with ER stress

Thus far, the presented data clearly shows that noncanonical SPC cleavage plays an important role in membrane protein quality (folding and assembly) control. Furthermore, the computational analyses (see Fig. 1B-C and 4A-B) and the validation of several noncanonical substrates (Cx32, Cx26, Cx30.3, PMP22, Hrd1 and iRhom2)[1] indicate that this phenomenon is very likely widespread. Hence, I hypothesized that proteolysis of membrane proteins by the SPC might be relevant for cell adaptation and resistance toward protein folding stress in the ER. Factors such as chaperones and ERAD components, that are important for cell response to ER stress (i.e. unfolded protein response UPR) are normally upregulated when needed, even if general translation and ER import drop[75]. Therefore, I initially assessed if the SPC subunits were upregulated in response to ER stress induction. Consistently with previous studies overexpressing the unfolded protein response transcription factors ATF6α and XBP1(S) in NIH-3T3 cells[186,187], mRNA levels of the regulatory subunit SPCS1 and the catalytic subunit SEC11A are slightly but significantly upregulated upon induction of ER stress with cyclopiazonic acid (CPA)[188], a reversible inhibitor of the sarcoplasmic reticulum/ER calcium ATPase[189](Fig. 12A). The same effect upon ER stress induction was reflected at the protein level for SPCS1 and BiP but, interestingly, not for SEC11A (Fig.12 B-C), suggesting that the novel quality control function of the SPC helps cells to cope with ER stress. To corroborate this idea, I monitored cell growth

under CPA-induced ER stress. Indeed, SPCS1 KO cells grew significantly worse under stress conditions compared to wt cells (Fig. 12D). This highlights a role for SPCS1 and the SPC in protein homeostasis under conditions of protein folding stress. It should be also noted that, in SPCS1 KO cells no reduction of the cleavage of classical signal sequences of ER-resident[1] and secreted proteins (see Fig. 6F) had been observed, suggesting that the growth defect displayed under ER stress conditions is primarily due to the lack of the quality control function of the SPC and not to its classical function in processing ER-targeted proteins.

In addition to upregulated transcription of UPR target genes, re-establishment of normal protein levels of ER chaperones and the ERAD machinery once ER stress ceases is also key for restoring cell homeostasis[190]. Hence, I sought to address whether SPCS1 plays a role in recovery after ER stress by triggering turnover of proteins upregulated during the stress phase. A previous study reported that ER chaperones, but not ERAD factors, are cleared to restore steady state levels post-ER stress via an autophagic pathway using Sec62, a component of the translocon, as autophagy receptor[190]. Consequently, I decided to test whether SPCS1 is involved in clearance of ERAD factors during the recovery phase. Having already identified an ERAD player as noncanonical substrate of the SPC (see Fig. 9C and 11C), I focused on Hrd1. Interestingly, while Hrd1 levels, upregulated upon ER stress, returns to pre-stress levels in wt HEK293T cells, Hrd1 levels remains elevated in SPCS1 KO cells (Fig. 12E). Of note, this can be reversed by SPCS1 expression in SPCS1 KO cells (Fig. 12E). Together, these results suggest a role of noncanonical SPC cleavage in ER stress adaptation by tuning the amount of the ERAD E3 ligase Hrd1.

Conclusively, the data presented so far reveals that the human SPC does not process only ER-targeted proteins but also multipass membrane proteins without containing a signal sequence. This unravel a novel important function of the SPC in membrane protein quality control and ER protein homeostasis and identifies the previously ill-defined accessory subunit SPCS1 as a key mediator of this unprecedented quality control function.

2.6 Putative novel role of the SPC beyond protein quality control

Having unravelled that the SPC plays an important role in tuning the level of the E3 ubiquitin ligase Hrd1, I set out to investigate if there might be a more general role of the SPC in controlling protein abundance. Based on the computational analyses performed (see Fig. 1B-C and 4A-B), I identified ~1500 membrane proteins which potentially contain at least one cryptic SPC cleavage sites (~80% after internal TMDs), accounting for ~18% of the whole human membrane proteome[191]. This indicates that cryptic cleavage sites are widespread and likely not all are used for the quality control function of the SPC. To validate other noncanonical substrates with the aim to uncover other putative roles of the SPC, I initially performed an enrichment analysis of protein classes on the list of proteins containing internal cryptic cleavage sites (Fig. 13A). Additionally, with the idea to find out cellular processes in which the SPC may play a role, I performed label-free mass spectrometry analysis of the interactome of SPCS1 (Fig. 13B). To assess specific SPCS1 interactors, I compared pull-down fractions of wt HEK293T and SPCS1 KO cells. Importantly, the identification of the other SPC subunits (SEC11A, SPCS2 and SPCS3) amongst the most enriched proteins confirmed the technical quality of the experiment (Fig. 13B). Another identified interactor is SSR3 (Fig. 13B), the gamma subunit of the translocon associated protein (TRAP) complex, important for initiation of protein translocation[46,192]. Due to its role, the interaction with SSR3 is most likely relevant for the canonical function of the SPC. Interestingly, other two putative interactors were identified in the analysis: CNIH4, a protein involved in trafficking of G-protein coupled receptors (GPCRs)[193], and SLC38A2, a sodium-coupled neutral amino acid transporter[194]. Of note, interactors relevant for the quality control function of the SPC, e.g. Hrd1 and FAM8A1 (see Fig. 10C), have not been identified in this interactome analysis, suggesting that their interaction with the SPC may become particularly prominent in presence of folding stress. In light of the GPCRs and amino acid transporters protein classes being identified in the enrichment analysis (Fig. 13A), CNIH4 and SLC38A2 may be relevant hits. I therefore decided to perform a first analysis on the amino acid transporter SLC38A2. SLC38A2 is localized at the plasma membrane and contains three glycosylation sites (Fig. 13C). When ectopically expressed in HEK293T cells, it runs in different forms on SDS-PAGE. By means of a glycosylation analysis using EndoH and PNGaseF, enzymes that can respectively digest simple glycans formed in the ER or complex glycans formed in the

Golgi, I assigned the 55 kDa form to the immature ER-localized form and the 70-100 kDa forms to the mature, fully glycosylated forms (Fig. 13D).
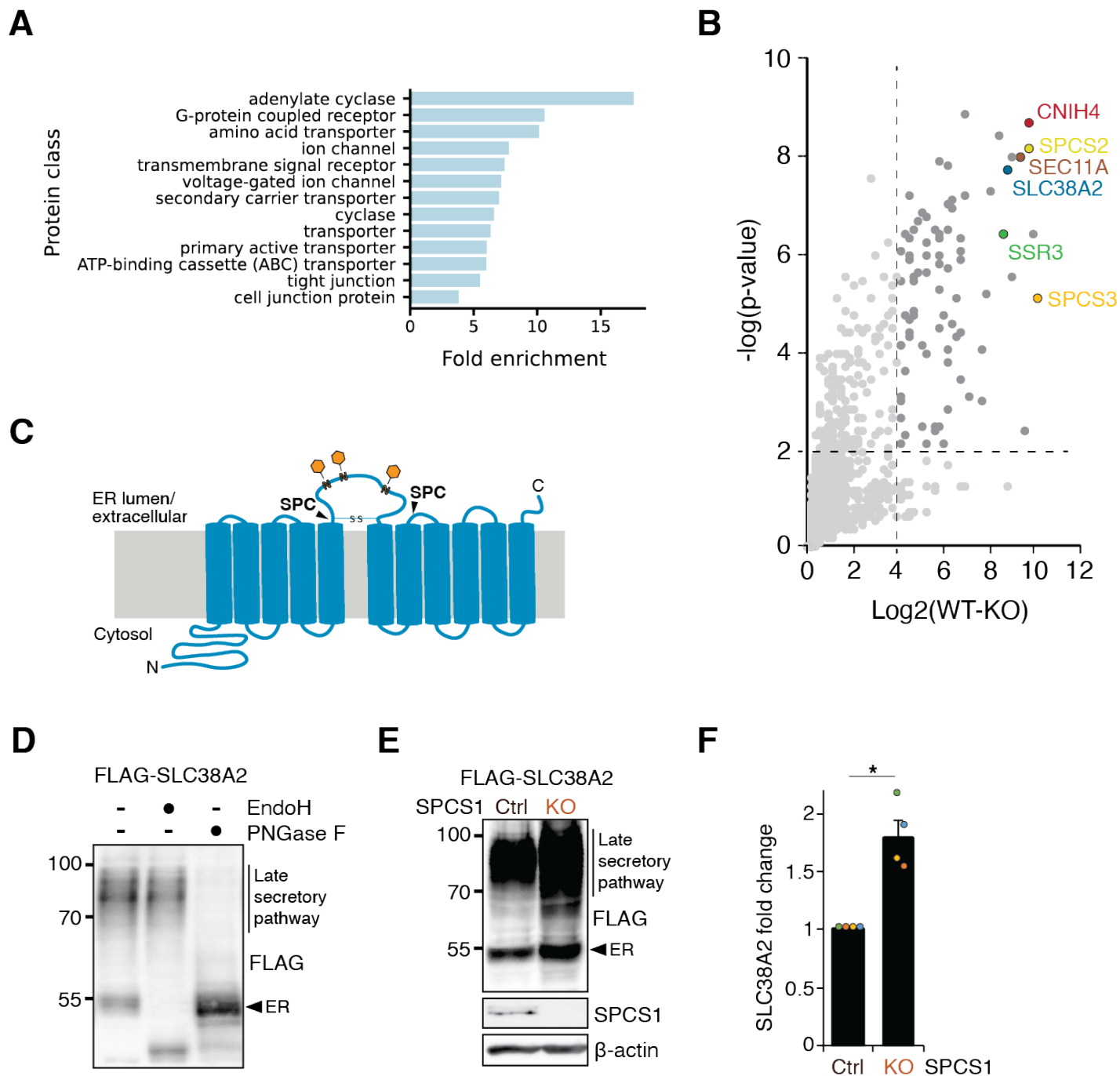
Figure 13. Possible role of the SPC in controlling protein abundance. A. Fold enrichment analysis of protein classes in the list of protein containing putative SPC cryptic cleavage sites after internal TMDs, performed by using

Gene Ontology Resource[151–153]. **B.** Volcano plot displaying SPCS1 interactome analysed via label-free mass spectrometry. Interesting hits discussed here are highlighted in different colours. **C.** Schematic representation of the amino acid transporter SLC38A2. Predicted SPC cleavage sites and glycosylation sites are indicated. **D.** Immunoblot analysis of the glycosylated forms of FLAG-tagged SLC38A2 ectopically expressed in HEK293T cells. **E.** Immunoblot analysis of FLAG-tagged SLC38A2 ectopically expressed in HEK293T wt (Ctrl) or SPCS1 KO cells. Actin was used as loading control. **F.** Quantification of SLC38A2 amount relative to Ctrl cells (n=4; coloured dots represent different replicates; mean ± s.e.m.; * P<0.05; paired t test).

Surprisingly, despite not being able to observe any SPC-dependent fragment (data not shown), I observe a significant increase in SLC38A2 protein steady-state levels in SPCS1 KO cells (Fig. 13E-F), suggesting a possible role of the SPC in controlling its abundance.

3. Discussion

The SPC has been known since the 1970s to uniquely cleave off signal sequences from ER-targeted and secretory proteins. However, very recently, it has been reported that it can also help the maturation process of viral polyproteins by cleaving at several sites[141,145,195], suggesting that other functions of this complex may have been overlooked for years.

In this thesis, I identified and characterised a previously unknown function of the SPC as a quality control enzyme. This yet uncharacterized activity of the SPC not only facilitates the degradation of misfolded membrane proteins but also controls the physiological level of functional proteins and mitigates ER stress responses in the resolution phase, increasing cellular fitness. First, in collaboration with Dr. Gurdeep Singh, I identified approximately 1500 membrane proteins containing putative cryptic cleavage sites for the SPC. I subsequently validated proteins of the connexin family (Cx32, Cx26 and Cx30.3), iRhom2 and Hrd1 as noncanonical SPC substrates, which are cleaved at cryptic cleavage sites when misfolded or when failing to assemble in complexes correctly. I then showed that this SPC cleavage facilitates clearance of the cleaved proteins by synergistically working with the ERAD pathway. Moreover, I uncovered that the accessory subunit SPCS1 is essential for this novel function. Together, these findings highlight the importance and essentiality of the SPC in general cellular functions and raise two important questions: (i) how are non-canonical substrates selected by the SPC, and (ii) how are membrane proteins protected from unwanted SPC cleavage in the process of folding and complex assembly.

3.1 The SPCS1 subunit as a recruitment factor for noncanonical substrates

In this thesis, I presented the SPCS1 subunit as the key subunit for the quality control function of the SPC. Based on the human SPC structure[40], the catalytic core of the complex is formed by SEC11A/C and SPCS3 and this is supported by the fact that both homologues in yeast are essential for signal peptidase activity and cell survival[131–134]. In contrast, the yeast homologues of the SPC accessory subunits SPCS1 and SPCS2 are not essential for signal peptidase activity[136]. This suggested that these accessory subunits must have distinct functions. However,

systematic analyses to identify their roles have only been partially performed in yeast[136], where the SPCS2 homologue is reported to interact with the translocon[138] and, therefore, is possibly important for the canonical function of the SPC in cleaving signal sequences from translocating nascent chains. Conversely, the SPCS1 homologue is only reported to be not essential[135] and, if anything, its absence leads to increased signal sequence processing[140].

Here, I finally uncover a functional role for the SPCS1 subunit. Based on the data provided, I propose that SPCS1 functions as a recruitment factor for noncanonical substrates, i.e. membrane proteins, helping the SPC in distinguishing them from its canonical substrates containing signal sequences (Fig. 14A).

The selectivity of proteases is commonly achieved by the specific recognition of the primary sequence surrounding the scissile peptide bond. Indeed, to bind to the SPC active site, ER-targeting signal peptides commonly present small and uncharged amino acid residues at the -1 and -3 positions and are devoid of prolines[174]. However, this feature is also shared by the TMDs containing cryptic SPC cleavage sites identified in this study (Fig. 5A). Thus, it was clear that there must be additional crucial determinants for SPC specificity towards signal sequences or TMDs, such as the conformation and position of the cleavage site region with respect to the membrane.

Recent cryo-EM structure of the SPC combined with molecular dynamics simulation showed that the SPC causes a local thinning of the ER membrane[40]. While this membrane thinning helps recruit only short hydrophobic regions of cleavable signal peptides, it blocks longer TMDs from entering the SPC catalytic core, hinting towards a secondary mechanism for the recognition of TMDs containing cryptic cleavage sites by the SPC. In this work, I could show that the SPCS1 subunit supports noncanonical substrate processing by the SPC by possibly binding to the TMDs containing cryptic cleavage sites when these are exposed. Therefore, I propose that SPCS1 might serve as a substrate-binding site outside the SPC active site (exosite) which may help to recruit type II-oriented TM segments independent of the membrane-thinned region.
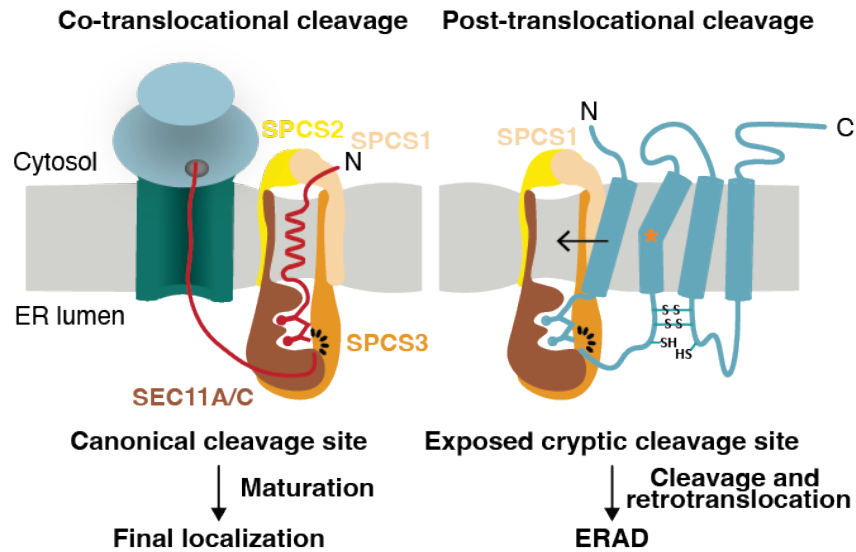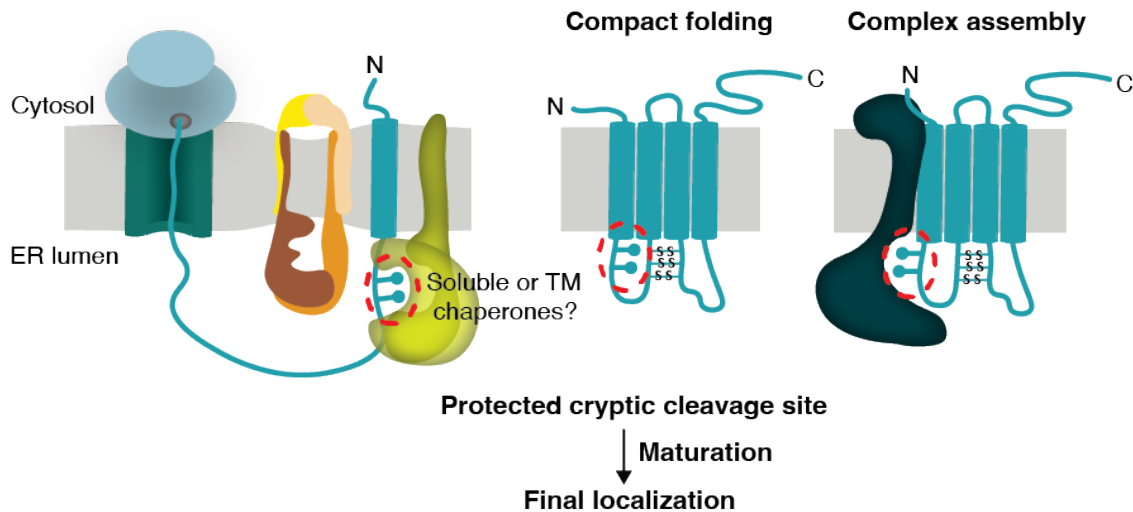
Figure 14. Model of the SPC noncanonical substrates cleavage. A. Schematic of canonical signal peptides processed by the SPC during the translocation process (left) and schematic of non-canonical substrates, containing cryptic cleavage sites, processed by the SPC posttranslocationally. Non-canonical cleavage depends on SPCS1, which serve in the recognition process via an exosite. Cleaved substrates are prone to ERAD involving Hrd1. **B.** Schematic of how cryptic cleavage sites are protected from unwanted SPC processing. During the translocation process, when the site can be exposed and accessible, cleavage may be prevented by soluble or TM chaperones. Compact folding and complex assembly also maintain the cryptic cleavage site buried and inaccessible by the SPC.

Interestingly, in contrast to what I observed for noncanonical SPC substrates, deletion of the SPCS1 homologue in yeast enhances classical signal peptide cleavage of soluble proteins[140], suggesting that SPCS1 might have opposing roles in canonical versus noncanonical SPC-mediated cleavage. Consistent with this, I observed increased prolactin secretion in cells depleted of SPCS1 (Fig. 6F). This strongly suggests that SPCS1 is, thus, the determinant subunit in the selection of canonical versus noncanonical SPC substrates (Fig. 14A).

Although I also identified crucial SPCS1 residues for this function in the TMD2 (Fig. 7), the exact molecular mechanism leading to the cleavage by the catalytic subunit remains unclear. Therefore, I propose that even though the interaction between SPCS1 and a substrate TMD is relatively non-specific and is predicted to have a low affinity, additional recognition of the cleavage site region adjacent to the TMD by the SPC active site might bypass the accommodation into the thinned region of the ER membrane, allowing processing of noncanonical substrates (Fig. 14A).

The relevance of the other subunits in the SPC noncanonical function still needs to be determined. Removal of each subunit independently causes destabilisation of the complex[1]. Despite this, SEC11A knockdown does not affect cleavage of the noncanonical substrate Cx32, whereas SPCS1, SPCS2 and SPCS3 affect it to various extents[1]. This surprising effect of SEC11A depletion might be explained by the upregulation of the orthologue catalytic subunit SEC11C. These two subunits coexist in mammalian cells and form orthologous complexes[40], thereby allowing for speculation of redundancy. However, detection of SEC11C in different cell lines containing normal levels of SEC11A has failed[40], suggesting that this subunit might be used as a backup, at least in the type of cells analysed. Indeed, inhibition of the SEC11A subunit with cavinafungin, which is in theory also able to bind to SEC11C[146], results in a complete block of noncanonical cleavage (Fig. 2B). Nevertheless, to fully characterise the impact of each subunit, systematic analysis of canonical versus noncanonical substrates in knockdown/knockout conditions would be required.

Recently, a large-scale meta-analysis on RNA data from Alzheimer's disease patients revealed SPCS1 to be one of the only three genes whose expression is significantly downregulated in all patients and all analysed regions of the brain[196]. Additionally, despite being non-essential in yeast, the only other study at the organismal level performed in *Drosophila* reported SPCS1 deletion to be embryonic lethal (Haase Gilbert et al., 2013), highlighting the importance of this

subunit in higher eukaryotes. My discovery now provides a rationale for these important findings since it presents SPCS1 as a critical factor for the membrane protein quality function of the SPC. The importance of the SPCS1 subunit is also corroborated by the growth defect I observed in cells lacking SPCS1 under ER stress conditions (Fig. 12D). Moreover, SPCS1 seems to be necessary also for restoring Hrd1 levels in the recovery phase post ER stress (Fig. 12E). Restoring physiological levels of chaperones and ERAD factors once stress subsides is crucial. A recent study discovered the function of the translocon component Sec62 as an autophagic receptor for clearance of chaperones, but not of ERAD factors, in the recovery phase post ER stress[190]. My data provide a starting point that may indicate an SPCS1-linked pathway to clear ERAD factors, such as Hrd1, in the recovery phase post ER stress. Further analyses extended towards a broad range of ERAD factors upregulated upon ER stress may confirm the hypothesis of the SPCS1-dependent SPC-mediated cleavage of ERAD factors or the attractive speculation of SPCS1 function as an autophagic receptor, in parallel to Sec62, to facilitate removal of ERAD factors once ER stress subsided.

All in all, the abovementioned findings in Alzheimer's disease patients, in *Drosophila* and those reported in this thesis might suggest that the newly identified quality control function of the SPC, guided by the SPCS1 subunit, is highly relevant for the general protein homeostasis of cells during stress conditions (e.g. ER stress or aging) and that is conserved in higher eukaryotes. Studies in different organisms, such as mice or *C.elegans*, might provide future evidence for this speculation.

3.2 Mechanisms to prevent unregulated SPC cleavage of membrane proteins

The second important question emerging from this thesis is how membrane protein folding and complex assembly intermediates are protected from unwanted SPC cleavage. In contrast to the cleavage of signal peptides from translocating nascent chains, which occurs early when the cleavage site region enters the ER lumen, my data show that cleavage of noncanonical TMDs occurs posttranslationally, when the protein is already inserted into the membrane and folded. Consequently, the folding state surrounding the cryptic cleavage site might be sampled, as only accessible protein regions that are capable of entering and binding the SPC active site

in an extended confirmation can get cleaved (Fig. 14A). Indeed, my work suggests that once correctly folded, potential SPC cleavage sites may be shielded. Likewise, assembly into higher-order complexes can shield cryptic cleavage sites (Fig. 14B). Recent work has revealed a large number of membrane-integral chaperones, including the EMC[42,53] and the PAT complex[52,197], which are all in close proximity to the Sec61 translocon. Together with soluble ER-resident chaperones like BiP[198] and ERdj3[199] that also interact with the growing nascent polypeptide chains, these factors might protect folding and complex assembly intermediates of membrane proteins from unwanted SPC cleavage (Fig. 14B). Of note, for one of the noncanonical SPC substrates I investigated, chaperone interaction analyses are available: Cx32 interacts with BiP, ERdj3, CNX and the EMC[54], substantiating these ideas. Another possibility is that the SPC exists in different assembly states with specialised functions, as recent proteomic profiling of detergent-solubilised SPC failed to recover stoichiometric binding of all four subunits[40]. This suggests that the SPC may require at least the catalytic core (SEC11A/C and SPCS3) and assemble the accessory subunits SPCS1 and SPCS2 when needed for distinct functions. Nevertheless, this remains highly speculative until the physiological composition of endogenous SPC complexes is analysed in different conditions, e.g. high secretion demand or folding stress.

Overall, post-translocational processing by the SPC shows striking parallels to N-linked glycosylation. While STT3A is associated with the Sec61 translocon and glycosylates only nascent polypeptide chains[44], in a slower process, that is also linked to the recognition of misfolded proteins for ERAD[200], its paralogue STT3B recognizes glycosylation signals (sequons) that were missed co-translocationally[201].

In general, it appears that the surroundings of the translocation machinery for membrane proteins grant a protected environment during membrane protein biogenesis[48,49,52]. On the contrary, when the protein is fully inserted and folded into the membrane in the native conformation, quality control mechanisms have more freedom to take place[202]. In line with these ideas, my thesis reveals another previously unanticipated post-translocational quality control function for the SPC as a major player in the ER protein biogenesis and quality control machinery.

3.3 The SPC as a quality control factor

As a degradation signal in the ERAD pathway, similar to the ubiquitin code, cryptic SPC cleavage sites might have been selected during evolution as predetermined breaking points that, if accessible, irreversibly mark misfolded or misassembled proteins for degradation. Membrane-embedded ERAD substrates are generally ubiquitinated as a signal for the AAA-ATPase p97/VCP to extract these proteins for proteasomal degradation[74,203]. In this thesis, I show that the SPC interacts with the E3 ubiquitin ligase Hrd1 to facilitate ERAD-mediated degradation (Fig.10-11). Notably, I have not performed any analysis on the ubiquitination state of the noncanonical substrates, even though the p97- and Hrd1-dependent degradation of the cleaved substrates might suggest that ubiquitination is occurring. Since the Hrd1 complex has been shown to act also as a retrotranslocation machinery by creating a channel in the membrane[106,108,109], I speculate that the role of Hrd1 in the clearance of noncanonical SPC substrates might be twofold, involving both ubiquitination and retrotranslocation of substrates. Other known proteases that synergize with the ERAD machinery in a similar manner are the rhomboid intramembrane protease RHBDL4[116] and SPP[114,115]. Furthermore, the membrane-embedded metalloprotease ZMPSTE24 (Ste24 in yeast) cleaves proteins stuck in the membrane plane during ER protein import, thereby clearing clogged Sec61 translocons[204]. While these proteases all have their active site in the plane of the membrane, my work reveals that, as for its canonical function, SPC cleaves membrane proteins for quality control purposes adjacent to the lipid bilayer on the lumen side of the ER. In agreement with a generally different cleavage site localization, I report that both SPP and RHBDL4 are not able to cleave the noncanonical SPC substrate Cx32 (Fig. 3), indicating that these ER proteases have a complementary substrate spectrum to the SPC to allow for a comprehensive action on the diverse membrane proteome.

Whereas previous studies had only investigated individual cases of SPC-catalysed cleavage of TMDs[158,205–207] and standard prediction algorithms had been created to negatively select against these examples[147,208,209], my proteome-wide computational analyses and experimental validation in SPCS1 KO cells show that the quality control function of the SPC is widespread. In several cases, it affects mutant membrane proteins associated with human diseases including neuropathies. Importantly, I reveal that the SPC-catalysed cleavage and downstream

handling of cleavage products by the ERAD machinery are linked to the folding state of the membrane protein substrates. Together, these findings significantly extend our understanding of cellular SPC functions beyond signal peptide cleavage and membrane protein homeostasis.

3.4 Future perspectives

In this thesis, I uncover a novel function of the SPC as a quality control factor for membrane proteins. To fully understand this new mechanism, a few aspects still need to be investigated. To mechanistically address substrate's engagement with the SPC through SPCS1, structural analyses would be required. Additionally, the interaction with noncanonical substrates could be investigated by employing co-immunoprecipitation analyses using the SPCS1 mutants generated in this work, in order to further corroborate the relevance of the amino acids patch in the TMD2 of SPCS1 in substrates engagement (Fig. 7). Moreover, the link with the ERAD pathway would also benefit from further investigation. Besides the specific interaction of the SPC with the Hrd1 complex (Fig. 10A-C) and the requirement of Hrd1 in the clearance of cleaved noncanonical substrates (Fig.10D-E), there might be other factors interacting with the SPC involved in this branch of the ERAD pathway. To investigate this possibility, a pull-down experiment followed by mass spectrometry similar to the one already carried out (Fig. 13B) could be performed in conditions of folding stress to possibly enhance transient interactions that might occur only under specific conditions. I also show that SPC cleavage is, partially, a prerequisite for substrate degradation (Fig. 11A-B). Nevertheless, radioactive pulse-chase analyses in the presence of the SPC inhibitor cavinafungin might be beneficial to better understand the kinetics of the process and to conclusively corroborate this hypothesis.

Overall, the findings presented in this work expand the substrate's range of a well-known and crucial protease for cellular homeostasis and open various future research directions. Taken together, the fitness advantage of SPCS1 KO cells under ER stress conditions, the key role of SPCS1 in the quality control of membrane proteins and the recent study reporting SPCS1 to be one of the only genes downregulated in Alzheimer's disease brains[196] lead to the exciting speculation that SPCS1 might be a key factor in the aging process by helping to maintain a healthy proteome[210–212]. To validate this hypothesis, studies at the organismal level with model systems commonly used for aging-related analyses (e.g. *C.elegans* or mice) would be critical.

Another interesting direction would be to investigate the SPC putative function in controlling protein abundance. In line with this idea, I observed an SPCS1-dependent control of Hrd1 protein levels during the recovery phase post-ER stress (Fig. 12E). Moreover, the computational analysis shows the enrichment of amino acids transporters in the list of proteins containing cryptic SPC cleavage sites (Fig. 13A) and I report SLC38A2 to interact with SPCS1 and to be more abundant in the absence of SPCS1 (Fig. 13B-F). This might have implications in cell metabolism. However, further studies would be required to address this intriguing hypothesis.

All in all, this thesis revealed a novel function of the SPC in the quality control of membrane proteins, consequently expanding the knowledge on the cellular functions of this essential ER-resident protease and setting the basis for new research lines to identify new links between this enzyme and neurodegeneration, aging and cancer.

4. Materials and Methods

4.1 Materials

Antibodies		
Rabbit polyclonal anti-Connexin-32	Proteintech	Cat#10450-1-AP
Mouse monoclonal anti-FLAG (M2)	Sigma	Cat#F1804
Rabbit polyclonal anti-SPCS1	Proteintech	Cat#11847-1-AP
Mouse monoclonal anti-β-actin	Sigma	Cat#A1978
Rabbit polyclonal anti-SEC11A	Proteintech	Cat#14753-1-AP
Rabbit polyclonal anti-SEL1L	Sigma	Cat#S3699
Mouse monoclonal anti-Climp63	Enzo	Cat#ENZ-ABS669-0100
Rabbit polyclonal anti-Hrd1	Bethyl Laboratories	Cat#A302-945A
Mouse monoclonal anti-Hrd1	Proteintech	Cat#67488-1-Ig
Rabbit polyclonal anti-FAM8A1	Proteintech	Ca#t24746-1-AP
Rabbit polyclonal anti-Bip	Abcam	Cat#Ab21685
Mouse monoclonal anti-HA	Biolegend	Cat#901502
Rabbit polyclonal anti-p97	Gift from Bernard Dobberstein	N/A
Donkey anti-mouse	Dianova	711-035-153
Donkey anti-rabbit	Dianova	715-035-150

Table 1. List of antibodies used.

Chemicals		
EasyTag^{TM} EXPRESS^{35}S Protein Labeling Mix	PerkinElmer	NEG772007MC
Triton X-100 (10%)	Calbiochem	Cat#648463-50ML
CHAPS	AppliChem	Cat#A1099,0025
Digitonin	AppliChem	Cat#A1905,0005
Cycloheximide (CHX)	AppliChem	Cat#A0879,0005
DMSO	AppliChem	Cat#A3672,0050
CB-5083	APExBIO	Cat#B6032
MG-132	Calbiochem	Cat#474790-5MG
epoxomicin	Calbiochem	Cat#324800
EndoH	NEB	Cat#P0703
PNGaseF	NEB	Cat#P0704
DTT	AppliChem	Cat#A1101-5G
CPA	Sigma	Cat#C1530-5MG
Cavinafungin	Gift from Martin Spiess	
(Z-LL)$_2$-ketone	Calbiochem	Cat#421050
cOmplete^{TM} Protease Inhibitor, EDTA-free	Roche	Cat#11836170001

Pierce Protein A/G Agarose beads	Thermo Fisher Scientific	Cat# 20421
WesternBright^{TM} ECL solution	Biozym	Cat#541005
Amersham ECL Prime Western Blotting Detection	Sigma	Cat# GERPN2236

Table 2. List of chemicals used.

Cell lines	
HEK293T Ctrl sg.95	Zhang et al.[141]
HEK293T SPCS1$^{-/-}$ sg.80	Zhang et al.[141]
HEK293T Hrd1 KO	Bock et al.[117]
HEK293T RHBDL4 KO	Bock et al.[117]
HEK293T SPP KO	Heidasch et al.[167]

Table 3. List of cell lines used.

Recombinant DNA	
pcDNA3.1(+)-Cx32^{wt}-FLAG	Created by Feige Lab
pcDNA3.1(+)-Cx32^{C201R}-FLAG	Created by Feige Lab
pcDNA3.1(+)-Cx26-FLAG	Created by Feige Lab
pcDNA3.1(+)-Cx26^{R32H}-FLAG	Created by Feige Lab
pcDNA3.1(+)-Cx30.3-FLAG	Created by Feige Lab
pcDNA3.1(+)-Cx30.3^{F189Y}-FLAG	Created by Feige Lab
pcDNA3.1(+)-SPCS1^{wt}	This study
pcDNA3.1(+)-SPCS1^{W47A}	This study
pcDNA3.1(+)-SPCS1^{M53A}	This study
pcDNA3.1(+)-SPCS1^{F58A}	This study
pcDNA3.1(+)-SPCS1^{L61A,L62A}	This study
pcDNA3.1(+)-SPCS1^{P65G}	This study
pcDNA3.1(+)-SPCS1^{W67A}	This study
pcDNA3.1(+)-SPCS1^{Y70A}	This study
pcDNA3.1(+)-SPCS1^{W67A,Y70A}	This study
pcDNA3.1(+)-SPCS1^{R71A,R72}	This study
pcDNA3.1(+)-FLAG-Prolactin	Fleig et al.[116]
pcDNA3.1(+)-Hrd1-FLAG	This study
pcDNA3.1(+)-Hrd1$^{1-251}$-FLAG	This study
pcDNA3.1(+)-FLAG-gp78	Gift from Ivan Robert Navi
pEGFP-N1-iRhom2-FLAG	This study
pEFGP-N1-iRhom2-HA	This study
pcDNA3.1(+)-FLAG-TACE(minus)	This study
pcDNA3.1(+)-PMP22^{L80R}-FLAG	This study

Table 4. List of plasmids used

Oligonucleotides
RT-qPCR primer for SPCS1: forward CTGAACAGTTCGGGTGGACT
RT-qPCR primer for SPCS1: reverse AACCACTTGAGAGGATGCCG
RT-qPCR primer for SEC11A: forward ATGAACAAGCGGCAGCTCTA
RT-qPCR primer for SEC11A: reverse CCTTCCAGATCATTAGTGCCGA
RT-qPCR primer for β-actin: forward GCATTGCCGACAGGATGC
RT-qPCR primer for β-actin: reverse GCAATGATCTTGATCTTCATTGTGC
RT-qPCR primer for TBP: forward CCGGCTGTTTAACTTCGCTT
RT-qPCR primer for TBP: reverse ACGCCAAGAAACAGTGATGC
RT-qPCR primer for Bip: forward CCAACGCCAAGCAACCAAAG
RT-qPCR primer for Bip: reverse TGCCGTAGGCTCGTTGATG
Quick change primer for SPCS1^{W47A}: forward GCTGAACAGTTCGGGGCGACTGTCTATATAGTT
Quick change primer for SPCS1 ^{W47A}: reverse AACTATATAGACAGTCGCCCCGAACTGTTCAGC
Quick change primer for SPCS1^{Y50A}: forward TTCGGGTGGACTGTCGCTATAGTTATGGCCGGA
Quick change primer for SPCS1^{Y50A}: reverse TCCGGCCATAACTATAGCGACAGTCCACCCGAA
Quick change primer for SPCS1^{M53A}: forward ACTGTCTATATAGTTGCGGCCGGATTTGCTTTT
Quick change primer for SPCS1^{M53A}: reverse AAAAGCAAATCCGGCCGCAACTATATAGACAGT
Quick change primer for SPCS1^{F58A}: forward ATGGCCGGATTTGCTGCTTCATGTTTGCTGACA
Quick change primer for SPCS1^{F58A}: reverse TGTCAGCAAACATGAAGCAGCAAATCCGGCCAT
Quick change primer for SPCS1^{L61A,L62A}: forward TTTGCTTTTTCATGTGCGGCGACACTTCCTCCATGG
Quick change primer for SPCS1^{L61A,L62A}: reverse CCATGGAGGAAGTGTCGCCGCACATGAAAAAGCAAA
Quick change primer for SPCS1^{P65G}: forward TGTTTGCTGACACTTGGTCCATGGCCCATCTAT
Quick change primer for SPCS1^{P65G}: reverse ATAGATGGGCCATGGACCAAGTGTCAGCAAACA
Quick change primer for SPCS1^{W67A}: forward CTGACACTTCCTCCAGCGCCCATCTATCGCCGG
Quick change primer for SPCS1^{W67A}: reverse CCGGCGATAGATGGGCGCTGGAGGAAGTGTCAG
Quick change primer for SPCS1^{Y70A}: forward CCTCCATGGCCCATCGCTCGCCGGCATCCTCTC
Quick change primer for SPCS1^{Y70A}: reverse GAGAGGATGCCGGCGAGCGATGGGCCATGGAGG
Quick change primer for SPCS1^{R71A,R72A}: forward CCATGGCCCATCTATGCCGCGCATCCTCTCAAGTGG

Quick change primer for SPCS1[R71A,R72A]: reverse CCACTTGAGAGGATGCGCGGCATAGATGGGCCATGG

Table 5. List of primers used for RT-qPCR and generation of SPCS1 mutants.

4.2 Methods

4.2.1 Cell culture

All HEK293T cells were cultured in Dulbecco's modified Eagle's Medium (DMEM) supplemented with 10% fetal bovine serum (FBS) at 37°C, 5% CO_2 and splitting at the desired dilution by means of trypsinitation.

4.2.2 Transfection of cultured cells

All HEK293T cells were transfected with polyethylenimine (PEI) following an adapted protocol[213]. Cells were split 1:20 in 6-well plates from a 10-cm confluent dish and grown until 70-80% confluency. Based on the experiment, plasmid mixtures were prepared to a total amount of 2 µg of DNA per well. 250 µL of DMEM supplemented with 1% Pen-Strep and 5 µL of PEI was added to the plasmid mixture, vortexed and incubated for 5 min. Next, 750 µL of DMEM supplemented with 5% FBS and 1% Pen-Strep were added to the mixture and incubated for 10 min. The mixture was added onto the cells, which were then incubated for approximately 4 h at 37°C in 5% CO_2. The medium was changed to DMEM supplemented with 10% FBS and 1% Pen-Strep and cells were grown overnight at 37°C, 5% CO_2. Expression of transfected constructs was analysed after 24 h.

4.2.3 Generation of SPCS1 mutant constructs

All mutants of SPCS1 were generated by site-directed mutagenesis following the protocol of the QuickChange Site-Directed Mutagenesis kit (Stratagene) using the primers listed in Table5.

4.2.4 Computational analyses of cryptic SPC cleavage sites

Initially, the analyses were performed by myself using two different version of the software: SignalP3.0 and SignalP4.1[147]. SignalP3.0, in contrast to SignalP4.1, does not recognise the presence of a proper TMD in the sequence. A list of 5233 annotated membrane proteins was downloaded from UniprotKB[148] and run on the online versions of the SignalP software, obtaining s-, c-, y-scores as output. Next, few arbitrary thresholds were set: (i) SignalP3.0 > 0.5 and (ii) SignalP4.1 < 0.6. Then, topology, localisation and presence of disease-linked mutations were assessed manually.

To make the computational approach more robust and to expand it to the whole proteome, these analyses were performed again together with Dr. Gurdeep Singh (Russel Lab, BioQuant, Heidelberg). Briefly, a command-line version of the SignalP4.1 program[147] was used to predict the SPC cryptic cleavage sites in the whole proteome. FASTA-formatted sequences of 70 amino acids were given to the program. The program relies on an internal algorithm to assign the number of TM residues in the input sequence. If the number of TM residues (assigned to the variable TMCount; set to 0 by default) is greater than a threshold (assigned to the variable TM_TRESHOLD; set to 4 by default), the program runs the sequence in the TM network, otherwise in the no-TM network. In order to force the program in either of the modes, the SignalP4.1 program was modified to generate 2 different versions: SignalP-TM and SignalP-noTM. For the SignalP-noTM, the TM_TRESHOLD was set to -1, so less than TMCount, and therefore forces the program to run in the no-TM network mode. For the SignalP-TM, we set the TM_TRESHOLD to 100, so greater than TMCount, forcing the program to run in the TM network mode. The maximum value of TMCount cannot be more than 70. Any input sequence more than 70 amino acids long is truncated after the 70th amino acid by default by the program. All protein sequences and their associated informations were retrieved from the UniProt/Swiss-Prot[148] data set (release 2020_05). The start and end points of TM segments and signal peptides were determined from the keyword (KW) and feature table (FT) annotations.

Two set of proteins sequences were created: (i) containing first N-terminal 70 aa sequences of the whole proteome, (ii) containing 70 aa sequences from all membrane proteins starting from the first aa of the TMD. The Y-scores of both sets were predicted using the SignalP-TM and SignalP-noTM versions described above. A protein sequence was considered to have a non-

canonical cryptic SPC cleavage site if (i) the Y-score in the SignalP-TM was less than 0.6, (ii) more than 0.5 in SignalP-noTM, (iii) the TMD has a type-II orientation and (iv) the protein was localized along the secretory pathway.

Furthermore, mutational information were assigned to each peptide derived from the protein. Missense mutations were downloaded from (a) UniProt[148] (pathogenic variants provided in *humsavar.txt.gz*; version 2020_05), COSMIC[150] (pathogenic variants, if reported in at least 3 samples, in *CosmicMutantExport.txt.gz*; version 72), and ClinVAR[149] (pathogenic variants annotated as pathogenic/likely pathogenic in *variant_summary.txt.gz*; version November 2021). The results from these analyses can be interactively visualised on the web application created by Dr. Gurdeep Singh (https://russelllab.shinyapps.io/webAppSPC/).

4.2.5 Protein enrichment analysis

This analysis was performed on the list of hits from the computational analysis to identify cryptic SPC cleavage sites (see section 4.2.4) using the Gene Ontology Resource PANTHER[153].

4.2.6 Computational comparison between signal peptides and noncanonical SPC substrates

These analyses were performed together with Dr. Gurdeep Singh (Russel Lab, BioQuant, Heidelberg). Signal peptides or TMDs truncated at the predicted SPC cleavage site were used for the analyses. Sequence logos were made by using the package logomaker[173]. Only experimentally validated signal peptides, supported by at least one PubMed entry, were considered in the analyses. ΔG prediction server (v1.0)[214] was used to predict the free energy difference, ΔG_{app}, for membrane insertion. Sequences satisfying the Y-score thresholds (see section 4.2.3) were considered hits. Lengths of both canonical (signal peptides) and non-canonical SPC substrates were analysed.

4.2.7 Protein sample preparation

Cells transfected with the required constructs were washed once with ice-cold PBS. For Connexins, PMP22 and Hrd1 samples, 300 µL of lysis buffer (50 mM Tris-HCl pH 7.5, 150 mM NaCl, 1% TritonX-100, 0.5% sodium deoxycholate and 1x protease inhibitors cocktail (Roche)) were added to each well of 6-well plates and incubated for 15 min while shaking. Cells were

collected by scraping into cold tubes and centrifuged at 15,000 x g at 4°C for 15 min. 180 μL of the supernatant were mixed with 60 μL of 4x Laemmli sample buffer and incubated at 37°C for 30 min (Connexins) or 95°C for 5 min (PMP22) while shaking. Samples were run directly on SDS-PAGE gels. For all the other proteins, 300 μL of 1x Laemmli sample buffer were added directly in the wells. Cells lysates were then incubated at 65°C for 15 min.

4.2.8 Radioactive pulse-chase analyses

Cells were rinsed once with PBS and starved for 1 h at 37°C, 5% CO_2 in DMEM without methionine and cysteine supplemented with 10% dialyzed FCS. 0.06 mCi of EasyTag™ EXPRESS[35]S Protein Labeling Mix containing ^{35}S-L-cysteine and ^{35}S-L-methionine were added to the medium of each well of a 6-well plate in order to label newly synthesized proteins for 2 min (Fig. 2C), 5 min (Fig. 6E) or 10 min (Fig. 8A and 11A). After labeling, cells were washed once with DMEM supplemented with 10% FBS and 1% Pen/Strep and then incubated in the same medium with or without different chemicals (DMSO, CB-5083 or DTT), where required for the experiments, at 37°C, 5% CO_2 until sample collection at different time points. At specific time points, cells were washed once with PBS, collected by scraping in 1 mL PBS + 10 mM EDTA into 1.5 mL tubes and centrifuged at 900 x g for 3 min at 4°C. The pellet obtained was then snap-frozen in liquid nitrogen. Once all the samples from different time points were collected, cell pellets were re-suspended by pipetting in 300 μL of solubilization buffer (50 mM HEPES-KOH pH 7.4, 150 mM NaCl, 2 mM MgOAc$_2$, 10% glycerol, 1 mM EGTA) + 1% Triton X-100 + EDTA-free complete Protease Inhibitor Cocktail (Roche) and incubated on ice for 30 min. Next, samples were centrifuged at 14,000 x g for 15 min at 4°C, supernatants were collected into 1.5 mL tubes with 10 μL of Protein G beads for preclearing and incubated for 2 h rotating overhead at 4°C. Following beads precipitation at 1,500 x g for 2 min at 4°C, supernatants were collected into new 1.5 mL tubes and 1 μL of anti-FLAG antibody was added. Samples were incubated overnight rotating overhead at 4°C. The next day, 20 μL of Protein G beads were added and the samples were incubated rotating overhead for additional 2h at 4°C. Beads were then washed three times in solubilisation buffer + 0.1% Triton X-100 by centrifugation at 1500 x g for 2 min at 4°C. 25 μL of 2x Laemmli Buffer were added and the beads were incubated for 30 min at 37°C while shaking. Samples were run on a SDS-PAGE gel. The gel was then fixed by incubation with Fix-Mix solution (10% acetic acid, 40% Methanol, 0.4 % glycerol) for 30 min

while shaking and dried on Whatman paper for 50 min at 70°C. Labelled proteins were visualized by a FLA-7000 phosphorimager (Fuji).

4.2.9 Analysis of prolactin secretion

Cells transfected with FLAG-tagged Prl were harvested as described in section 4.2.6. Previously, 500 μL of the medium were collected and centrifuged at 20,000 x g for 20 min to remove cell debris. The supernatant was collected and mixed with the same volume of 20% trichloroacetic acid, vortexed briefly and centrifuged for 2 min at full speed at 4°C. Next, 180 μL of acetone were added to the pellet. The sample was then centrifuged for 1 min at 20,000 x g, the supernatant was discarded and the tube was incubated at 37°C to let the acetone evaporate. The pellet was suspended in 100 μL of 1x Laemmli sample buffer. Samples were then run on 15% SDS-PAGE gels.

4.2.10 Co-immunoprecipitation analysis

Cells were washed once with ice-cold PBS, collected by scraping with 1 mL of ice-cold PBS + 10mM EDTA into 1.5 mL tubes and centrifuged at 900 x g for 3 min at 4°C. 300 μL of solubilisation buffer + 1% CHAPS (Figure 7A, 7E, 10A and 10B) or 1% Digitonin (Figure 10C) + EDTA-free complete Protease Inhibitor Cocktail (Roche) were added to the cell pellet and incubated for 30 min at 4°C. The following steps were performed as for radioactive pulse-chase analysis described in section 4.2.8 with the following exceptions: an input fraction was taken before the overnight incubation step with the antibody and the washing steps were done in solubilisation buffer + 0.1% CHAPS or 1% Digitonin based on the experiment. Samples were analysed by western blotting.

4.2.11 Cycloheximide chase analysis

Following transfection with the required constructs, cells were treated with cycloheximide (100 μg/mL) and with DMSO, MG132 (10 μM), epoxomicin (2 μM) or cavinafungin (5 μM), based on the experiment, and collected at different time points as described in section 4.2.7. Cell lysates were then analysed by western blotting.

4.2.12 EndoH and PNGaseF treatment

Samples were diluted to 0.5% SDS. Next, from each sample, 3 different solutions were obtained, containing (i) 12 μL of sample + 3 μL of H_2O, (ii) 12 μL of sample + 1.5 μL G3 buffer (NEB) + 0.2 μL EndoH (NEB) + 1.3 μL H_2O, or (iii) 12 μL of sample + 1.5 μL G2 buffer (NEB) + 0.2 μL PNGaseF (NEB) + 1.5 μL NP40 (NEB). All samples were then incubated for 1.5h at 37°C. 5 μL of 4X Laemmli sample buffer and 1 μL of β-mercaptoethanol were added to each reaction. Samples were incubated for 5 minutes at 65°C and run directly on SDS-PAGE gels.

4.2.13 Quantitative real-time PCR

This method was used to assess SPC subunits mRNA levels in cells under ER stress conditions (CPA 10 μM, 16h). Total RNA was isolated using the NucleoSpin RNA isolation kit (Macherey-Nagel) according to manufacturer's protocol. 2 μg RNA were reverse transcribed using the RevertAid First Strand cDNA Synthesis Kit (Thermo Scientific) according to manufacturer's protocol. Quantitative PCR was performed in a 348-well plate using the SensiFAST SYBR No-ROX kit (Bioline) and the LightCycler480 Instrument II (Roche) using the primers listed in Table 5. Each reaction was performed in technical triplicates. The 2^$\Delta\Delta$Ct method was used to calculate relative changes in gene expression and normalized to the geometric mean of the housekeeping genes (β-actin and TATA-binding protein (TBP)).

4.2.14 Analysis of cell growth

To analyse the growth of HEK293T wt and SPCS1 KO cells under different conditions, 6,000 cells were seeded in a 96-well plate in DMEM supplemented with 10% FBS. Cells were treated with DMSO or CPA (25-50 μM) and incubated for 72 h. Photomicrographs were acquired every 3h by the Incucyte live cell imager (Essen BioScience). Confluency of the cells was measured using the Incucyte software (Essen BioScience).

4.2.15 ER stress recovery

Cells were treated for 16h with CPA (10 μM) to induce ER stress. Next, cells were rinsed with 1x PBS and incubated for additional 10h in DMEM supplemented with 10% FBS in order to

recover from ER stress, as descried previously[190]. Cells were collected as described in section 4.2.7. Samples were then analysed by western blotting.

4.2.16 Mass spectrometry analysis of SPCS1 interactome

Pull-down fractions were collected as described in 4.2.8 and 4.2.10. Subsequent sample preparation for mass spectrometry analysis was performed as advised from the Proteomics Core Facility Cologne. Analysis of the results was carried out following instruction previously reported[215].

4.2.17 Immunoblotting

Samples were prepared differently based on the experiment as described in the previous sections. Samples were then loaded on Tris-Glycine SDS-PAGE gels at different percentages based on the protein of interest. Proteins were then transferred onto PVDF membranes via semi-dry blotting and membranes were blocked using 5% (w/v) nonfat dried milk solution in TBS-T for 30 min, incubated with primary antibodies overnight at 4°C and with secondary antibodies for 1 h at room temperature. Western blot analysis was then performed using either Westernbright[TM] ECL solution (Advansta Inc.) and imaged using a LAS-4000 system (Fuji).

4.2.18 Images quantification and statistical analyses

Western blot quantifications were performed using Fiji[216]. Quantification of autoradiograms was performed using Multi Gauge (Fuji). Statistical analyses were performed using Microsoft Excel. The statistical tests used, the statistical significance and the number of replicates are reported in the figure legends.

5. Bibliography

1. Zanotti, A. *et al.* The human signal peptidase complex acts as a quality control enzyme for membrane proteins. *Science* **378**, 996–1000 (2022).

2. Krogh, A., È rn Larsson, B., von Heijne, G. & L Sonnhammer, E. L. Predicting Transmembrane Protein Topology with a Hidden Markov Model: Application to Complete Genomes. *J Mol Biol* **305**, 567–580 (2001).

3. Uhlén, M. *et al.* Tissue-based map of the human proteome. *Science* **347**, 1260419 (2015).

4. von Heijne, G. The membrane protein universe: what's out there and why bother? *J. Intern. Med.* **261**, 543–557 (2007).

5. Xie, K. & Dalbey, R. E. Inserting proteins into the bacterial cytoplasmic membrane using the Sec and YidC translocases. *Nat. Rev. Microbiol.* **6**, 234–244 (2008).

6. Aviram, N. & Schuldiner, M. Targeting and translocation of proteins to the endoplasmic reticulum at a glance. *J. Cell Sci.* **130**, 4079–4085 (2017).

7. Shao, S. & Hegde, R. S. Membrane Protein Insertion at the Endoplasmic Reticulum. *Annu. Rev. Cell Dev. Biol.* **27**, 25–56 (2011).

8. White, S. & Vonheijne, G. Transmembrane helices before, during, and after insertion. *Curr. Opin. Struct. Biol.* **15**, 378–386 (2005).

9. Hegde, R. S. & Keenan, R. J. The mechanisms of integral membrane protein biogenesis. doi:10.1038/s41580-021-00413-2.

10. Nyathi, Y., Wilkinson, B. M. & Pool, M. R. Co-translational targeting and translocation of proteins to the endoplasmic reticulum ☆. *BBA - Mol. Cell Res.* **1833**, 2392–2402 (2013).

11. Von Heijne, G. *Signal Sequences. The Limits of Variation. J. Mol. Biol* vol. 184 99–105 (1985).

12. Martoglio, B. & Dobberstein, B. Signal sequences: more than just greasy peptides. *Trends Cell Biol.* **8**, 410–415 (1998).

13. Hegde, R. S. & Bernstein, H. D. The surprising complexity of signal sequences. *Trends Biochem. Sci.* **31**, 563–571 (2006).

14. Johnson, N., Powis, K. & High, S. Post-translational translocation into the endoplasmic reticulum ☆. *BBA - Mol. Cell Res.* **1833**, 2403–2409 (2013).

15. Keenan, R. J., Freymann, D. M., Stroud, R. M. & Walter, P. The Signal Recognition Particle. *Annu. Rev. Biochem.* **70**, 755–775 (2001).

16. Saraogi, I. & Shan, S.-O. Molecular Mechanism of Co-translational Protein Targeting by the Signal Recognition Particle. *Traffic* **12**, 535–542 (2011).

17. Pool, M. R. Signal recognition particles in chloroplasts, bacteria, yeast and mammals (Review). *Mol. Membr. Biol.* **22**, 3–15 (2005).

18. Halic, M. *et al.* Structure of the signal recognition particle interacting with the elongation-arrested ribosome. **427**, (2004).

19. Voorhees, R. M. & Hegde, R. S. Structures of the scanning and engaged states of the mammalian SRP-ribosome complex. *eLife* **4**, e07975 (2015).

20. Shan, S., Schmid, S. L. & Zhang, X. Signal Recognition Particle (SRP) and SRP Receptor: A New Paradigm for Multistate Regulatory GTPases. *Biochemistry* **48**, 6696–6704 (2009).

21. Hsieh, H.-H., Lee, J. H., Chandrasekar, S. & Shan, S. A ribosome-associated chaperone enables substrate triage in a cotranslational protein targeting complex. *Nat. Commun.* **11**, 5840 (2020).

22. Gamerdinger, M., Hanebuth, M. A., Frickey, T. & Deuerling, E. The principle of antagonism ensures protein targeting specificity at the endoplasmic reticulum. *Science* **348**, 201–207 (2015).

23. Borgese, N., Coy-Vergara, J., Colombo, S. F. & Schwappach, B. The Ways of Tails: the GET Pathway and more. *Protein J.* **38**, 289–305 (2019).

24. Shan, S. Guiding tail-anchored membrane proteins to the endoplasmic reticulum in a chaperone cascade. *J. Biol. Chem.* **294**, 16577–16586 (2019).

25. Wang, F., Brown, E. C., Mak, G., Zhuang, J. & Denic, V. A Chaperone Cascade Sorts Proteins for Posttranslational Membrane Insertion into the Endoplasmic Reticulum. *Mol. Cell* **40**, 159–171 (2010).

26. Stefanovic, S. & Hegde, R. S. Identification of a Targeting Factor for Posttranslational Membrane Protein Insertion into the ER. *Cell* **128**, 1147–1159 (2007).

27. Mateja, A. *et al.* The structural basis of tail-anchored membrane protein recognition by Get3. *Nature* **461**, 361–366 (2009).

28. Mateja, A. *et al.* Structure of the Get3 targeting factor in complex with its membrane protein cargo. *Science* **347**, 1152–1155 (2015).

29. Schuldiner, M. *et al.* The GET Complex Mediates Insertion of Tail-Anchored Proteins into the ER Membrane. *Cell* **134**, 634–645 (2008).

30. Hegde, R. S. & Keenan, R. J. Tail-anchored membrane protein insertion into the endoplasmic reticulum. *Nat. Rev. Mol. Cell Biol.* **12**, 787–798 (2011).

31. Mariappan, M. *et al.* The mechanism of membrane-associated steps in tail-anchored protein insertion. *Nature* **477**, 61–66 (2011).

32. Wang, F., Chan, C., Weir, N. R. & Denic, V. The Get1/2 transmembrane complex is an endoplasmic-reticulum membrane protein insertase. *Nature* **512**, 441–444 (2014).

33. Anghel, S. A., McGilvray, P. T., Hegde, R. S. & Keenan, R. J. Identification of Oxa1 Homologs Operating in the Eukaryotic Endoplasmic Reticulum. *Cell Rep.* **21**, 3708–3716 (2017).

34. McDowell, M. A. *et al.* Structural Basis of Tail-Anchored Membrane Protein Biogenesis by the GET Insertase Complex. *Mol. Cell* **80**, 72-86.e7 (2020).

35. Guna, A., Volkmar, N., Christianson, J. C. & Hegde, R. S. The ER membrane protein complex is a transmembrane domain insertase. *Science* **359**, 470–473 (2018).

36. Berg, B. van den *et al.* X-ray structure of a protein-conducting channel. *Nature* **427**, 36–44 (2004).

37. Voorhees, R. M., Fernández, I. S., Scheres, S. H. W. & Hegde, R. S. Structure of the Mammalian Ribosome-Sec61 Complex to 3.4 Å Resolution. *Cell* **157**, 1632–1643 (2014).

38. Rapoport, T. A., Li, L. & Park, E. Structural and Mechanistic Insights into Protein Translocation. *Annu. Rev. Cell Dev. Biol.* **33**, 369–390 (2017).

39. Voorhees, R. M. & Hegde, R. S. Structure of the Sec61 channel opened by a signal sequence. *Science* **351**, 88–91 (2016).

40. Liaci, A. M. *et al.* Structure of the human signal peptidase complex reveals the determinants for signal peptide cleavage. *Mol. Cell* **81**, 3934-3948.e11 (2021).

41. High, S. *et al.* Sec61p is adjacent to nascent type I and type II signal-anchor proteins during their membrane insertion. *J. Cell Biol.* **121**, 743–750 (1993).

42. Chitwood, P. J., Juszkiewicz, S., Guna, A., Shao, S. & Hegde, R. S. EMC Is Required to Initiate Accurate Membrane Protein Topogenesis. *Cell* **175**, 1–13 (2018).

43. Wu, H. & Hegde, R. S. Mechanism of signal-anchor triage during early steps of membrane protein insertion. *Mol. Cell* **83**, 961-973.e7 (2023).

44. Braunger, K. *et al.* Structural basis for coupling protein transport and N-glycosylation at the mammalian endoplasmic reticulum. *Science* **360**, 215–219 (2018).

45. Weng, T. *et al.* Architecture of the active post-translational Sec translocon. *EMBO J.* (2020) doi:10.15252/embj.2020105643.

46. Pfeffer, S. *et al.* Dissecting the molecular organization of the translocon-associated protein complex. *Nat. Commun.* **8**, 14516 (2017).

47. Voigt, S., Jungnickel, B., Hartmann, E. & Rapoport, T. A. Signal sequence-dependent function of the TRAM protein during early phases of protein transport across the endoplasmic reticulum membrane. *J. Cell Biol.* **134**, 25–35 (1996).

48. McGilvray, P. T. *et al.* An ER translocon for multi-pass membrane protein biogenesis. *eLife* **9**, e56889 (2020).

49. Sundaram, A. *et al.* Substrate-driven assembly of a translocon for multipass membrane proteins. *Nature* **611**, 167–172 (2022).

50. Braakman, I. & Hebert, D. N. Protein Folding in the Endoplasmic Reticulum. *Cold Spring Harb. Perspect. Biol.* **5**, a013201 (2013).

51. Young, J. C., Agashe, V. R., Siegers, K. & Hartl, F. U. Pathways of chaperone-mediated protein folding in the cytosol. *Nat. Rev. Mol. Cell Biol.* **5**, 781–791 (2004).

52. Smalinskaitė, L., Kim, M. K., Lewis, A. J. O., Keenan, R. J. & Hegde, R. S. Mechanism of an intramembrane chaperone for multipass membrane proteins. *Nature* **611**, 161–166 (2022).

53. Volkmar, N. & Christianson, J. C. Squaring the EMC-how promoting membrane protein biogenesis impacts cellular functions and organismal homeostasis. (2020) doi:10.1242/jcs.243519.

54. Coelho, J. P. L. *et al.* A network of chaperones prevents and detects failures in membrane protein lipid bilayer integration. *Nat. Commun.* **10**, 672 (2019).

55. Bloemeke, N. *et al.* Intramembrane client recognition potentiates the chaperone functions of calnexin. *EMBO J.* **41**, (2022).

56. Juszkiewicz, S. & Hegde, R. S. Quality Control of Orphaned Proteins. *Mol. Cell* **71**, 443–457 (2018).

57. Bertolini, M. *et al.* Interactions between nascent proteins translated by adjacent ribosomes drive homomer assembly. *Science* **371**, 57–64 (2021).

58. Shiber, A. *et al.* Cotranslational assembly of protein complexes in eukaryotes revealed by ribosome profiling. *Nature* **561**, 268–272 (2018).

59. Marinko, J. T. *et al.* Folding and Misfolding of Human Membrane Proteins in Health and Disease: From Single Molecules to Cellular Proteostasis. (2019) doi:10.1021/acs.chemrev.8b00532.

60. Sun, Z. & Brodsky, J. L. Protein quality control in the secretory pathway. *J. Cell Biol.* **218**, 3171–3187 (2019).

61. Guerriero, C. J. & Brodsky, J. L. The Delicate Balance Between Secreted Protein Folding and Endoplasmic Reticulum-Associated Degradation in Human Physiology. *Physiol. Rev.* **92**, 537–576 (2012).

62. Joazeiro, C. A. P. Mechanisms and functions of ribosome-associated protein quality control. *Nat. Rev. Mol. Cell Biol.* **20**, 368–383 (2019).

63. Brandman, O. & Hegde, R. S. Ribosome-associated protein quality control. *Nat. Struct. Mol. Biol.* **23**, 7–15 (2016).

64. Phillips, B. P. & Miller, E. A. Ribosome-associated quality control of membrane proteins at the endoplasmic reticulum. *J. Cell Sci.* **133**, jcs251983 (2020).

65. Hessa, T. *et al.* Protein targeting and degradation are coupled for elimination of mislocalized proteins. *Nature* **475**, 394–397 (2011).

66. Rodrigo-Brenni, M. C., Gutierrez, E. & Hegde, R. S. Cytosolic Quality Control of Mislocalized Proteins Requires RNF126 Recruitment to Bag6. *Mol. Cell* **55**, 227–237 (2014).

67. Dederer, V. *et al.* Cooperation of mitochondrial and ER factors in quality control of tail-anchored proteins. *eLife* **8**, e45506 (2019).

68. Matsumoto, S. *et al.* Msp1 Clears Mistargeted Proteins by Facilitating Their Transfer from Mitochondria to the ER. *Mol. Cell* **76**, 191-205.e10 (2019).

69. McKenna, M. J. *et al.* The endoplasmic reticulum P5A-ATPase is a transmembrane helix dislocase. *Science* **369**, eabc5809 (2020).

70. Adams, B. M., Oster, M. E. & Hebert, D. N. Protein Quality Control in the Endoplasmic Reticulum. *Protein J.* **38**, 317–329 (2019).

71. Araki, K. & Nagata, K. Protein Folding and Quality Control in the ER. *Cold Spring Harb. Perspect. Biol.* **3**, a007526–a007526 (2011).

72. Eletto, D., Dersh, D. & Argon, Y. GRP94 in ER quality control and stress responses. *Semin. Cell Dev. Biol.* **21**, 479–485 (2010).

73. Hammond, C., Braakman, I. & Helenius, A. Role of N-linked oligosaccharide recognition, glucose trimming, and calnexin in glycoprotein folding and quality control. *Proc. Natl. Acad. Sci.* **91**, 913–917 (1994).

74. Lemberg, M. K. & Strisovsky, K. Maintenance of organellar protein homeostasis by ER-associated degradation and related mechanisms. *Mol. Cell* **81**, 2507–2519 (2021).

75. Walter, P. & Ron, D. The unfolded protein response: from stress pathway to homeostatic regulation. *Science* **334**, 1081–6 (2011).

76. Hetz, C. & Papa, F. R. The Unfolded Protein Response and Cell Fate Control. *Mol. Cell* **69**, 169–181 (2018).

77. Hou, N. S. *et al.* Activation of the endoplasmic reticulum unfolded protein response by lipid disequilibrium without disturbed proteostasis in vivo. *Proc. Natl. Acad. Sci.* **111**, (2014).

78. Halbleib, K. *et al.* Activation of the Unfolded Protein Response by Lipid Bilayer Stress. *Mol. Cell* **67**, 673-684.e8 (2017).

79. Preissler, S. & Ron, D. Early Events in the Endoplasmic Reticulum Unfolded Protein Response. *Cold Spring Harb. Perspect. Biol.* **11**, a033894 (2019).

80. Cox, J. S., Shamu, C. E. & Walter, P. Transcriptional induction of genes encoding endoplasmic reticulum resident proteins requires a transmembrane protein kinase. *Cell* **73**, 1197–1206 (1993).

81. Bertolotti, A., Zhang, Y., Hendershot, L. M., Harding, H. P. & Ron, D. Dynamic interaction of BiP and ER stress transducers in the unfolded-protein response. *Nat. Cell Biol.* **2**, 326–332 (2000).

82. Gardner, B. M. & Walter, P. Unfolded Proteins Are Ire1-Activating Ligands That Directly Induce the Unfolded Protein Response. *Science* **333**, 1891–1894 (2011).

83. Calfon, M. *et al.* IRE1 couples endoplasmic reticulum load to secretory capacity by processing the XBP-1 mRNA. *Nature* **415**, 92–96 (2002).

84. Yoshida, H., Matsui, T., Yamamoto, A., Okada, T. & Mori, K. XBP1 mRNA Is Induced by ATF6 and Spliced by IRE1 in Response to ER Stress to Produce a Highly Active Transcription Factor. *Cell* **107**, 881–891 (2001).

85. Yoshida, H. *et al.* A Time-Dependent Phase Shift in the Mammalian Unfolded Protein Response. *Dev. Cell* **4**, 265–271 (2003).

86. Haze, K., Yoshida, H., Yanagi, H., Yura, T. & Mori, K. Mammalian Transcription Factor ATF6 Is Synthesized as a Transmembrane Protein and Activated by Proteolysis in Response to Endoplasmic Reticulum Stress. *Mol. Biol. Cell* **10**, 3787–3799 (1999).

87. Ye, J. *et al.* ER Stress Induces Cleavage of Membrane-Bound ATF6 by the Same Proteases that Process SREBPs. *Mol. Cell* **6**, 1355–1364 (2000).

88. Wang, P., Li, J., Tao, J. & Sha, B. The luminal domain of the ER stress sensor protein PERK binds misfolded proteins and thereby triggers PERK oligomerization. *J. Biol. Chem.* **293**, 4110–4121 (2018).

89. Harding, H. P., Zhang, Y. & Ron, D. Protein translation and folding are coupled by an endoplasmic-reticulum- resident kinase. **397**, (1999).

90. Marciniak, S. J. *et al.* CHOP induces death by promoting protein synthesis and oxidation in the stressed endoplasmic reticulum. *Genes Dev.* **18**, 3066–3077 (2004).

91. Ruggiano, A., Foresti, O. & Carvalho, P. ER-associated degradation: Protein quality control and beyond. *J. Cell Biol.* **204**, 869–879 (2014).

92. Christianson, J. C. & Carvalho, P. Order through destruction: how ER-associated protein degradation contributes to organelle homeostasis. *EMBO J.* (2022) doi:10.15252/embj.2021109845.

93. Christianson, J. C. *et al.* Defining human ERAD networks through an integrative mapping strategy. *Nat. Cell Biol.* **14**, 93–105 (2012).

94. Ye, Y., Meyer, H. H. & Rapoport, T. A. The AAA ATPase Cdc48/p97 and its partners transport proteins from the ER into the cytosol. *Nature* **414**, 652–656 (2001).

95. Khmelinskii, A. *et al.* Protein quality control at the inner nuclear membrane. *Nature* **516**, 410–413 (2014).

96. Foresti, O., Rodriguez-Vaello, V., Funaya, C. & Carvalho, P. Quality control of inner nuclear membrane proteins by the Asi complex. *Science* **346**, 751–755 (2014).

97. Fenech, E. J. *et al.* Interaction mapping of endoplasmic reticulum ubiquitin ligases identifies modulators of innate immune signalling. *eLife* **9**, (2020).

98. van de Weijer, M. L. *et al.* Quality Control of ER Membrane Proteins by the RNF185/Membralin Ubiquitin Ligase Complex. *Mol. Cell* **79**, 768-781.e7 (2020).

99. Carvalho, P., Goder, V. & Rapoport, T. A. Distinct Ubiquitin-Ligase Complexes Define Convergent Pathways for the Degradation of ER Proteins. *Cell* **126**, 361–373 (2006).

100. Schulz, J. *et al.* Conserved cytoplasmic domains promote Hrd1 ubiquitin ligase complex formation for ER-associated degradation (ERAD). *J. Cell Sci.* (2017).

101. Horn, S. C. *et al.* Usa1 Functions as a Scaffold of the HRD-Ubiquitin Ligase. *Mol. Cell* **36**, 782–793 (2009).

102. van der Goot, A. T., Pearce, M. M. P., Leto, D. E., Shaler, T. A. & Kopito, R. R. Redundant and Antagonistic Roles of XTP3B and OS9 in Decoding Glycan and Non-glycan Degrons in ER-Associated Degradation. *Mol. Cell* **70**, 516-530.e6 (2018).

103. Lilley, B. N. & Ploegh, H. L. A membrane protein required for dislocation of misfolded proteins from the ER. *Nature* **429**, 834–840 (2004).

104. Ye, Y., Shibata, Y., Yun, C., Ron, D. & Rapoport, T. A. A membrane protein complex mediates retro-translocation from the ER lumen into the cytosol. *Nature* **429**, 841–847 (2004).

105. Neal, S. *et al.* The Dfm1 Derlin Is Required for ERAD Retrotranslocation of Integral Membrane Proteins. *Mol. Cell* **69**, 306-320.e4 (2018).

106. Wu, X. *et al.* Structural basis of ER-associated protein degradation mediated by the Hrd1 ubiquitin ligase complex. *Science* **368**, (2020).

107. Rao, B. *et al.* The cryo-EM structure of an ERAD protein channel formed by tetrameric human Derlin-1. *Sci. Adv.* **7**, eabe8591 (2021).

108. Schoebel, S. *et al.* Cryo-EM structure of the protein-conducting ERAD channel Hrd1 in complex with Hrd3. *Nature* **548**, 352–355 (2017).

109. Vasic, V. *et al.* Hrd1 forms the retrotranslocation pore regulated by auto-ubiquitination and binding of misfolded proteins. *Nat. Cell Biol.* **22**, 274–281 (2020).

110. Nejatfard, A. *et al.* Derlin rhomboid pseudoproteases employ substrate engagement and lipid distortion to enable the retrotranslocation of ERAD membrane substrates. *Cell Rep.* **37**, 109840 (2021).

111. Guerriero, C. J. *et al.* Transmembrane helix hydrophobicity is an energetic barrier during the retrotranslocation of integral membrane ERAD substrates. *Mol. Biol. Cell* **28**, 2076–2090 (2017).

112. Weihofen, A., Binns, K., Lemberg, M. K., Ashman, K. & Martoglio, B. Identification of signal peptide peptidase, a presenilin-type aspartic protease. *Science* **296**, 2215–2218 (2002).

113. Avci, D. *et al.* The Yeast ER-Intramembrane Protease Ypf1 Refines Nutrient Sensing by Regulating Transporter Abundance. *Mol. Cell* **56**, 630–640 (2014).

114. Chen, C. -y. *et al.* Signal peptide peptidase functions in ERAD to cleave the unfolded protein response regulator XBP1u. *EMBO J.* **33**, 2492–2506 (2014).

115. Boname, J. M. *et al.* Cleavage by signal peptide peptidase is required for the degradation of selected tail-anchored proteins. *J. Cell Biol.* **205**, 847–862 (2014).

116. Fleig, L. *et al.* Ubiquitin-Dependent Intramembrane Rhomboid Protease Promotes ERAD of Membrane Proteins. *Mol. Cell* **47**, 558–569 (2012).

117. Bock, J. *et al.* Rhomboid protease RHBDL4 promotes retrotranslocation of aggregation-prone proteins for degradation. *Cell Rep.* **40**, 111175 (2022).

118. Avci, D. *et al.* The intramembrane protease SPP impacts morphology of the endoplasmic reticulum by triggering degradation of morphogenic proteins. *J. Biol. Chem.* **294**, 2786–5585 (2019).

119. Mark Paetzel, †, Andrew Karla, ‡, Natalie C. J. Strynadka, † and & Ross E. Dalbey*, ‡. Signal Peptidases. *Chem. Rev.* **102**, 4549–4579 (2002).

120. von Heijne, G. The signal peptide. *J. Membr. Biol.* **115**, 195–201 (1990).

121. von Heijne, G. Membrane-protein topology. *Nat. Rev. Mol. Cell Biol.* **7**, 909–918 (2006).

122. Paetzel, M., Dalbey, R. E. & Strynadka, N. C. J. The structure and mechanism of bacterial type I signal peptidases: A novel antibiotic target. *Pharmacol. Ther.* **87**, 27–49 (2000).

123. Tjalsma, H. *et al.* The Role of Lipoprotein Processing by Signal Peptidase II in the Gram-positive Eubacterium Bacillus subtilis. *J. Biol. Chem.* **274**, 1698–1707 (1999).

124. Strom, M. S., Nunn, D. N. & Lory, S. A single bifunctional enzyme, PilD, catalyzes cleavage and N-methylation of proteins belonging to the type IV pilin family. *Proc. Natl. Acad. Sci.* **90**, 2404–2408 (1993).

125. Zwizinskis, C. & Wicknerfj, W. Purification and Characterization of Leader (Signal) Peptidase from Escherichia coli*. *J. Biol. Chem.* **255**, 7973–7977 (1980).

126. Dalbey, R. E., Wang, P. & van Dijl, J. M. Membrane Proteases in the Bacterial Protein Secretion and Quality Control Pathway. *Microbiol. Mol. Biol. Rev.* **76**, 311–330 (2012).

127. Craney, A. & Romesberg, F. E. The inhibition of type I bacterial signal peptidase: Biological consequences and therapeutic potential. *Bioorg. Med. Chem. Lett.* **25**, 4761–4766 (2015).

128. Blobel, G. & Dobberstein, B. Transfer of proteins across membranes. I. Presence of proteolytically processed and unprocessed nascent immunoglobulin light chains on membrane-bound ribosomes of murine myeloma. *J. Cell Biol.* **67**, 835–851 (1975).

129. Evans, E. A., Gilmore, R. & Blobel, G. Purification of microsomal signal peptidase as a complex. *Proc. Natl. Acad. Sci. U. S. A.* **83**, 581–5 (1986).

130. Kalies, K.-U. & Hartmann, E. *Membrane Topology of the 12-and the 25-kDa Subunits of the Mammalian Signal Peptidase Complex*. http://www.jbc.org/ (1996).

131. Yadeau, J. T., Kleint, C. & Blobel, G. Yeast signal peptidase contains a glycoprotein and the Sec11 gene product. *Proc Nati Acad Sci USA* **88**, 517–521 (1991).

132. Böhni, P. C., Deshaies, R. J. & Schekman, R. W. SEC11 is required for signal peptide processing and yeast cell growth. *J. Cell Biol.* **106**, 1035–42 (1988).

133. Meyer, H.-A. & Hartmann, E. The Yeast SPC22/23 Homolog Spc3p Is Essential for Signal Peptidase Activity*. *J. Biol. Chem.* **272**, 13159–13164 (1997).

134. Fang, H., Mullins, C. & Green, N. In addition to SEC11, a newly identified gene, SPC3, is essential for signal peptidase activity in the yeast endoplasmic reticulum. *J. Biol. Chem.* **272**, 13152–8 (1997).

135. Fang, H., Panzner, S., Mullins, C., Hartmann, E. & Green, N. The Homologue of Mammalian SPC12 Is Important for Efficient Signal Peptidase Activity in Saccharomyces cerevisiae*. *J. Biol. Chem.* **271**, 16460–16465 (1996).

136. Mullins, C., Meyer, H.-A., Hartmann, E., Green, N. & Fang, H. Structurally Related Spc1p and Spc2p of Yeast Signal Peptidase Complex Are Functionally Distinct*. *J. Biol. Chem.* **271**, 29094–29099 (1996).

137. Kalies, K.-U., Rapoport, T. A. & Hartmann, E. The Subunit of the Sec61 Complex Facilitates Cotranslational Protein Transport and Interacts with the Signal Peptidase during Translocation. *J. Cell Biol.* **141**, 887–894 (1998).

138. Antonin, W., Meyer, H.-A. & Hartmann, E. Interactions between Spc2p and Other Components of the Endoplasmic Reticulum Translocation Sites of the Yeast Saccharomyces cerevisiae*. *J. Biol. Chem.* **275**, 34068–34072 (2000).

139. Gilbert, H. H., Kwak, E., Chen, S.-J. & Mardon, R. Drosophila Signal Peptidase Complex Member Spase12 Is Required for Development and Cell Differentiation. *PLoS ONE* **8**, 60908 (2013).

140. Yim, C. *et al. Spc1 regulates the signal peptidase-mediated processing of membrane proteins.* (2021).

141. Zhang, R. *et al.* A CRISPR screen defines a signal peptide processing pathway required by flaviviruses. *Nature* **535**, 164–168 (2016).

142. Bintintan, I. & Meyers, G. A New Type of Signal Peptidase Cleavage Site Identified in an RNA Virus Polyprotein * Downloaded from. *J. Biol. Chem.* **285**, 8572–8584 (2010).

143. Ma, L. *et al.* Host Factor SPCS1 Regulates the Replication of Japanese Encephalitis Virus through Interactions with Transmembrane Domains of NS2B. (2018) doi:10.1128/JVI.00197-18.

144. Hongo, S. *et al.* Influenza C virus CM2 protein is produced from a 374-amino-acid protein (P42) by signal peptidase cleavage. *J. Virol.* **73**, 46–50 (1999).

145. Suzuki, R. *et al.* Signal Peptidase Complex Subunit 1 Participates in the Assembly of Hepatitis C Virus through an Interaction with E2 and NS2. *PLOS Pathog.* **9**, e1003589 (2013).

146. Estoppey, D. *et al.* The Natural Product Cavinafungin Selectively Interferes with Zika and Dengue Virus Replication by Inhibition of the Host Signal Peptidase Report The Natural Product Cavinafungin Selectively Interferes with Zika and Dengue Virus Replication by Inhibition o. *CellReports* **19**, 451–460 (2017).

147. Nordahl Petersen, T., Brunak, S., von Heijne, G. & Nielsen, H. SignalP 4.0: discriminating signal peptides from transmembrane regions. *Nat. Methods* **8**, 785–786 (2011).

148. Apweiler, R. UniProt: the Universal Protein knowledgebase. *Nucleic Acids Res.* **32**, 115D – 119 (2004).

149. Landrum, M. J. *et al.* ClinVar: improvements to accessing data. *Nucleic Acids Res.* **48**, D835–D844 (2020).

150. Tate, J. G. *et al.* COSMIC: the Catalogue Of Somatic Mutations In Cancer. *Nucleic Acids Res.* **47**, D941–D947 (2019).

151. Ashburner, M. *et al.* Gene Ontology: tool for the unification of biology. *Nat. Genet.* **25**, 25–29 (2000).

152. The Gene Ontology Consortium *et al.* The Gene Ontology resource: enriching a GOld mine. *Nucleic Acids Res.* **49**, D325–D334 (2021).

153. Mi, H., Muruganujan, A., Ebert, D., Huang, X. & Thomas, P. D. PANTHER version 14: more genomes, a new PANTHER GO-slim and improvements in enrichment analysis tools. *Nucleic Acids Res.* **47**, D419–D426 (2019).

154. Kumar, N. M. & Gilula, N. B. The Gap Junction Communication Channel. *Cell* **84**, 381–388 (1996).

155. Sohl, G. Gap junctions and the connexin protein family. *Cardiovasc. Res.* **62**, 228–232 (2004).

156. Delmar, M. *et al.* Connexins and Disease. *Cold Spring Harb. Perspect. Biol.* **10**, a029348 (2018).

157. Falk, M. M., Kumar, N. M. & Gilula, N. B. Membrane Insertion of Gap Junction Connexins: Polytopic Channel Forming Membrane Proteins. *J. Cell Biol.* **127**, 343–355 (1994).

158. Falk, M. M., Buehler, L. K., Kumar, N. M. & Gilula, N. B. Cell-free synthesis and assembly of connexins into functional gap junction membrane channels. *EMBO J.* **16**, 2703–2716 (1997).

159. Falk, M. M. & Gilula, N. B. Connexin Membrane Protein Biosynthesis Is Influenced by Polypeptide Positioning within the Translocon and Signal Peptidase Access* Downloaded from. *J. Biol. Chem.* **273**, 7856–7864 (1998).

160. Bone, L. J., Deschenes, S. M., Balice-Gordon, R. J., Fischbeck, K. H. & Scherer, S. S. Connexin32 and X-linked Charcot–Marie–Tooth Disease. (1997).

161. Scherer, S. S. & Kleopa, K. A. X-linked Charcot-Marie-Tooth disease. *J. Peripher. Nerv. Syst.* **17**, 9–13 (2012).

162. Kleopa, K. A., Abrams, C. K. & Scherer, S. S. How do mutations in GJB1 cause X-linked Charcot–Marie–Tooth disease? *Brain Res.* **1487**, 198–205 (2012).

163. Sillén, A., Annerén, G. & Dahl, N. A novel mutation (C201R) in the transmembrane domain of connexin 32 in severe x-linked charcot-marie-tooth disease. *Hum. Mutat.* **11**, S8–S9 (1998).

164. Fluhrer, R., Steiner, H. & Haass, C. Intramembrane Proteolysis by signal peptide peptidases: A comparative discussion of GXGD-type aspartyl proteases. *J. Biol. Chem.* **284**, 13975–13979 (2009).

165. Wunderle, L. *et al.* Rhomboid intramembrane protease RHBDL4 triggers ER-export and non-canonical secretion of membrane-anchored TGFα. *Sci. Rep.* **6**, 27342 (2016).

166. Knopf, J. D. *et al.* Intramembrane protease RHBDL4 cleaves oligosaccharyltransferase subunits to target them for ER-associated degradation. (2020) doi:10.1242/jcs.243790.

167. Heidasch, R. *et al. Intramembrane protease SPP defines a cholesterol-regulated switch of the mevalonate pathway.* http://biorxiv.org/lookup/doi/10.1101/2021.07.19.452877 (2021) doi:10.1101/2021.07.19.452877.

168. Colin Adrain,1† Markus Zettl,1*† Yonka Christova,1 Neil Taylor, 2 Matthew Freeman1‡. Tumor Necrosis Factor Signaling Requires iRhom2 to Promote Trafficking and Activation of TACE. *Science* **335**, 225–228 (2012).

169. Künzel, U. *et al.* FRMD8 promotes inflammatory and growth factor signalling by stabilising the iRhom/ADAM17 sheddase complex. *eLife* **7**, (2018).

170. Dulloo, I. *et al. Cleavage of the pseudoprotease iRhom2 by the signal peptidase complex reveals an ER-to-nucleus signalling pathway.* http://biorxiv.org/lookup/doi/10.1101/2022.11.28.518246 (2022) doi:10.1101/2022.11.28.518246.

171. Hattori, N. *et al.* Demyelinating and axonal features of Charcot-Marie-Tooth disease with mutations of myelin-related proteins (PMP22, MPZ and Cx32): a clinicopathological study of 205 Japanese patients. *Brain* **126**, 134–151 (2003).

172. Marinko, J. T., Carter, B. D. & Sanders, C. R. Direct relationship between increased expression and mistrafficking of the Charcot–Marie–Tooth–associated protein PMP22. *J. Biol. Chem.* **295**, 11963–11970 (2020).

173. Tareen, A. & Kinney, J. B. Logomaker: beautiful sequence logos in Python. *Bioinformatics* **36**, 2272–2274 (2020).

174. Von Heijne, G. Patterns of Amino Acids near Signal-Sequence Cleavage Sites. *Eur. J. Biochem.* **133**, 17–21 (1983).

175. Madeira, F. *et al.* Search and sequence analysis tools services from EMBL-EBI in 2022. *Nucleic Acids Res.* **50**, W276–W279 (2022).

176. Calligaris, M. *et al.* Strategies to Target ADAM17 in Disease: From Its Discovery to the iRhom Revolution. *Molecules* **26**, 944 (2021).

177. Nadav, E. *et al.* A novel mammalian endoplasmic reticulum ubiquitin ligase homologous to the yeast Hrd1. *Biochem. Biophys. Res. Commun.* **303**, 91–97 (2003).

178. Kikkert, M. *et al.* Human HRD1 Is an E3 Ubiquitin Ligase Involved in Degradation of Proteins from the Endoplasmic Reticulum. *J. Biol. Chem.* **279**, 3525–3534 (2004).

179. Hwang, J. *et al.* Characterization of protein complexes of the endoplasmic reticulum-associated degradation E3 ubiquitin ligase Hrd1. *J. Biol. Chem.* **292**, 9104–9116 (2017).

180. Vembar, S. S. & Brodsky, J. L. One step at a time: endoplasmic reticulum-associated degradation. *Nat. Rev. Mol. Cell Biol.* **9**, 944–957 (2008).

181. Hampton, R. Y. & Sommer, T. Finding the will and the way of ERAD substrate retrotranslocation. *Curr. Opin. Cell Biol.* **24**, 460–466 (2012).

182. Wu, X. & Rapoport, T. A. Mechanistic insights into ER-associated protein degradation. *Curr. Opin. Cell Biol.* **53**, 22–28 (2018).

183. Kostova, Z., Tsai, Y. C. & Weissman, A. M. Ubiquitin ligases, critical mediators of endoplasmic reticulum-associated degradation. *Semin. Cell Dev. Biol.* **18**, 770–779 (2007).

184. Kaneko, M. *et al.* Genome-wide identification and gene expression profiling of ubiquitin ligases for endoplasmic reticulum protein degradation. *Sci. Rep.* **6**, 30955 (2016).

185. Zhou, H.-J. *et al.* Discovery of a First-in-Class, Potent, Selective, and Orally Bioavailable Inhibitor of the p97 AAA ATPase (CB-5083). *J. Med. Chem.* **58**, 9480–9497 (2015).

186. Sriburi, R., Jackowski, S., Mori, K. & Brewer, J. W. XBP1: a link between the unfolded protein response, lipid biosynthesis, and biogenesis of the endoplasmic reticulum. *J. Cell Biol.* **167**, 35–41 (2004).

187. Bommiasamy, H. *et al.* ATF6alpha induces XBP1-independent expansion of the endoplasmic reticulum. *J. Cell Sci.* **122**, 1626–36 (2009).

188. Seidler, N. W., Jona, I., Vegh, M. & Martonosi, A. Cyclopiazonic Acid is a Specific Inhibitor of the Ca2+-ATPase of Sarcoplasmic Reticulum. *J. Biol. Chem.* **264**, 17816–17823 (1989).

189. Pirot, P. *et al.* Global profiling of genes modified by endoplasmic reticulum stress in pancreatic beta cells reveals the early degradation of insulin mRNAs. *Diabetologia* **50**, 1006–1014 (2007).

190. Fumagalli, F. *et al.* Translocon component Sec62 acts in endoplasmic reticulum turnover during stress recovery. *Nat. Cell Biol.* **18**, 1173–1184 (2016).

191. Almén, M. S., Nordström, K. J. V., Fredriksson, R. & Schiöth, H. B. Mapping the human membrane proteome: a majority of the human membrane proteins can be classified according to function and evolutionary origin. *BMC Biol.* **7**, 50 (2009).

192. Fons, R. D., Bogert, B. A. & Hegde, R. S. Substrate-specific function of the translocon-associated protein complex during translocation across the ER membrane. *J. Cell Biol.* **160**, 529–539 (2003).

193. Sauvageau, E. *et al.* CNIH4 Interacts with Newly Synthesized GPCR and Controls Their Export from the Endoplasmic Reticulum: CNIH4 Controls GPCR Export from the ER. *Traffic* **15**, 383–400 (2014).

194. Mackenzie B, Erickson JD. Sodium-coupled neutral amino acid (System N/A) transporters of the SLC38 gene family. *Pflugers Arch* **447**, 784–95 (2004).

195. Lavie, M. & Goffard, A. Assembly of a Functional HCV Glycoprotein Heterodimer.

196. Patel, H., Dobson, R. J. B. & Newhouse, S. J. A Meta-Analysis of Alzheimer's Disease Brain Transcriptomic Data. *J. Alzheimers Dis.* **68**, 1635–1656 (2019).

197. Chitwood, P. J. & Hegde, R. S. An intramembrane chaperone complex facilitates membrane protein biogenesis. *Nature* **584**, 630–634 (2020).

198. Dudek, J. A novel type of co-chaperone mediates transmembrane recruitment of DnaK-like chaperones to ribosomes. *EMBO J.* **21**, 2958–2967 (2002).

199. Guo, F. & Snapp, E. L. ERdj3 Regulates BiP Occupancy in Living Cells. *J. Cell Sci.* jcs.118182 (2013) doi:10.1242/jcs.118182.

200. Sato, T. *et al.* STT3B-Dependent Posttranslational N-Glycosylation as a Surveillance System for Secretory Protein. *Mol. Cell* **47**, 99–110 (2012).

201. Ruiz-Canada, C., Kelleher, D. J. & Gilmore, R. Cotranslational and Posttranslational N-Glycosylation of Polypeptides by Distinct Mammalian OST Isoforms. *Cell* **136**, 273–283 (2009).

202. Zhang, S., Xu, C., Larrimore, K. E. & Ng Correspondence, D. T. W. Slp1-Emp65: A Guardian Factor that Protects Folding Polypeptides from Promiscuous Degradation In Brief A dedicated cellular mechanism protects folding polypeptides from degradation. *Cell* **171**, 346-350.e12 (2017).

203. Avci, D. & Lemberg, M. K. Clipping or Extracting: Two Ways to Membrane Protein Degradation. *Trends Cell Biol.* **25**, 611–622 (2015).

204. Ast, T., Michaelis, S. & Schuldiner, M. The Protease Ste24 Clears Clogged Translocons. *Cell* **164**, 103–114 (2016).

205. Lara, P. *et al.* Topology and cleavage of astrotactins 1 Murine astrotactins 1 and 2 have similar membrane topology and mature via endoproteolytic cleavage catalyzed by signal peptidase. *J. Biol. Chem.* **294**, 4538–4545 (2019).

206. Matczuk, A. K., Kunec, D. & Veit, M. Co-translational Processing of Glycoprotein 3 from Equine Arteritis Virus: N-GLYCOSYLATION ADJACENT TO THE SIGNAL PEPTIDE PREVENTS CLEAVAGE. *J. Biol. Chem.* **288**, 35396–35405 (2013).

207. Nilsson, I., Johnson, A. E. & von Heijne, G. Cleavage of a tail-anchored protein by signal peptidase. *FEBS Lett.* **516**, 106–108 (2002).

208. Bendtsen, J. D., Nielsen, H., Von Heijne, G. & Brunak, S. Improved prediction of signal peptides: SignalP 3.0. *J. Mol. Biol.* **340**, 783–795 (2004).

209. Emanuelsson, O., Brunak, S., Von Heijne, G. & Nielsen, H. Locating proteins in the cell using TargetP, SignalP and related tools. *Nat. Protoc.* **2**, 953–971 (2007).

210. Vilchez, D., Saez, I. & Dillin, A. The role of protein clearance mechanisms in organismal ageing and age-related diseases. *Nat. Commun.* **5**, 5659 (2014).

211. Kikis, E. A., Gidalevitz, T. & Morimoto, R. I. Protein Homeostasis in Models of Aging and Age-Related Conformational Disease. in *Protein Metabolism and Homeostasis in Aging* (ed. Tavernarakis, N.) vol. 694 138–159 (Springer US, 2010).

212. Ladiges, W. The quality control theory of aging. *Pathobiol. Aging Age-Relat. Dis.* **4**, 24835 (2014).

213. Durocher, Y., Perret, S. & Kamen, A. High-level and high-throughput recombinant protein production by transient transfection of suspension-growing human 293-EBNA1 cells. *Nucleic Acids Res.* **30**, e9 (2002).

214. Hessa, T. *et al.* Molecular code for transmembrane-helix recognition by the Sec61 translocon. *Nature* **450**, 1026–1030 (2007).

215. Aguilan, J. T., Kulej, K. & Sidoli, S. Guide for protein fold change and *p*-value calculation for non-experts in proteomics. *Mol. Omics* **16**, 573–582 (2020).

216. Schindelin, J. *et al.* Fiji: an open-source platform for biological-image analysis. *Nat. Methods* **9**, 676–682 (2012).

Acknowledgements

First, I would like to thank Marius. You've been an amazing and supportive mentor throughout this challenging journey. Your enthusiasm towards science in general and towards the project helped me grow as a scientist and enjoy the process.

I would like to thank Matthias Mayer and Rob Russell for being part of my thesis committee for the past three years and for the helpful discussions during our meetings. A special thanks to Matthias also for hosting me over the last year and subsequently allowing me to complete my PhD in Heidelberg and to Rob for the support in the computational aspects of my project.

I want to thank Nora Voegtle for being part of my defence committee.

A big thanks to Matthias Feige, Joao Coelho and Dinah Kaylani for the extraordinary collaboration, the long discussions and for helping in bringing the project to the level it reached. Big thanks also to Gurdeep for the tireless support in the computational part of the project and for the enthusiasm you put into this every moment of the way.

Next, I would like to thank the ZMBH, particularly Elmar Schiebel, Angret Joester and Ralf Tolle, for providing support over the last few years. Also, special thanks go to Alex Merx for the invaluable help with the hot lab.

I would also like to thank the Schlaitz and the Duarte Campos Labs for the sharing and positive environment created in 329.

I sincerely thank Wilhelm Palm and Catarina Pechincha for making me part of a fantastic and exciting project that led to my next chapter in the scientific world. I cannot wait to start!

I also owe a special thanks to the ZMBH cleaning/kitchen ladies for the irreplaceable and indispensable job they carry out every day.

I would like to thank the Proteomics Core Facility Cologne for the help with the SPCS1 interactome analysis.

Next, I would like to profoundly thank the entire Lemberg Lab for the awesome environment that made this journey less stressful and even joyful. Immense gratitude goes to the "office gang": Dönem, my scientific "mom", you taught me basically everything lab-related and if I achieved what I achieved, this is also thanks to your tireless support; Martina, for the laughter and tears together during the insanely long hours in the hot lab; and Julia, for the assistance

and encouragement during these years, inside and also outside the lab. You all have no idea how much I missed you in the last year.

My sincere and countless gratitude goes to all the Schuck Lab past and present members (Rolf, Inge, Anna, Sibi, Oli, Petra, Niklas, Lis, Aye and Dimitris) for adopting me as one of your own lab members over the last few years. Thanks for all the lunches, walks and coffee&cake breaks. In particular, thanks to Oli, Lis, and Niklas for making me discover what is now one of my favourite sports: bouldering. Thanks for driving me there every single Monday to enjoy climbing, relax and begin the week with a good spirit, but mostly for the countless Flammkuchens post-session enjoyed together.

I want to thank with all my heart all the friends I made during these years.

Special thanks to Oli and Lena for sharing the passion for food, all the dinners together and the lovely summer holidays. Thank you for all the moments we have spent together and I am sure there will be many more in the next years. By the way, you have to learn Italian because we all know we are going to end up in Italy at some point, right?

Thanks to the Italian cluster, Fabio, Roberto and Alessandra. Thank you for making me laugh so bad that I end up with hiccups every time (maybe I actually should not thank you for that…). Sono comunque felicissimo di avervi conosciuto e rimpiango che non sia accaduto prima. Avremo in ogni caso tante altre occasioni per divertirci insieme, tanto lo sappiamo tutti che non ce ne andremo mai da qui.

Endless gratitude with all my heart to my family, mom, dad, Nonna Silvana for always being there and for helping me become the person I am now, and to my acquired family, Paola, Peppo, Benny, Nonna Aurora, Dodo and Manu, for the support and the long video calls during these years abroad, especially during the lockdown. A special thought to Nonna Liliana and Nonno Gugliemo, which unfortunately cannot be here to enjoy this moment with us. I am sure Nonna would be happy to know that our job "in the fields" is going great.

Last but not least, I immensely thank my best friend, the love of my life, and now also my wife, Giulia. We started this life journey together more than ten years ago and, since then, we have always been there for each other, in good and bad times. I cannot wait to see what life brings us next and I am happy that, whatever it will be, we will be together.